UNIVERSIDADE DE SÃO PAULO

FACULDADE DE ECONOMIA, ADMINISTRAÇÃO, CONTABILIDADE E ATUÁRIA

DEPARTAMENTO DE CONTABILIDADE E ATUÁRIA

PROGRAMA DE PÓS-GRADUAÇÃO EM CONTROLADORIA E CONTABILIDADE

WHEN THERE'S NO NOVEMBER RAIN: DEVELOPING A PARAMETRIC INSURANCE FOR HYDROELECTRIC ENERGY GENERATORS IN BRAZIL

"WHEN THERE'S NO NOVEMBER RAIN": DESENVOLVENDO UM SEGURO PARAMÉTRICO PARA GERADORES DE ENERGIA HIDRELÉTRICA NO BRASIL

Nathalia Costa Fonseca

Orientador:

Prof. Dr. João Vinícius de França Carvalho

SÃO PAULO

2023

Prof. Dr. Carlos Gilberto Carlotti Júnior
Reitor da Universidade de São Paulo

Prof.ª Dr.ª Maria Dolores Montoya Diaz
Diretora da Faculdade de Economia, Administração, Contabilidade e Atuária

Prof.ª Dr.ª Mara Jane Contrera Malacrida
Chefe do Departamento de Contabilidade e Atuária

Prof. Dr. Renê Coppe Pimentel
Coordenador do Programa de Pós-Graduação em Controladoria e Contabilidade

Catalogação na Publicação (CIP)
Ficha Catalográfica com dados inseridos pelo autor

Fonseca, Nathalia Costa
When There's no November Rain: Developing a Parametric Insurance for Hydroelectric Energy Generators in Brazil / Nathalia Costa Fonseca – São Paulo, 2023.
124p.
Dissertação (Mestrado) – Universidade de São Paulo, 2023.
Orientador: Prof. Dr. João Vinícius de França Carvalho.

1. Parametric Insurance. 2. Hydrological Risk. 3. Spatial Econometrics. 4. Copulas. 5. Energy Generators. Universidade de São Paulo. Faculdade de Economia, Administração, Contabilidade e Atuária

Nathalia Costa Fonseca
WHEN THERE'S NO NOVEMBER RAIN: DEVELOPING A PARAMETRIC INSURANCE FOR HYDROELECTRIC ENERGY GENERATORS IN BRAZIL.

Dissertação apresentada à Faculdade de Economia, Administração, Contabilidade e Atuária da Universidade de São Paulo para obtenção do título de Mestre em Ciências.

Aprovado em:

Banca Examinadora

Prof. Dr. Luiz Paulo Lopes Fávero

Instituição: FEA-USP Julgamento:

Prof.ª Dr.ª Wesley Mendes da Silva

Instituição: EAESP-FGV- Externo Julgamento:

Prof. Dr. César da Rocha Neves

Instituição: UERJ/SUSEP - Externo Julgamento:

NATHALIA COSTA FONSECA

WHEN THERE'S NO NOVEMBER RAIN: DEVELOPING A PARAMETRIC INSURANCE FOR HYDROELECTRIC ENERGY GENERATORS IN BRAZIL

"WHEN THERE'S NO NOVEMBER RAIN": DESENVOLVENDO UM SEGURO PARAMÉTRICO PARA GERADORES DE ENERGIA HIDRELÉTRICA NO BRASIL

Dissertação apresentada ao Programa de Pós-Graduação em Controladoria e Contabilidade do Departamento de Contabilidade e Atuária da Faculdade de Economia, Administração, Contabilidade e Atuária da Universidade de São Paulo como requisito parcial para obtenção do título de Mestre em Ciências.

Área de Concentração: Controladoria e Contabilidade.

Orientador: Prof. Dr. João Vinícius de França Carvalho

Versão corrigida

(versão original disponível na Biblioteca da Faculdade de Economia, Administração, Contabilidade e Atuária)

SÃO PAULO

2023

ACKNOWLEDGEMENTS

Writing this dissertation has been a long, interesting and fulfilling process. Much has happened in these past two years that contributed to both my academic, professional and personal evolution. Most of all, the connections from the past that remain, the ones that recently surged and the ones that got stronger, they are somehow responsible, directly or not, for the quality of this research, as none of this would have been possible to be done alone.

Accomplishing this has taken a great deal of talent and effort, as my supervisor once stated, but more than that, it has taken the help and support of all those connections, all those people, that gave me the basis to achieve what I have done so far.

First of all, I thank my family for providing me the bases I needed to enter such a prestigious institution as USP. And for always believing and routing for me. To my mom, Andréa, who always gave her best so I could have the best opportunities in life. To my father, Marcos, who always supported my dreams, no matter how crazy they were, and introduced me to so many of the things I love most in life, like reading, rock music and fantasy stories. And who helped me so much through understanding how accounting spreadsheets work. To my stepfather, José Custódio, who has always been a second father to me and showed as much interest, support and happiness for me and my endeavors as my biological parents. To my aunt, Annelise, who has always been a best friend to me, as well as an example of courage and life joy. And to her daughter Anna Julia, that always looked up to me and never lets me forget that I am amazing, even when I don't feel like it.

To my grandparents, Iva, Elias, Leida and Oswaldo. All four whom I am so lucky to still have present in my life, and that have always looked after me and cared for me. Even if they still cannot really explain what I do for a living or what an actuary is, they always show how proud they are and tell all their friends about me. And, most important, my grandmas always make me the best food, which I deeply value.

Of those who directly contributed to the content in this dissertation, I especially thank my supervisor, João Vinícius. Ever since my undergraduate years, he has been more than a professor, becoming a true friend. I am happy that we have shared pizza, scary plane rides, good music and life adventures as well as research meetings, successful congresses, papers and prizes. He is one of my greatest academical references and inspirations. Thank you so much for always believing in me, pushing me to be better, showing me opportunities and seeing my potential further than I could ever see by myself.

I also thank Thiago ("Thithi"), my dearest friend, for helping me with the development and analyses of the copulas models in this study. This is not our first academic collaboration and I am certain that it won't be the last. It has been great working with you, and sharing meals and conversations as well. I am glad to have this friendship.

I also enormously thank André Chagas and Leonardo Merlini, for all the support with the spatial econometrics' concepts and coding. You have deeply contributed to my learning and the development of this dissertation. I hope to keep touch in the future for I am certain we can collaborate in many other applications of these techniques for actuarial issues.

To Alice Tinoco, my deepest thanks, as I could not have treated those databases in time without your help. I am sure a bright future in programming and actuary lies ahead of you.

To all the other professors and faculty members that have helped me with punctual doubts and suggestions, I extend my thanks. I especially thank Luis Eduardo Afonso, who has

not only evaluated the initial project, but also contributed to my evolution in teaching practice activities, encouraging and allowing me more responsibilities and experiences that I am sure will contribute to my development until someday I become a professor myself.

A kind thanks to Andrés Torres, from the post-graduation secretary, who is always so kind and considerate, and proudly routes for me every time we speak about how things are going.

I would also like to acknowledge my former physics teacher, from high school, Michelle Neves. She was the first to really encourage me when I was deciding to study actuaries. And, more than that, she told me that if I ever had the chance to involve myself in research, I should do it. Because she already knew, from my profile, I would be great in it. I deeply thank her for her support and this advice, which I took with me for life.

Special thanks are also due to my friends and colleagues at Youse. To my leaders, thank you for allowing me the opportunity of carrying on this master's program while balancing my working hours. I deeply esteem that I was able to conciliate both the academic and professional life, for they are two worlds that I love and which offer me complementary experiences. And thanks to all my work friends, who always supported me, showed interest in my research and listened to my class and congresses' stories. I am happy to say that we can see each other every day at the office and still meet after hours to play board games, because you are all amazing people for whom I deeply care.

Last but not least, I thank all the friends that have accompanied me through this journey, that always supported me and helped me keep my mental sanity. It was not easy, and I love each and everyone of you for sticking with me throughout these years. I specially thank Mirella, Catarina and Fernanda, my closest friends that I have kept for more years than I can tell. Thithi, Caio, Tuanny, Laryssa and Vitoria, dear friends I have made in the master's program and hope to keep for many years ahead. And, more recently, my rock band companions, that every week help me discount my anxieties thorough singing my lungs out, always encouraging my evolution. To my rugby team, Feaodonto, even if we hardly play together now, given my schedules, you girls are always there for me when I need, and I thank you for the big part you have played in my life these past years.

As J.R.R. Tolkien once said: "If more of us valued food and cheer and song above hoarded gold, it would be a merrier world". Hence, I thank all my friends for being by my side throughout life, and gladly share this accomplishment with them. Let us all cheer.

RESUMO

A indústria de seguros não-vida desempenha um papel crucial na proteção da sociedade contra uma miríade de perigos. No entanto, existem algumas lacunas de proteção por meio de seguros, especialmente para riscos fundamentais. O seguro paramétrico oferece uma solução para essas lacunas ao mesmo tempo em que melhora a eficiência do mercado segurador. Uma aplicação possível é em questões de alterações climáticas. A crescente frequência e intensidade das secas no Brasil, agravadas pelas mudanças climáticas, tem causado crises econômicas e energéticas. Este estudo aborda essa questão urgente ao introduzir um produto de seguro paramétrico adaptado às hidroelétricas brasileiras, com o objetivo de melhorar a resiliência da geração de energia durante crises de seca e mitigar os riscos hidrológicos sistêmicos. O objetivo principal deste estudo foi desenhar e avaliar a viabilidade deste produto de seguro inovador. A proposta inicial era indexar o seguro em índices de precipitação, porém, os resultados apontam para um índice combinado de precipitação e de vazão de água dos rios ou volume de reservatórios, dependendo das características da usina hidroelétrica. Relativamente aos procedimentos metodológicos, este trabalho é pioneiro no uso de econometria espacial e cópulas para modelar a geração de energia de usinas hidroelétricas brasileiras, uma abordagem não comumente explorada na literatura existente. Nossas principais conclusões enfatizam a utilidade da econometria espacial, particularmente o modelo SARAR de efeitos fixos, na modelagem eficaz da geração de energia para ambos os tipos de usinas hidrelétricas. Esse modelo leva em conta a influência das usinas vizinhas, o que é vital no contexto do sistema elétrico interligado do Brasil. Além disso, o estudo esclarece o potencial do seguro paramétrico na mitigação dos riscos hidrológicos durante crises de seca, mas reitera a necessidade de produtos de seguros diferenciadas para usinas fio-d'água e de armazenamento, devido às suas diferentes características. Um aspecto crucial e pioneiro deste estudo foi utilizar modelos de cópulas condicionais como mecanismo de verificação de robustez, para garantir a não-endogeneidade do modelo espacial. Os resultados iniciais não apresentam viabilidade imediata para as seguradoras, devido ao elevado índice de sinistralidade, mas melhorias podem ser feitas, principalmente com a introdução de um componente dinâmico nos modelos, pois todos foram estimados de maneira estática. Por fim, ao introduzir metodologias inovadoras e fornecer informações valiosas sobre a modelagem de geração de energia, este estudo oferece um caminho promissor para aumentar a sustentabilidade e a resiliência do fornecimento de energia do Brasil, dada a crescente ameaça de secas induzidas pelas mudanças climáticas.

Palavras-Chave: Seguro Paramétrico; Risco Hidrológico; Econometria Espacial; Copulas; Geradores de Energia.

ABSTRACT

The nonlife insurance industry plays a crucial role in safeguarding societal members against a myriad of perils. However, there are some insurance protection gaps (IPGs), especially for fundamental risks. Parametric insurance offers a solution for IPGs while improving the insurance market's efficiency. One possible application is towards climate change issues. The increasing frequency and intensity of droughts in Brazil, exacerbated by climate change, have caused economical and energetic crises. This study addresses this pressing issue by introducing a parametric insurance product tailored to Brazilian hydroelectric companies, aiming to improve the resilience of energy generation during drought crises and mitigating hydrological systemic risks. The primary objective of this study was to design and evaluate the feasibility of this innovative insurance product. The initial proposal was to link the insurance solely on precipitation indexes, however, the results point out to a combined index of precipitation and rivers' water flow or reservoir's volume, depending on hydroelectric powerplant's characteristics. Regarding to methodological procedures, this research lies in its pioneering use of spatial econometrics and copulas to model energy generation of Brazilian hydroelectric powerplants, an approach not commonly explored in the existing literature. Our main findings emphasize the utility of spatial econometrics, particularly the fixed-effects SARAR model, in effectively modeling energy generation for both hydroelectric powerplants' types. This model takes into account the influence of neighboring powerplants, which is vital in the context of Brazil's interconnected electrical system. Moreover, the study sheds light on the potential of parametric insurance in mitigating hydrological risks during drought crises, but it underscores the need for differentiated insurance designs for run-of-river and water store powerplants, due to their diverse characteristics. A crucial and pioneering aspect of this study was to use vine copulas models as a robustness check mechanism, to ensure the non-endogeneity of the spatial model. The primary design does not show immediate viability for insurance companies, due to a high loss ratio, but improvements can be made, especially by introducing a dynamic component in the models, as they were all estimated in a static way. Ultimately, by introducing innovative methodologies and providing valuable insights into energy generation modeling, this study offers a promising avenue to enhance the sustainability and resilience of Brazil's energy supply given the growing threat of climate change-induced droughts.

Keywords: Parametric Insurance; Hydrological Risk; Spatial Econometrics; Copulas; Energy Generators.

TABLE OF CONTENTS

LIST OF ACRONYMS AND ABBREVIATIONS

ANEEL	National Electric Energy Agency
CRFR	climate-related financial risks
DG	decentralized generation
ERM	Enterprise Risk Management
ESG	Environmental, Social, and Governance
GDP	gross domesthic product
GHG	global greenhouse gases
GLM	Generalized linear models
GSF	Generation Scaling Factor
IFRS	International Financial Reporting Standards
IIRC	International Integrated Reporting Council
IPG	insurance protection gap
IR	integrated reporting
ISSB	International Sustainability Standards Board
MRE	Energy Reallocation Mechanism
MRL	Maximum Retention Limit
NDC	National Determined Contributions
NGFS	Network for Greening the Financial System
OLS	Ordinary least squares
ONS	National System Operator
PCH	small hydroelectric plants
PG	Physical Guarantee
PI	parametric insurance
PLD	Settlement Price for Differences
PROINFA	Program for Incenting Alternative Sources of Electric Energy
SAR	Spatial Autoregressive Model
SARAR	Spatial Autoregressive model with Autoregressive Errors
SDM	Spatial Durbin Model
SDEM	Spatial Durbin Error Model
SEM	Spatial Error Model
SIN	National Interconnected System
SLX	Spatial Model with lag in X

TABLES LIST

FIGURES LIST

1. INTRODUCTION

Insurance can be defined as a legal and economic mechanism whereby individuals replace potential uncertain and substantial financial losses, stemming from contingent future events, for a smaller certain cost – the insurance premium (Vaughan & Vaughan, 2008). The nonlife insurance industry assumes a crucial role in safeguarding societal members against a myriad of perils. However, not all risks are insurable (for their nature or the insurers' underwriting choices) and not all insurable risks are insured (given supply and demand issues) (Lin & Kwon, 2020; Schanz, 2018; Vaughan & Vaughan, 2008). This is reflected by a concept called *insurance protection gap* (IPG), meaning "the difference between the amount of insurance that is economically beneficial and the amount of coverage actually purchased" (Schanz, 2018, p. 1), which is common for fundamental risks, such as natural catastrophes, cyber-risks and epidemic related risks (Singer, 2019).

Parametric insurance can offer a new opportunity to solve some IPG problems while improving the insurance market's efficiency, as it is an effective mechanism especially in regions prone to natural catastrophes (Lin & Kwon, 2020). Also, it enables insurance companies to indemnify losses faster, as it requires no claim investigations, whilst reducing problems of moral hazard and adverse selection (Bokusheva, 2018; Lin & Kwon, 2020; Singer, 2019).

Parametric insurance (PI), also known as index-based insurance, is an innovative actuarial scheme, most suitable for low-frequency, high-intensity losses. Unlike indemnity-based insurance, PI does not cover the pure loss, but rather indemnifies the policyholder according to the variation of an index (parameter) that is observable, reliable, and ideally correlated with sustained losses (Eabrasu, 2021; Enríquez et al., 2020; Singer, 2019). This means that, even though the parameter is supposed to be correlated with a sustained loss, the insurance payouts are only triggered by the index, regardless of real losses. In this case, the insurance company provides a payout whose value is established in advance, diverging from the conventional practice of determining the indemnity value based on the real losses incurred (Eabrasu, 2021; Enríquez et al., 2020).

Within this framework, such scheme empowers policyholders to self-assess the potential impact of an event, i.e., the risk measurement is made not only by the insurance company, but the policyholder also plays an active role in this process by determining which levels of the index would represent a sustainable loss, and which levels would demand insurance coverage (Eabrasu, 2021). Furthermore, it can be a viable product for insurance companies to offer when there is insufficient information to underwrite the severity of actual losses, also overcoming the problem of information asymmetry, mitigating adverse selection and preventing moral hazards (Bokusheva, 2018; Enríquez et al., 2020; Han et al., 2019).

PI fosters innovative insurance designs against the unconventional risks that fail to satisfy the criteria of conventional indemnity insurance (Lin & Kwon, 2020). The index may concern any triggering event (e.g., the magnitude of seismic activity or fluviometric levels), so the new generation of parametric insurance solutions include protection for events of terrorism or cyber-attacks, coverages for shipping and manufacturing companies when river water-levels fall and protection against the economic impact of infectious disease outbreaks (Moro, 2020; Singer, 2019). What these new solutions have in common is that they are not protecting against direct physical damage, but rather the indirect consequences of events, such as business interruption costs (Singer, 2019). One possible application of PI is related to weather issues, especially as we experience climate change effects (Horton, 2018).

Climate change has become a pressing global issue, with far-reaching implications for different regions. These effects are expected to intensify with further warming (Bolton et al.,

2020; Diffenbaugh et al., 2018; Domínguez-Tuda & Gutiérrez-Jurado, 2021; Gürtürk et al., 2022; Lesk et al., 2021; Li et al., 2022; Mansoor et al., 2022; Montoya et al., 2021; Paltán et al., 2021; Qi et al., 2022; Tollefson, 2021; van Houtan et al., 2021; Wu et al., 2021; C. Zhang et al., 2021). We are witnessing unprecedented flooding, heatwaves, and wildfires which have already incurred billions of dollars in damages. These climate-related changes are raising concerns among governments and institutions worldwide (C. C. Lee et al., 2022; Mansoor et al., 2022; Mendes-Da-Silva et al., 2021; Verma, 2021).

Discussions and proposals to address potential consequences of global warming have emerged in sectors that had not traditionally paid a lot of attention to it. The financial institutions, in particular, are increasingly involved, when not true drivers of changes to come (Campiglio et al., 2018; C. C. Lee et al., 2022; Michel-Kerjan & Morlaye, 2008). Central banks can have an additional role to play in mitigating climate change, by establishing policies such as carbon pricing, and integrating sustainability principles into financial practices and accounting frameworks (Bolton et al., 2020; Campiglio et al., 2018).

The IFRS Foundation, a leading organization responsible for developing global accounting standards, has recently established the International Sustainability Standards Board (ISSB). ISSB's primary responsibility is to define sustainability accounting standards to be applied in the upcoming financial years, with great focus on ESG (environmental, social and corporate governance) dynamics, as investors and stakeholders increasingly recognize the find it an urgent need for comprehensive information on climate-related matters (Tettamanzi et al., 2022). Climate change, in fact, poses a systemic risk akin to a "ruin problem", i.e., where the system might be exposed to irreversible harm, eventually leading to the risk of total failure (Chenet et al., 2021). Notably, at the 2015 Paris Agreement, the promotion of risk transfer emerged as the key policy instrument for managing losses and damages associated with the adverse effects of climate change (Broberg, 2020; Horton, 2018).

Thus, numerous applications of PI have arisen addressing climate change challenges. Insurance for agriculture is one of the most common applications (Horton, 2018; Jibril et al., 2022), but there is also a growing use of parametric schemes for natural disasters (Broberg, 2020; Horton, 2018; Lin & Kwon, 2020; Pai et al., 2022) and a novel and innovative application regards renewable energy generation.

Examples of the latter include (i) wind farms, as the energy generation is affected by absent or low-speed wind, both conditions that could be affected by current climate change; (ii) hydropower generation systems, as hydroelectric reservoirs are susceptible to droughts that reduce their water storage, and high temperatures that increase evaporation rates; and even (iii) photovoltaic energy is susceptible to weather conditions, as the electricity generation is proportional to the solar radiation flux that reaches the cells, which can be affected by cloudy, rainy or dusty conditions during daylight hours (Drewing & Lanavère, 2021; Enríquez et al., 2020). The demand for parametric insurance for renewable energy is likely to grow with continued expansion of power generation from renewable sources and concerns about weather and climate risks (Enríquez et al., 2020).

In this study, we aim to evaluate the costs and viability of a parametric insurance scheme for renewable energy generation applied to Brazil. Brazil, bestowed with the world's largest fresh water reserves, relies predominantly on hydroelectric power, which accounts for approximately 65% of its energy consumption. However, in recent years, the nation has grappled with adverse impacts of climate change, notably prolonged periods of severe drought (Getirana et al., 2021; Hochberg & Poudineh, 2021; Paim et al., 2019).

One of the main contributors to this, locally and globally, is deforestation. Brazil holds two major biomes, Amazon and Pantanal, which have suffered with wildfires and

deforestation, culminating in adverse modifications on air temperature, humidity, and consequential precipitation patterns. These changes are not restricted to these biomes. The hydroclimate in the south-central region – responsible for most of Brazil's gross domestic product (GDP) –, for instance, is partly controlled by moisture transfer from the rainforest. Almost one-quarter of Brazil's GDP comes from agriculture and livestock. One of the major exporters of soy, coffee and sugar cane, among other primary products, Brazil's economy highly depends on water (Getirana et al., 2021; Silva et al., 2022).

Regarding the energy generation, the country has the world's second-largest installed hydropower capacity (behind only China), with Itaipu Power Plant. But, in 2021, river discharges on this powerplant's area have fallen to their lowest levels in 91 years (Getirana et al., 2021). Droughts are not a new problem in Brazil. However, climate change has made them more intense and more frequent (Getirana et al., 2021; Hunt et al., 2018; Paim et al., 2019). There is a high cost in dealing with energy crises resulting from drought, as thermoelectric power plants need to be actioned (and besides being more costly, many of them run on fossil fuels, which may worsen global warming) and sometimes even electricity rationing (with possible blackouts) is imposed (Hunt et al., 2018; Paim et al., 2019). These costs hit the consumers by elevating the electricity tariffs and can worsen economic crises already present in the nation (Getirana et al., 2021; Hunt et al., 2018; Paim et al., 2019).

Our study proposes to design a parametric insurance product for Brazilian hydroelectric companies, indexed on Brazil's National Institute of Meteorology (INMET)'s rainfall index, which could improve the companies' operations sustainability and mitigate effects of drought crises. Such financial product will be constructed based on other parametric insurance studies in the literature, using GLM models and also more advanced techniques, such as spatial econometrics and copulas, to determine pricing methods. In the end, we will be able to not only unravel the spatial interdependence between climatic variables and energy generation, but also to elucidate the intricate conditional non-linear dependency structures to different power plant facilities.

2. THEORETICAL BACKGROUND

This chapter is divided in 4 subsections, comprehending (i) the effects of climate change onto the financial sector; (ii) the history, main characteristics and functioning of the Brazilian electric sector; (iii) an overview of non-life insurance pricing in actuarial literature, and; (iv) the historical and most recent applications of weather-index insurance and its pricing methods.

2.1. Climate change and its impact on the financial sector

Within the context of the business community, climate change and the behavior of individuals have become determinant factors in companies' long-term perspectives. After a number of climate related disasters and resulting events, there is a growing pressure for companies to increase their efforts to manage the operational risks and potential liabilities caused by climate change (Mendes-Da-Silva et al., 2021). In an attempt to mitigate climate change's effects, the 2015 Paris Agreement, for instance, introduced a new compliance model, based on National Determined Contributions (NDC), to reduce global greenhouse gases (GHG) emissions (Galletta et al., 2022; C. C. Lee et al., 2022).

Globally, nations are actively collaborating to attain environmental sustainability by implementing diverse strategies for reducing GHG emissions, from cleaner energy sources, such as wind power, photovoltaics and hydropower, to the creation of global carbon trading markets (C. C. Lee et al., 2022). These initiatives are integral to climate finance, a concept that aligns financial systems and sustainability, to foster green growth while concurrently mitigating carbon dioxide emissions. Climate finance is an essential tool in addressing climate change and has regained prominence as a top priority in international climate negotiations (C. C. Lee et al., 2022).

It is now widely accepted that unmitigated climatic change poses serious threats to financial stability and, therefore, is material to central banks and financial supervisors' mandates (Campiglio et al., 2018; Chenet et al., 2021). Such recognition was a key catalyst in the creation of the Network for Greening the Financial System (NGFS), an international group of central banks, financial supervisors and observers focused on how financial policy needs to adjust to the risks posed by climate change and the low-carbon transition (Chenet et al., 2021).

An example of the effect of climate change onto the financial sector is that the increase in climate-induced physical risks (e.g., heatwaves and floods) directly affects insurers. Uninsured risks may harm the financial situation of households and businesses, resulting in potential losses for the banks that serve them (Campiglio et al., 2018). Thus, climate change poses new challenges and opportunities for insurers (and actuaries) as stakeholders demand that insurance solutions go beyond traditional risk transfer to explicitly address climate risk adaptation and seize new opportunities, providing aid for companies to adapt to this new climate scenario (Can & Musulin, 2023).

In 2020, the Australian Institute of Actuaries released an information note for its members with recommendations on actuarial practices, including Enterprise Risk Management (ERM) related to climate change issues (Actuaries Institute Australia, 2020). Figure 1, extracted from this information note, illustrates the impact of climate-related risks on diverse insurance processes within financial institutions.

Figure 1. Climate-Related Risks and Insurance Processes

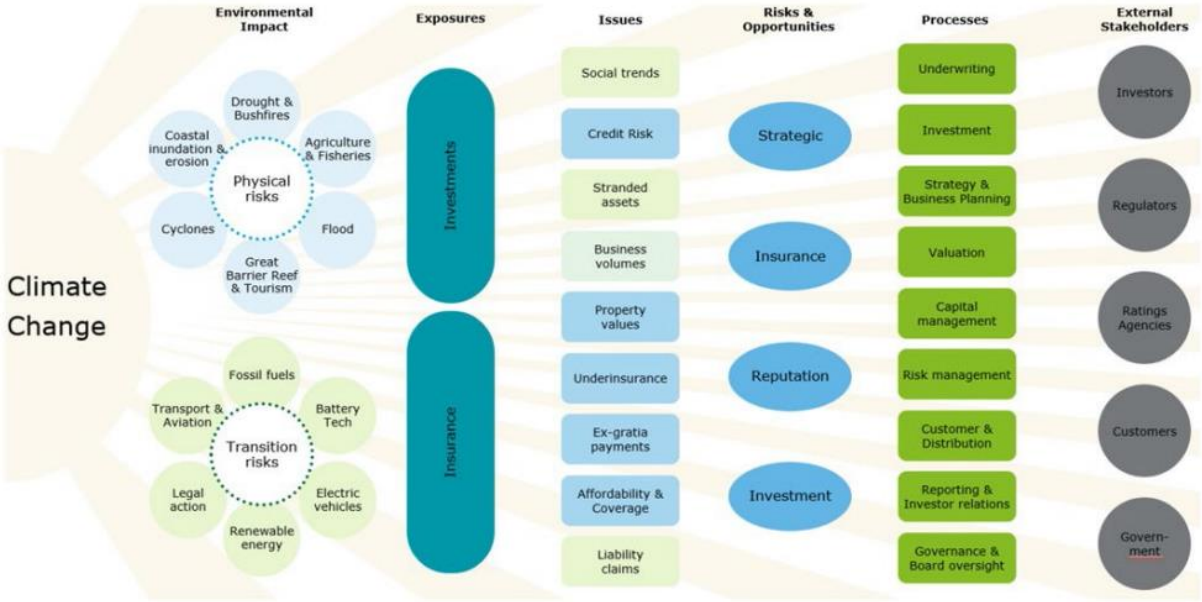

Source: Actuaries Institute Australia (2020).

Figure 1 depicts the extensive influence of climate change on insurance procedures, encompassing property and casualty, life and pension products, as well as external stakeholders associated with insurance companies. Climate-related financial risks (CRFR) comprehend physical, transition and liability risks (Bolton et al., 2020; Chenet et al., 2021). Distinguished by their profound reach, unpredictable character, and irreversibility, climate-related financial risks, CRFR are endogenous and systemic in nature, with the potential to affect entire economies and financial systems (Chenet et al., 2021). Government climate policies alone might not prevent financial instability during the transition., and, in fact, if implemented too abruptly and without the adequate safeguards, they might increase transition risks (Campiglio et al., 2018).

A key obstacle to the achievement of a smooth low-carbon transition is the limited awareness among companies and investors regarding their exposure to CRFR. Most companies are not used to assessing the impact of these risks on their business models, while most investors are unaware of how exposed their portfolios are. Hence, despite CRFR unique characteristics, the emerging policy framework for addressing them has largely focused on market-oriented solutions which seek to reduce perceived information deficits. These solutions include disclosure, transparency, scenario analysis and stress testing (Campiglio et al., 2018; Chenet et al., 2021).

The International Integrated Reporting Council (IIRC) was established in 2010 to lay the foundations for the development of integrated reporting (IR) principles (Havlová, 2015). Its primary objective is to issue IR standards for global adoption by companies, thereby providing enhanced clarity in disclosures for users.

Havlová (2015) focuses on the early adopters of IR and investigates how the reporting changed since its adoption. The author shows that the most relevant information included in IR relate to environment, safety, employees' welfare, community engagement, and corporate governance, all of which align with Environmental, Social and Governance (ESG) dynamics. Furthermore, accordingly to Chen et al. (2022), climate change crises accelerated ESG promotion.

ESG principles are important drivers of financial actors' decisions regarding sustainable finance. This concept and its implications have been extensively discussed in the

academic literature and by market players and regulators, especially in the banking industry (Galletta et al., 2022).

Galletta et al. (2022) conducted a bibliometric analysis regarding ESG in the financial sector on 271 publications over the 1986-2021 period. It is pointed out that the literature has increased considerably over the last decade, and scholars have mainly focused on the social dimension of ESG. It seems to exist a gap on the environmental issue, as only in more recent years it has been investigated as a new direction of studies in the banking sector. These studies are motived by the recent regulators' actions towards green finance sustainability.

Several studies on ESG dynamics can be cited in 2022 alone. Cankaya & Naeem (2022), Chen et al. (2022), Escobar-Anel (2022), Ford et al. (2022), Lai & Zhang (2022), Liu et al. (2022), Lööf et al. (2022), Prol & Kim (2022), Shanaev & Ghimire (2022), Shin et al. (2022), Umar et al. (2022) and Wen et al. (2022) analyze the impacts of ESG information on investors, stock returns or the investments that companies receive. Generally, companies with better ESG rates receive more investments or are perceived in a more optimistic way by investors. Besides that, when testing the relation between ESG factors and short-term investor sentiment in USA, Ford et al. (2022) reveal that only the environmental and ESG controversies scores are significant factors in option traders' sentiment, with better scores in these factors significantly improving sentiment. The authors conclude that the most sophisticated investors are considering companies' environmental risks. Prol & Kim (2022) also show that high ESG optimized portfolios have lower volatility (although also lower returns). This is endorsed by Lööf et al. (2022) findings, who also argue that good ESG performance mitigates financial risk.

Besides the investment focus, Fafaliou et al. (2022) argue that ESG reputational risk has a negative impact on firm growth opportunities, mitigating market longevity. To show that, the author uses a panel dataset, comprising US firms over the period 2007-2019 . They conduct dynamic empirical analysis to quantitatively assess the connections between firms' ESG reputational risk and their market sustainability. M. T. Lee et al. (2022) show that firms use ESG achievements as a means of brand valuation. The brands signal to consumers by communicating advertising spending, research and development investments, social media participation and ESG reputation (M. T. Lee et al., 2022).

Q. Huang et al. (2022) examine how natural disasters affect the ESG disclosure policies of firms located close to disaster areas. Their research focuses on companies situated in areas adjacent to regions affected by natural disasters. As a general trend, these companies enhance their ESG disclosure transparency in the aftermath of such disasters. The changes in disclosure transparency after the disasters are consistent with managers increasing their preference for transparency as their risk salience increases.

Tan & Zhu (2022) investigate how ESG ratings affect corporate green innovation based on data relating to Chinese A-share listed companies between 2010-2018. The results show that ESG ratings significantly promote the quantity and quality of corporate green innovation, alleviate financial constraints, and increase managers' environmental awareness. In this context, the higher the ESG rating score, the more pronounced the promotion effect.

Mu et al. (2023) investigate the effect of digital finance on corporate ESG, using a large sample of Chinese listed firms over the period 2011-2020. The authors found that digital finance positively affects corporate ESG performance, and digital finance enhances the ESG by mitigating corporate financial constraints. On a related matter, D. Zhang et al. (2022) estimate the impact of green finance and digital finance on environmental protection throughout a quantile regression model. The findings reveal that environmental CO2 emissions decrease due to green finance, renewable energy investment, and technological

innovation, whereas CO2 emissions are increased by factors such as economic growth, energy consumption, trade, and foreign direct investment.

Martins (2022) investigates how competition affects firms' ESG practices in 22 emerging markets, using the difference-in-differences technique and matched samples, from 2011 to 2019. The results suggest that firms in emerging markets adjust ESG practices negatively after a shock in competition, contrasting with previous results from developed economies. Pineau et al. (2022) analyze the importance of ESG factors in sovereign credit ratings, by using a data-driven methodology. By employing a statistical shadow rating model, the authors compute variable importance scores to explore the relative importance of ESG and non-ESG factors in sovereign creditworthiness assessment. They found that the importance of ESG factors is different in emerging markets and developing economies (EMDEs) and in advanced economies (AEs): governance is the most important factor for AEs and non-ESG factors drive the creditworthiness of EMDEs.

Focusing on the banking sector, Citterio & King (2023) use a sample of 362 American and European commercial banks, from 2012 to 2019. They construct a predictive model for bank financial distress and subsequently assess the influence of ESG indicators on its predictive performance. The outcomes highlight that ESG factors enhance the model's accuracy in correctly identifying distressed banks and significantly reduce the chances of misclassifying distressed or defaulted banks as healthy.

Agnese & Giacomini (2023) analyze whether ESG factors affect the pricing of bank bonds in the primary market. Using a dataset of fixed-rate senior bonds issued by 63 EU banks between 2006-2021, they find that, *caeteris paribus*, banks with higher ESG scores benefit from lower issuance costs. In accordance with Galletta et al. (2022), these results are not driven by the environmental friendliness of the issuer, but are rather attributed to robust corporate governance standards, ESG reporting and transparency practices.

Finally, ESG inherently impacts the energy sector, driving investments away from conventional energy sources towards renewables, as heightened global awareness of climate risks takes hold (Kumar, 2023). Boldeanu et al. (2022) show that, for renewable electricity companies, returns are positively impacted by the environmental and social ESG scores, while governance favors traditional energy sources companies. Recent crises have further accelerated this investment shift. For instance, following the Russian invasion of Ukraine, European stocks linked to the low-carbon transition witnessed gains, reflecting market expectations of more robust policy measures in favor of renewable energy sources. This response was prompted by Europe's increased dependence on Russian oil and gas (Deng et al., 2022).

2.2. The Brazilian electric sector

2.2.1. The Brazilian electricity sector's history and the role of hydroelectric powerplants

Electrification in Brazil traces its origins back to the last quarter of the 19th century and is intricately linked with the nation's geographical features. The plateau relief and abundant rainfall created favorable conditions for substantial investments in hydroelectric power. Initially, national companies supplied energy with imported technology (Cataia, 2019).

In a still predominantly agrarian nation with sparse population density, the introduction of electricity was a gradual and uneven process. The primary needs revolved around lighting services, public transportation, and power for nascent industries (Carneiro, 2000). Throughout the beginning of the 20th century, there was an upsurge in the expansion of electricity services, marked by the establishment of numerous energy companies,

encompassing both domestic and international investments, envisioning the industrial development (Cataia, 2019).

Throughout the entirety of the 20th century, the hydroelectric model was dominant, even though it coexisted with thermoelectric power stations, with diversification beginning only in the 21st century (Carneiro, 2000). Initially, the generation and consumption of electricity were local and predominantly within major cities, often state capitals, along the Atlantic coast of the country (Cataia, 2019). It was not until the 1960s that long distances electric power transmission lines were established. This marked the transition from decentralized systems to the formation of a National Interconnected System (SIN), enabling energy generation at one location and its widespread distribution throughout the territory (Hermes de Araújo, 2006).

Originally under complete state control, the sector underwent a substantial wave of privatizations during the 1990s, in line with the prevailing neoliberal policy stance of the government at that time (Campos et al., 2020; Hochberg & Poudineh, 2021). Nevertheless, diminished investment yields, coupled with uncertainties surrounding the energy market and the currency devaluation that occurred towards the end of the decade, posed obstacles to the continued expansion of this model. This led to a mismatch between the growing demand and the available supply, ultimately culminating in an energy crisis. The situation was further exacerbated by fluctuations in the dollar exchange rates, which escalated operational costs for many electric companies, particularly those reliant on natural gas, like thermoelectric plants (Campos et al., 2020).

In 2002-2003, with a change of government, the electrical sector underwent a reform, which saw the State, previously relegated to a regulatory role, assuming a more active role, especially regarding the market expansion planning and monitoring. The National System Operator (ONS) became responsible for the operational planning, programming, and dispatching of the generation and transmission activities across the entire interconnected system of a competitive market (Campos et al., 2020; Hermes de Araújo, 2006). Brazil’s electricity policy has since focused primarily on the security of supply and, to some extent, cost efficiency, which is pursued through a combination of auctions, long-term contracts, and central coordination mechanisms (Hochberg & Poudineh, 2021). The energy distribution is negotiated through auctions in which investors submitted energy price proposals for government projects' included plants, with the lowest rate securing the auction (Campos et al., 2020; Hochberg & Poudineh, 2021). Additionally, Brazil incorporated a bilateral market (ACL) within its auction system, allowing industries and large corporations to directly negotiate their electricity purchases with electricity suppliers. The Brazilian electricity auction system is schematized in Figure 2.

Figure 2. Brazil's market design for long-term electricity auctions

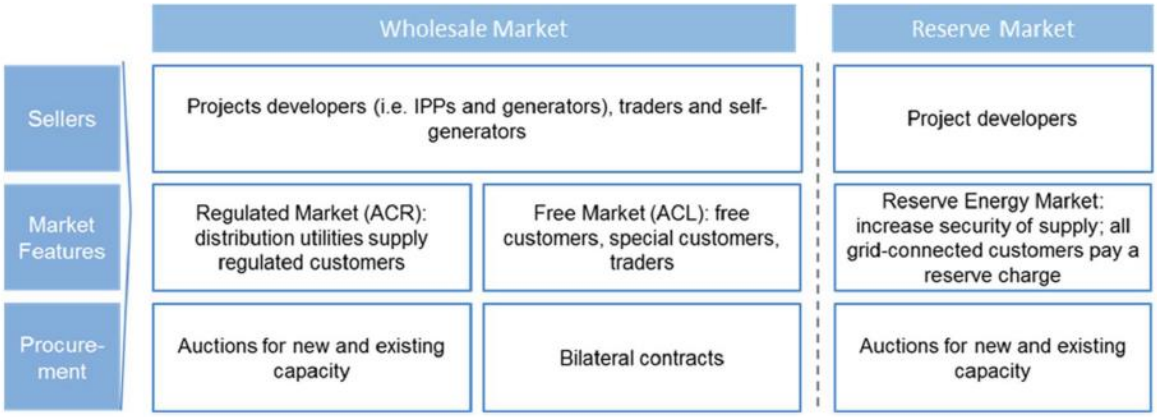

Source: Hochberg & Poudineh (2021).

According to Hochberg & Poudineh (2021), auctions achieve efficiency and maximize social welfare, and have become the mainstay of power generation capacity development in Brazil. The country was among the early adopters, introducing both general electrical power auctions in 2004 and renewable-specific auctions in 2007, effectively replacing its feed-in tariff (FiT) . Tolmasquim et al. (2021) also examined the Brazilian experience with auction design for integrating renewable energy sources, highlighting it as a successful model now embraced globally. In Brazil, the government maintains a pivotal role in the electricity market by specifying critical auction parameters, including eligible technologies, procurement volume, and contract duration (Hochberg & Poudineh, 2021).

Furthermore, Hochberg & Poudineh (2021) provide a comprehensive overview of the current workings of the Brazilian electricity sector. While the auction system proves its efficiency, they contend that the present market architecture may not be the optimal long-term solution for a sustainable market. Their argument is based on several considerations, including the neglect of consumer preferences in influencing investment decisions, the transfer of risks to consumers, a diminished significance of the short-term market and complications stemming from regulatory and design complexities.

2.2.2. Main characteristics and Regulatory Frameworks of the Brazilian Electrical System

The Brazilian electricity system is the 9th largest globally and is the most extensive in Latin America. As of 2020, Brazil's installed capacity was distributed as follows: 62% hydro, 25% thermal generation, 10% wind, 2% solar, and 1% nuclear (Hochberg & Poudineh, 2021). Figure 3 displays a map of Brazilian transmission lines originating from the SIN, offering a visual representation of the scale and interconnectivity of the country's electrical network. Notably, Brazil hosts three of the world's longest power transmission lines[12].

[1] https://www.power-technology.com/features/featurethe-worlds-longest-power-transmission-lines-4167964/?cf-view&cf-closed
[2] https://www.statista.com/statistics/1305820/longest-power-transmission-lines-worldwide/

Figure 3. Brazil's Power Transmission Lines: 2024 Horizon

Source: (ONS & SIN, n.d.)

Notable among the primary hydroelectric plants in the country are those situated in the Paraná River basin, including Itaipu, the largest hydroelectric plant in Brazil and the second largest globally. Additionally, plants like Ilha Solteira and Jupiá have made significant contributions to Brazil's energy matrix (Bentemuller, 2018). Furthermore, within the Tocantins-Araguaia basin, powerhouses like Tucuruí and Belo Monte hold substantial generation capacities and serve as pivotal contributors to both regional and national energy supplies (Falcão et al., 2019).

There are mainly two types of hydroelectric powerplants: (i) run-of-river powerplants and (ii) water storage powerplants. The first type takes advantage of the natural flow of a watercourse, positioned on two different levels. Water is collected and routed through a channel equipped with a filtering grid to remove solid materials, such as debris, before flowing into a reservoir. It then descends a slope through a pressurized pipeline, reaching the power plant's turbine chamber. Here, it drives a turbine, which rotates due to the force of the flowing water. A generator, connected directly to the turbine shaft, converts the mechanical energy into electrical power. Subsequently, the water is channeled into a drainage conduit and returned to the watercourse. The output of run-of-river powerplants is contingent on the flow rate of the watercourse and the height differential between the water's intake and discharge points (Enel Green Power, n.d.).

The second type involves the storage of water in reservoirs, which can be of natural or artificial origin, allowing for more control over electricity generation by adjusting the water release and flow through the turbines. The water is routed to the dam used to store water at higher altitudes. After that, the process is similar to run-of-river powerplants. The water is removed from the reservoir and taken through a system of pipelines to the turbine, which will generate energy, then it goes into a drainage channel and is reintroduced into the watercourse. When power demand is high, water is released from the reservoir to generate electricity, and

during low-demand periods, excess energy can be used to pump water back into the reservoir, acting as a form of energy storage. This approach offers greater flexibility in managing electricity supply according to needs, at certain times of the day or at certain times of the year. Because of that, they are also known as regulated flow hydroelectric plants (Enel Green Power, n.d.).

Hydroelectricity stands as a vital renewable technology, making a significant contribution to grid regulation. It has the capability to swiftly and effectively respond to fluctuations in electricity demand, facilitated by water storage powerplants that enable the control of flow intensity from the reservoir (Enel Green Power, n.d.; Gonçalves & Mueller, 2019). Figure 4 illustrates the two types of hydroelectric powerplants.

Figure 4. Illustration of hydroelectric powerplants

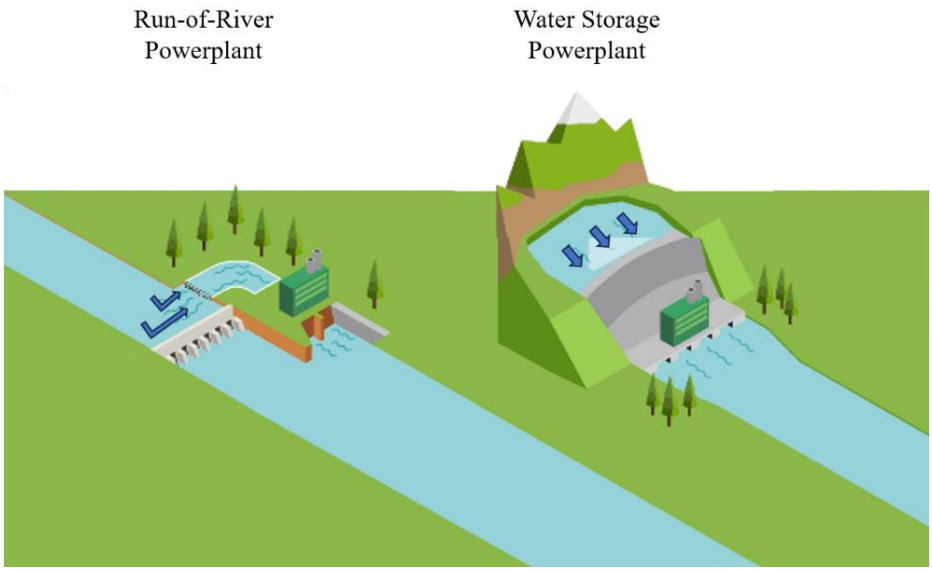

Source: (Enel Green Power, n.d.)

Policies and regulatory frameworks have played a fundamental role in stimulating the Brazilian energy sector's development. These evolving policies have consistently aimed to promote the expansion and utilization of the nation's abundant hydroelectric potential, all while ensuring a sustainable and reliable electricity supply in response to the escalating energy demand (Cataia, 2019; Hochberg & Poudineh, 2021).

One of the central policies and regulatory frameworks in this sector was the establishment of the National Electric Energy Agency (ANEEL) in 1996. ANEEL holds a central position in the sector, as it is tasked with regulating and overseeing the entire electricity industry. This includes setting the rules and guidelines governing power plant operation, concessions, and bidding processes. Moreover, ANEEL defines the technical and environmental criteria for the establishment and operation of these plants, contributing significantly to the sector's management and sustainability (Golfetto, 2023; Hermes de Araújo, 2006).

Laws 8987/1995, 9074/1995, 9427/1996, 9648/1998 and 2655/1998 played a relevant role in shaping the norms for the granting and extension of concessions and permissions for public services, encompassing energy generation and transmission contracts (Ganim, 2009; Mayon & Parodi, 2018). Notably, Law 9648/1998 was responsible for establishing the ONS, which holds the mandate to coordinate and oversee the operation of electricity generation and

transmission within the SIN. This oversight and regulation fall under the purview of ANEEL (Ganim, 2009).

Another important milestone was the creation of the Program for Incenting Alternative Sources of Electric Energy (PROINFA), in 2002 (Clauberg et al., 2021; Gonçalves & Mueller, 2019). The PROINFA program was initiated with the aim of promoting the utilization of renewable energy sources through the provision of financial and tariff incentives. It was conceived in response to the energy crises of 1999-2001 as a means to mitigate hydrological risk, thereby encouraging the growth of smaller hydroelectric projects, known as PCH, and alternative sources like wind power plants. This initiative effectively facilitated the diversification of the energy matrix and made a significant contribution to the sector's sustainability (Clauberg et al., 2021; Ganim, 2009; Gonçalves & Mueller, 2019).

These regulatory frameworks provided a favorable environment for the development of Brazil's energy sector, encouraging investments and guaranteeing the necessary legal security for the implementation of the powerplants, transmission and distribution projects. The creation of bidding mechanisms, auctions and concessions was also essential for attracting investors and making these projects economically viable (Gonçalves & Mueller, 2019; Hochberg & Poudineh, 2021; Melo et al., 2019).

Regarding recent policies, Costa, Capaz, et al. (2022) model the possible long-term consequences of a recently approved law (Ordinary Law 14300/2022) for regulating on-grid renewable distributed generation in Brazil. This new law states that compensation for electricity injected into the grid by prosumers will no longer be 100%, to safeguard distribution companies and conventional consumers. The results show that the new law successfully mitigates tariff increases and reduces social inequality, which are its main goals. However, it shows negative implications to the decentralized generation business, market welfare, and the environment.

Also, Costa, Bonatto, et al. (2022) propose an optimization of energy tariff pricing in Brazil. The existing tariff model, designed for fixed rates and grids lacking distributed energy resources, is now being reimagined. The proposed model incorporates static time-of-use rates, distributed generation, and energy storage, thus enabling optimization of the regulated electricity market. A significant policy insight from this study is the potential to reduce the compensation parameter once distributed generation and energy storage systems become established in the market. This approach helps avert tariff increases, safeguards traditional consumers, aligns with societal interests, and aligns with the Ordinary Law 14300/2022 analyzed by Costa, Capaz, et al. (2022).

Public policies and regulations aimed at hydrological risk management play a key role in promoting water security and reducing the impacts associated with extreme events by establishing guidelines and rules for the operation of hydroelectric plants, reservoir management and monitoring of water resources (Assed & Assed, 2020; Esposito, 2018; Melo et al., 2019; Mendes et al., 2016). These regulations can address aspects such as defining the rules for operating reservoirs, safety criteria and sizing of hydraulic structures, sharing costs and benefits, and establishing contingency policies to face extreme events. The implementation and compliance with these regulations are essential to ensure water security and the reduction of hydrological risks (Assed & Assed, 2020; Melo et al., 2019).

It is important to highlight that coordination between the different levels of government, such as federal, state and municipal, is fundamental for the success of public policies and regulations related to hydrological risk management. The harmonization of strategies and the exchange of information between the different agents are essential to ensure an integrated and effective approach (Bentemuller, 2018; Mayon & Parodi, 2018).

2.2.3. Hydrological Risk and the Energy Reallocation Mechanism

Historically, Brazil has had a strong dependence on hydroelectric generation, which is partly due to the abundance of water resources in its territory. From the inception of Brazil's electricity matrix, hydroelectric plants have been responsible for a significant portion of energy generation, reaching high levels in relation to other sources. This scenario is the result of both the available hydroelectric potential and the incentive policies and investments made in the sector (Assed & Assed, 2020).

The contribution of hydroelectric plants to the stability and reliability of the electrical system is still central in Brazil's energy context. These plants play a key role in ensuring the continuous supply of electricity, acting as a reliable and stable source of generation. Its quick and flexible response capacity to changes in demand and operational contingencies (for instance, with water storage capacity) gives it a significant advantage for balancing the electrical system (Golfetto, 2023).

Hydroelectric plants' rapid response capacity allows efficient control of the generation frequency, keeping it within established limits. This is fundamental to avoid unwanted oscillations in the electrical network, guaranteeing the operational stability of the system (Gonçalves & Mueller, 2019). These plants are designed and built to operate for many decades, with proper maintenance and continuous monitoring. This operational reliability is crucial for the availability of electrical energy in a consistent and safe way, reducing the probability of supply interruptions (Mayon & Parodi, 2018).

However, it is important to point out that the percentage of energy generated from hydroelectric plants is subject to fluctuations over time, varying accordingly to hydrological conditions, and may be influenced by climatic factors, such as rains and droughts, as well as the installed capacity and operation of the plants (Assed & Assed, 2020; Getirana et al., 2021).

It is noteworthy that, although hydroelectric plants have advantages in terms of stability and reliability of the electrical system, their socio-environmental impacts and the challenges related to hydrological variability must be taken into account. Relying exclusively on hydroelectric plants can expose the electrical system to vulnerabilities in the face of extreme events or climate changes (Melo et al., 2019; Paim et al., 2019).

Hydrological risks refer to issues related to the volume and/or quality of the water, which affect the operation of hydroelectric powerplants (Paim et al., 2019). For instance, there is the risk of having insufficient water supply to support expected levels of electricity generation, carrying the potential for physical, financial, environmental and social impacts (Paim et al., 2019).

Hydrological risk can be mitigated with different approaches. Over the last few decades, there has been a gradual diversification of the Brazilian energy matrix, with greater incentives for alternative energy sources, such as thermal, wind, solar and biomass generation (Esposito, 2018; Melo et al., 2019; Paim et al., 2019). This diversification seeks to reduce the exclusive dependence on hydroelectric plants and to mitigate the risks associated with hydrological variations, including extended dry spells. This strategy aims to ensure the long-term stability and reliability of the electrical system (Clauberg et al., 2021; Esposito, 2018; Paim et al., 2019).

Maestri & Andrade (2022) analyze the Brazilian electricity industry's history, focusing on the centralization of the energy generation, and arguing the need for expanding decentralized generation (DG). The benefits of DG expansion, according to the authors, are (i) the decentralization of the electricity market; (ii) the diversification of the electrical/energy

matrix; (iii) the expansion of electricity supply and GDP growth; and (iv) the reliability in the electricity supply, especially during periods of water scarcity, that may compensate the negative impacts of DG in the electricity tariff.

Fridgen et al. (2020) also analyze the effects of decentralization, as renewable energy sources are inherently decentralized and increasingly prioritized by many nations due to climate change concerns. The risk associated with uncertain long-term electricity price trends is generally seen as a hindrance to investments. However, the authors argue that investing in distributed energy resources can actually serve as a form of insurance for consumers against price volatility. This is achieved by enabling prosumers (consumers who also actively generate energy) to become more self-reliant and less susceptible to unpredictable price fluctuations.

It is worth noting that this insurance effect may diminish under certain circumstances. For instance, when a prosumer evolves into a predominant energy producer, they once again face risk in terms of uncertain revenues. Fridgen et al. (2020) underscore that this strategy is advisable once the integration of distributed energy resources reaches a significant level and the market is well-established.

Reducing the vulnerability of the electricity sector to hydrological risk requires the implementation of strategies that aim to minimize the impacts of variations in hydrological conditions and promote security and stability of energy supply (Barroso et al., 2007; Melo et al., 2019; Paim et al., 2019). These strategies involve an integrated approach that ranges from diversifying the energy matrix to improving the management of water resources and strengthening the energy storage systems (Mayon & Parodi, 2018; Melo et al., 2019; Paim et al., 2019).

Brazil has designed its own regulatory mechanism known as the Energy Reallocation Mechanism (MRE). This framework is designed to apportion hydrological risks among energy generators, facilitating more effective management of water reservoir levels and mitigating the financial vulnerability of energy producers (Paim et al., 2019).

In order to sell energy on the SIN, generators are required to hold a Physical Guarantee (PG) certificate. This certificate denotes the maximum volume of energy that each enterprise can commit to supply through electricity sales contracts, serving as a representation of a power plant's contribution to the system's security of supply (CCEE, 2023; Leonel et al., 2019).

The calculation of a powerplant's PG stems from the apportionment of the system's PG. The system's PG is established as the maximum annual average demand that a specific set of generators (both hydro and thermal) can meet while adhering to economic supply criteria. This alignment occurs when the anticipated operation marginal cost is equal to the expansion marginal cost. Furthermore, the system must uphold a 5% threshold for the annual deficit risk in each subsystem (CCEE, 2023; Leonel et al., 2019). Evaluating the connection between the energy production volume and the PG of each plant involves a metric known as Generation Scaling Factor (GSF), which operates as an adjustment factor in MRE calculations (Bentemuller, 2018; Paim et al., 2019).

If the computed GFS exceeds 100% (indicating more energy produced than the physical guarantees), each plant will be able to sell its surplus energy in the Short-Term Market. Conversely, if the GSF falls below 100%, the hydroelectric plants must acquire energy from the Short-Term Market, proportionally to their physical guarantee and the energy produced by all plants (Bentemuller, 2018).

The MRE operates through sharing hydrological risks among the participating powerplants. Each powerplant contributes with a portion of its energy PG to form an aggregate called the energy surplus. This surplus is then used to offset any generation shortfalls in other participating hydroelectric plants due to adverse hydrological conditions. In essence, plants generating in excess of their PG transfer the surplus to those generating below their PG, thereby minimizing the overall impact of hydrological variations on the system as a whole (CCEE, 2023; Ferreira et al., 2015).

It is important to point out that the MRE serves as an accounting mechanism, intended to promote the financial sharing of hydrological risk by creating an accounting portfolio of hydroelectric production. This portfolio leverages the diversity of hydrological patterns in Brazilian watersheds. However, it does not function as a tool capable of mitigating systemic risk; its primary role is to reduce the volatility to which an individual hydroelectric generator is exposed (CCEE, 2023; Paim et al., 2019).

During periods of water scarcity, when hydroelectric power plants cannot meet the energy demand, other sources, typically thermoelectric power plants, are required to compensate. This, unfortunately, incurs a significant economic cost as energy tariffs rise, and these thermoelectric plants rely on fossil fuels, which can exacerbate climate-related challenges (Getirana et al., 2021; Hunt et al., 2018; Paim et al., 2019).

By sharing risks among the participating plants, MRE mitigates the negative impacts arising from unfavorable hydrological conditions, such as drought or heavy rainfall periods (Gonçalves & Mueller, 2019). Its core objective is to minimize the financial repercussions resulting from fluctuations in energy generation, thereby enhancing the predictability of the financial outcomes for the plants and facilitating more effective management of the electricity sector's resources.

In addition, MRE promotes the stability and security of energy supply, contributing to the sustainability of the sector by averting disruptions in energy provision and reducing the associated environmental and socioeconomic impacts linked to water scarcity scenarios (Pereira et al., 2018). Participation in MRE assures power plants that any generation deficits will be compensated, thereby diminishing exposure to risks and uncertainties. This, in turn, permits more precise planning based on reliable forecasts of hydroelectric power generation. The security afforded by MRE enhances the overall stability and efficiency of the electrical system (Leonel et al., 2019).

A key feature of MRE is the so-called Reserve Energy Account, a record that tracks the energy surpluses and deficits of the participating plants. This account is regularly updated to compute the financial outcomes of the mechanism. In essence, it establishes the financial sums that powerplants must either pay or receive as a result of hydrological discrepancies that have occurred (Pereira et al., 2018). This calculation incorporates various factors, including water availability, the generation capacity of each plant and the electrical system's demand (Pereira et al., 2018).

In summary, the MRE process can be described as follows (Melo et al., 2019):

(1) For each subsystem, the generation surplus/deficit is determined by comparing the total hydroelectricity production with the total physical guarantee;

(2) In each subsystem with surplus generation, the deficit hydropower generators will receive "electricity rights" from the hydropower generators with surplus generation. After that, the subsystem's remaining surplus will be allocated to offset deficits in other subsystems;

(3) If the system's total hydroelectric generation is greater than the total physical guarantee, the difference is allocated among all the powerplants in the system, proportionally to their individual physical guarantee.

When a powerplant participant in the MRE process is unable to fulfill its contracted energy supply, it must purchase the shortfall electricity from the Short-Term Market. This transaction is subject to the payment of the Settlement Price for Differences (PLD), which is designed to mirror the market equilibrium price (Bentemuller, 2018). The Short-Term Market acts as a financial platform involving energy producers, suppliers, and free consumers. Here, energy producers hold credit, while energy consumers settle their debts, with the aim of achieving a zero balance at the conclusion of operations, except for cases of direct contracting (Bentemuller, 2018).

MRE undergoes periodic adjustments and revisions aimed at enhancing its efficiency and aligning with shifts in the electricity sector. These adaptations may be necessary to accommodate evolving hydrological conditions, modifications in the energy matrix, or shifts in government policies (Gonçalves & Mueller, 2019).

The implementation of MRE in the Brazilian electricity sector is not free of challenges and criticism, which arise due to the complexity and operational aspects of this mechanism (Golfetto, 2023). A primary challenge is related to hydrological variability and the inherent uncertainties in power generation forecasts. Relying on climatic conditions and water resources can lead to substantial disparities between anticipated and actual hydroelectric power generation. These discrepancies can impact the distribution of hydrological risks among the participating plants, requiring adjustments and adaptations in the mechanism (Golfetto, 2023).

Another issue concerns the definition of rules and criteria, which must be clear, transparent, and balanced. The definition of how energy surpluses and deficits are calculated and the procedures for financial compensation are crucial aspects for the effectiveness and reliability of the mechanism. The rules should be impartial and consistent, considering the specific characteristics of the participating plants and the regional hydrological conditions (Golfetto, 2023).

In addition to operational challenges, it also faces criticism related to its ability to ensure an equitable distribution of risks among participating powerplants (Mayon & Parodi, 2018). Some argue that plants with greater water storage capacity have a competitive advantage over plants with lower capacity, resulting in an asymmetrical distribution of MRE benefits and burdens. This asymmetry can generate distortions and imbalances between plants, requiring a review and improvement of the mechanism's rules (Mayon & Parodi, 2018).

Another common criticism is related to Brazil's high dependence on hydroelectric plants (Paim et al., 2019). Some experts argue that diversifying the energy matrix is essential to reduce the vulnerability of the electrical system to extreme events, notably extended drought. An overdependence on hydroelectric power plants can expose the system to additional risks, highlighting the importance of increased integration of alternative energy sources such as wind, solar and biomass (Assed & Assed, 2020).

MRE works well in times of typical hydrological patterns, but during severe drought periods it can aggravate financial challenges for some generators, as its design does not incorporate measures to mitigate systemic risk (Bentemuller, 2018; Paim et al., 2019). A pertinent illustration of this scenario unfolded during the hydrological crisis of 2014-2016, one of the greatest in Brazil's history (Bentemuller, 2018).

As previously mentioned, entities unable to produce sufficient energy to fulfill their contractual commitments are subject to the Short-Term Market's PLD, having to bear this additional cost (Bentemuller, 2018). In times of hydrological normality, the PLD cost is relatively lower for those who did not produce enough to meet their contractual obligations. However, during the hydrological crisis, the majority of generators experienced elevated PLD costs since the whole system' electricity generation fell below the levels defined by the GSF mechanism (Bentemuller, 2018). In this scenario, the hydroelectric powerplants were exposed to the Short-Term Market and compelled to buy energy (for instance, from thermal generators or other sources unaffected by the hydrological crisis), at the PLD rates, in order to fulfill their energy sale contracts.

This scenario led to some generators resorting to legal proceedings to request a revision of the GSF. In instances where these claims were granted, resulting in alleviated individual losses, the other participants in MRE were affected, as any debts exceeding the judicially imposed threshold were apportioned among the remaining members of the mechanism. This allocation of losses is necessitated by the requirement for the Short-Term Market to maintain a balanced account where credits and debits are mathematically annulled (Bentemuller, 2018). The financial ramifications extended beyond the generators and impacted consumers through elevated tariffs (Mendes et al., 2016). Given this backdrop, the GSF calculation is a point of criticism on MRE until today.

2.2.4. Necessities and Challenges for the Brazilian Electricity Sector

Examining the electricity sector's exposure to extreme weather events is fundamental for comprehending the risks and vulnerabilities it faces in the context of climate change (Falcão et al., 2019; Paim et al., 2019). This assessment entails an examination of the repercussions of extreme weather events, including storms, droughts and heatwaves, on the electricity generation, transmission and distribution (Falcão et al., 2019; Hochberg & Poudineh, 2021). Moreover, the deployment of climate and impact models on the electricity sector is indispensable for predicting the potential consequences of extreme weather events. These models consider climatic variables like temperature, precipitation and winds, and simulate the impacts of weather events on the electricity supply (Caceres et al., 2021; Fernandes et al., 2019; Lima et al., 2022). This approach facilitates the evaluation of risks linked to various extreme weather events, identifying geographically vulnerable areas and specific infrastructure (Leonel et al., 2019; Maceira et al., 2015). Climate change projections are also important, as they enable the estimation of how these events may evolve in the upcoming decades (Caceres et al., 2021; Domínguez-Tuda & Gutiérrez-Jurado, 2021; C. Zhang et al., 2021).

These projections and analyses are valuable for the strategic planning of the electricity sector, assisting the decision-making process and, for instance, guiding the adoption of risk adaptation and mitigation measures (Caceres et al., 2021). The insights gained from this analysis can contribute to the formulation of public policies to improve the electricity sector's resilience in the face of climate challenges (Caceres et al., 2021; Leonel et al., 2019). Strategies such as investments in infrastructure, diversification of the energy matrix, enhanced management of water resources and the implementation of energy efficiency measures are among the approaches that can be adopted to reduce exposure and mitigate the impacts of these events (Leonel et al., 2019).

Assessing the impacts of supply crises on the electrical system is also essential to understand the consequences and challenges faced during periods of energy shortages (Hunt et al., 2018; Melo et al., 2019). One of the main aspects considered is the energy supply capacity. During a supply crisis, demand may surpass available generation capacity, leading

to interruptions in electricity supply (Campos et al., 2020; Hunt et al., 2018; Melo et al., 2019). These interruptions can have profound impacts on critical sectors including hospitals, industries and public services, with repercussions for the economy and the well-being of the population (Melo et al., 2019). Extended power supply interruptions can also result in substantial economic losses for companies due to reduced productivity, damage to equipment and services disruption, besides potential for reputational damage (Falcão et al., 2019). Furthermore, the use of certain alternative energy sources, such as diesel generators, to meet demand may have adverse environmental implications, including increased GHG emissions and air pollution (Borba et al., 2023; Hunt et al., 2018; Melo et al., 2019; Montoya et al., 2021).

Another important aspect involves the examination of response and recovery mechanisms during supply crises. The response capacity of both private companies and the governmental authorities, demonstrated through emergency measures, such as the mobilization of additional generation resources, use of strategic energy reserves or implementation of rationing plans, can minimize the impacts of crises and expediting the restoration of the electric system (Hunt et al., 2018; Melo et al., 2019).

Additionally, the construction of new powerplants and the expansion of existing ones (such as reforming old hydroelectric facilities) are essential to increase generation capacity, ensure a secure energy supply and diversify the energy matrix. These investments aim to meet the growing demand for electricity, driven by economic growth and the expansion of various economy sectors such as industrial, commercial and real estate (Melo et al., 2019).

Efforts and investments are equally essential in the broader infrastructure of the electricity sector. This includes the development and modernization of the transmission and distribution network, which is crucial for efficiently transporting energy from the powerplants to the final consumers (Barroso et al., 2007). Investments in high voltage transmission lines, substations and monitoring and control systems are essential to guarantee the reliability and stability of the electrical system, as well as to facilitate the integration of new sources of wind, solar and biomass energy (Barroso et al., 2007; Falcão et al., 2019).

This also involves improving environmental licensing processes, defining socio-environmental criteria for the implementation of hydroelectric plants (given their high socioenvironmental impacts, with dam construction that can flood extensive areas, disrupt local ecosystems, and necessitate the relocation of populations) and promoting sustainable practices throughout project development (Bentemuller, 2018; Clauberg et al., 2021). Investment in advanced technologies, such as digitalizing the electrical network and implementing automation and real-time monitoring systems, contribute to operational efficiency and the overall optimization of the electrical system (Bentemuller, 2018; Clauberg et al., 2021).

It is important to emphasize that infrastructure investments and the expansion of the electricity sector require strategic planning, fostered through public-private partnerships and guided by a sustainability-oriented approach. Attracting private investments and ensuring a stable and predictable regulatory environment are essential aspects for securing the necessary investments within this sector (Esposito, 2018; Ferreira et al., 2015; Paim et al., 2019).

Assessing the additional challenges imposed by climate change on hydrological risk management is extremely important to understand the new demands and complexities emerging in this context. Climate change exerts impacts on hydrological patterns, amplifying the uncertainty and variability of events, thereby constituting an extra layer of complexity in the management of water resources (Caceres et al., 2021; Hunt et al., 2018; Paim et al., 2019).

One of the main challenges is the change in rainfall patterns and water availability, potentially resulting in a spatial and temporal redistribution of rainfall, resulting in changes in runoff patterns and aquifer recharge (Borba et al., 2023; Caceres et al., 2021; Wu et al., 2021). This requires a reevaluation of water resource management strategies, including the adoption of conservation practices, storage and efficient use of water, to cope with scarcity in certain regions and the occurrence of extreme events in others (Caceres et al., 2021; Gonçalves & Mueller, 2019).

Climate change also intensifies extreme weather events, contributing to lengthier droughts and more intense rainfall occurrences. This heightened risk increases the potential for floods and landslides (Domínguez-Tuda & Gutiérrez-Jurado, 2021; Paltán et al., 2021; Verma, 2021; W. Zhang et al., 2021). The ability to predict and adapt to these extreme events has become crucial, involving the improvement of early warning systems, the planning of resilient infrastructures and the development of post-disaster recovery strategies (Mayon & Parodi, 2018).

Due to Brazil's high dependency on the hydroelectric system and consequent vulnerability to droughts, exploiting the diversification of its electricity matrix could contribute to reducing hydrological risk (Borba et al., 2023; Nascimento et al., 2022; Paim et al., 2019). Paim et al. (2019) employ Integrated Assessment Modelling (IAM) techniques to access this issue, analyzing future macroeconomic and energy scenarios for Brazil within a global context, aligned with the Brazilian Nationally Determined Contributions under the 2015 Paris Agreement on Climate Change. Their analysis reveals that the addition of non-hydro renewables is advantageous from the perspective of the integrated Water-Energy-Food nexus, as it reduces trade-offs amongst the water and energy sectors.

Furthermore, Pinheiro Neto et al. (2017) show that, in the diversification process, the complementarity between sources helps reducing economic risk. The authors propose a methodology for risk analysis and portfolio optimization of power generation assets with hydro, wind, and solar power. The model, constructed with synthetic time series and Monte Carlo simulation, indicates that the initial correlation between the energy resources is altered by the cash flow model and, more notably, by the debt. An increase in debt augments the correlation, reduces the return and risk and, consequently, affects the diversification process and economic outcomes.

Machado & Bhagwat (2020) investigate the impact of the electricity matrix mix on two existing regulatory frameworks for hydropower remuneration in Brazil, namely MRE and Insurance Call Option Obligation (ICO). In MRE, as previously explained, individual operational risks are mitigated through a risk-sharing principle within a hydro pool structure. ICO, on the other hand, offers an insurance approach allowing hydro generators to transfer their risks to the consumers. The frameworks are assessed across three long-term scenarios, each featuring varying proportions of non-hydro renewables and thermal sources in the electricity matrix, using a SDDP approach. The findings indicate that the composition of the electricity matrix may considerably influence MRE's performance and economic feasibility of hydropower. Moreover, ICO's design may lead to an overall improvement in the market level welfare when compared to the MRE if a criterion of equivalent welfares (ensuring the same expected results for both generators and consumers) is established as a preferred design goal.

2.3. Non-life insurance pricing

The foundation of modern risk theory can be traced back to the works of Filip Lundberg in 1903 and Harald Cramér in 1930. Lundberg proposed the Poisson process as a solution for the problem of the first passage time. Cramér further expanded on Lundberg's work by modeling the ruin of an insurance company as a first passage time problem (Frees,

2015; Minkova, 2012). These seminal contributions paved the way for the development of the classical risk model (Cramér-Lundberg), which is a pillar of non-life insurance mathematics, and has been extensively treated in the literature (Bergel et al., 2013; Minkova, 2012). The Cramér-Lundberg model assumes that a given surplus process has constant deterministic gains (premiums) and random losses (claims) which occur at random times (Bergel et al., 2013; Frees, 2015).

When we acknowledge Cramér-Lundberg as one of the foundations of actuarial science, it is clear how insurance pricing takes an important role in this field, as it defines the premium, a vital part of the model. The fundamental premise underlying premium calculation is that insurance premiums should be set in a way that balances the risk associated with the potential occurrence of an adverse event covered by the policy. In other words, policyholders pay prices that correspond to the expected value of the insurance benefits, or the anticipated losses (Jha, 2012). This concept is known as actuarially fair price, which accounts for the entire insurance risk pool rather than individual risks, aligning with the principle of mutualism, a mechanism for sharing risk. Consequently, this calculation is founded on the principles of collective risk theory (Cummins, 1991; Vaughan & Vaughan, 2008).

Therefore, as premiums should match expected losses, one of the main components of this calculation is the distribution of aggregate claims. This concept can be defined as it follows (Bowers et al., 1987):

Let X_1 denote the amount of the first claim, X_k the amount of the k-th claim:

$$S = X_1 + X_2 + \cdots + X_k + \cdots + X_N$$

$$S = \begin{cases} 0, & N = 0 \\ \sum_{i=1}^{N} X_i, & N > 0 \end{cases} \quad (1)$$

S represents the aggregate claims generated by the portfolio for the period under study. The number of claims, N, is a random variable and it is associated with the frequency of claims. The individual claim amounts X_1, X_2… are also random variables, measuring the severity of claims, and are assumed to be independent and identically distributed.

Now let p_x denote the common distribution function of the X's.

$$p_k = E[X^k] \quad (2)$$

It can be deduced (Bowers et al., 1987) that:

$$E[S] = E\big[E[S|N]\big] = E[p_1 N] = p_1 E[N] \quad (3)$$

and

$$Var[S] = E\big[Var[S|N]\big] + Var\big[E[S|N]\big] = E[N]Var[X] + p_1^2 Var[N] \quad (4)$$

Meaning that the expected value of aggregate claims is the product of the expected individual claim amount and the expected number of claims, while the variance of claims is the sum of the variability of individual claim amounts and the variability of the number of claims.

Therefore, much of insurance pricing resumes in modelling the distribution of aggregate losses, which is usually done based on historical data (Cummins, 1991; Frees, 2015).

Other aspects of pricing include mechanisms of risk reduction (e.g., statistical loading, deductibles, maximum indemnity limits and reinsurance contracts), loading rates (to compensate commercial and administrative expenses, besides taxes and profit margin),

commercial decisions (changes in prices due to market competitiveness) and utility matters (Guelman et al., 2014; Kaas et al., 2008; Laas et al., 2016; Mourdoukoutas et al., 2021; Omerašević & Selimović, 2020; Verschuren, 2022).

The techniques for non-life insurance pricing modelling are constantly evolving. Earlier methods were much simpler and often showed reduced accuracy when compared to the new ones. Chang & Fairley (1979) and Sant (1980) both address the case of automobile insurance in Massachusetts in the 1970's, which was then priced based on a multiplicative method (instead of using the claim experience of combined variables, it was assumed that the claim amount ratios for one variable – e.g. a driver feature, as age – were the same for all classes of the second variable – e.g. driving region, so a specific age would present the same risk for all driving regions. And the claim amount ratios for the second variable were considered the same for all classes of the first variable – driving region risk is constant for all ages. Then a risk relativity would be applied for each class of each variable, and they were multiplied to achieve the final relativity). Both articles conclude that the traditional pricing procedures contained biases that result in overcharging individuals in the highest rated risk classes, in comparison with multivariate statistical analysis. Chang & Fairley (1979) state that the multiplicative method may still perform well when the differences in claim experiences among the classes of the variables of interest are small. However, it becomes an inaccurate estimator of claim amounts when substantial differences are found to exist. Sant (1980) also defends that increased accuracy is obtained from the use of a large data amount in the analysis. Fairley et al. (1981) extended the studies of Chang & Fairley (1979) to the case of New Jersey, and found similar results.

A few years later, Generalized Linear Models (GLM) rose as the main method for non-life insurance pricing estimation, and remain as a standard pricing method to this day (Andersen & Bonat, 2017; David, 2015; Embrechts & Wüthrich, 2022; Jong & Heller, 2008; Karim & Mutaqin, 2020; Laas et al., 2016; Laudagé et al., 2019; Lovick & Lee, 2012; Nielsen, 2010; Ohlsson & Johansson, 2010; Omerašević & Selimović, 2020; Verschuren, 2021; Wuthrich & Buser, 2018). GLM represents an extension of traditional linear models, in which the probability distribution of the dependent variable belongs to the family of exponential distributions (e.g., Normal, Poisson or Gamma). The expectation of the dependent variable is determined by a linear predictor based on nonlinear link function (Omerašević & Selimović, 2020). GLM is versatile and can be used to analyze the claims frequency and severity based on individual data at the insured level. For example, the number of claims in a specific time period can be modeled with a Poisson distribution, while the amount of claims with a Gamma distribution, which is a very common practice in auto insurance (Frees, 2015; Omerašević & Selimović, 2020). One of the reasons for the popularity of this method is its ability to address both frequency and severity effectively. Additionally, a critical requirement for pricing models in insurance is transparency and interpretability, as these models need to be easily explained to all stakeholders. GLM methods excel in providing this feature (Henckaerts et al., 2020).

Two strategies are commonly used to analyze claims distributions: the two-step and the pure premium approaches. While the first decomposes claims cost into a frequency and a severity component, as already exemplified, the latter uses the Tweedie distribution to accommodate the mass probability at zero (Shi et al., 2016). The Tweedie distribution is useful for analyses focused on the indemnifications amount. The Tweedie has a positive mass at zero (representing no claims) and a continuous component for positive values (representing the total amount for one or more claims), being characterized as highly right-skewed distribution, and can be defined as a Poisson sum of Gamma random variables (Denuit et al., 2021; Omerašević & Selimović, 2020; Qian et al., 2016).

Even though GLM methods still predominate in insurance pricing practices, more advanced methods have arisen in the past two decades, with the use of machine learning (Bellapu et al., 2021; Embrechts & Wüthrich, 2022). Shi et al. (2016) propose a copula regression combined with GLM for modelling property-casualty insurance claims. They use the Tweedie double GLM to examine the semi-continuous claim cost of each coverage type, then a Gaussian copula is specified to accommodate the cross-sectional and temporal dependence among the multilevel claims. Estimation and inference are based on the composite likelihood approach and the properties of parameter estimates were investigated through simulation studies. The authors applied their proposed copula model to a portfolio of personal automobile policies from a Canadian insurer, showing that it provides valuable insights to an insurer's claims management process. Wolny-Dominiak & Żædlo (2022) propose a similar model, also combining copulas and Tweedie, and apply it to the Polish insurance market data.

Yeo et al. (2002) proposed a pricing technique that combines clustering and neural networks to achieve an optimal portfolio in automobile insurance. The clustering procedure is used for risk group classification and prediction of claim costs, and the neural networks for predicting retention rates and price sensitivity analysis. The study shows benefits can come from this approach as, for instance, they observed an increase of revenue without affecting the predicted market share.

Henckaerts et al. (2020) predicted both frequency and severity for an insurance portfolio using tree-based Machine Learning (ML) methods (simple regression trees, random forests and boosted trees). The authors found that boosted trees outperform the classical GLMs, allowing the insurer to form profitable portfolios and to prevent against potential adverse risk selection. They also present visualization tools to obtain insights from the resulting models. Bellapu et al. (2021) conducted a similar analysis, starting from simple decision-making trees and developing random and gradient boosting machines to forecast the claims frequency for an all-risk insurance. The proposed gradient boost and random forests models surpass the individual decision trees.

Yu et al. (2021) trained and tested a three-layer backpropagation (BP) neural network model for automobile insurance pricing in China. The results showed the accuracy of the total claim amount prediction by the BP neural network to be over 95%. Then, the predicted total claim amount was used to calculate premiums for five cities in Shandong Province, according to credibility theory. The combination of BP neural network and credibility theory resulted in accurate claim amount estimation and pricing for automobile insurance, presenting itself as a method capable of improving the situation of the automobile insurance business and promoting the development of insurance industry.

Huang & Meng (2020) applied a Bayesian method for insurance pricing, as they argued that traditional parametric models are often inadequate to describe the distribution of losses as they require the data to meet specific distributional assumptions, which are often not well satisfied in complex insurance losses due to the existence of complicated features such as skewness, heavy tail, and multi-modality in non-life insurance. The authors use automobile insurance datasets to develop a Bayesian nonparametric model and compare the results to traditional GLM and ANOVA methods. The empirical results show that the proposed framework characterizes, with more flexibility, the actual loss distribution in the insurance datasets, and presents superior performance regarding the accuracy of data fitting and extrapolating predictions.

Besides the development of pricing methods for traditional insurance, new types of insurance coverages have emerged recently, along with digitalization and insurtechs,

requiring the adaptation of pricing strategies and methods. That is the case, for instance, of cyber insurance, intermittent insurance – also known as pay-as-you-drive (PAYD) when applied in automobile insurance –, and pay-how-you-drive (PHYD) – automobile insurance that offers different prices according to the policyholder's driving habits (Arumugam & Bhargavi, 2019; Ayuso et al., 2014; Biener et al., 2015; Braun & Schreiber, 2017; Corradin et al., 2022; Denuit et al., 2019; Dijksterhuis et al., 2015; Eling & Zhu, 2018; Khakifirooz et al., 2021; Malavasi et al., 2021; Reimers & Shiller, 2019; Stoeckli et al., 2018; Tselentis et al., 2018; Volosovych et al., 2021).

PAYD and PHYD are usually possible through telematics. Telematics is a monitoring technology that can effectively gather useful behavior-risk information, including speed, driving behavior and position parameters, in real-time (Denuit et al., 2019; Khakifirooz et al., 2021). The use of telematics data as a foundation for calculating automobile insurance rates is a developing trend, and, besides enhancing the predictability of future claims, PHYD tariffs offer several benefits, including improvements in driving behavior and mitigating moral hazard (Khakifirooz et al., 2021; Laas et al., 2016; Reimers & Shiller, 2019).

The change that telematics brings to traditional pricing is that the driving-behavior data are collected while the contract is in force, thus falling in the category of *a posteriori* (posterior) information, meaning it becomes available after the contract initiates. Therefore, they must be included in the actuarial pricing by means of credibility updating mechanisms, instead of being incorporated in the score as ordinary *a priori* (prior) observable features (Denuit et al., 2019).

Another challenge for insurers is cyber risk, as it is an emerging dynamic and difficult-to-quantify risk category (Eling & Zhu, 2018). According to Strupczewski (2021, p. 6), cyber risk can be defined as "an operational risk associated with performance of activities in the cyberspace, threatening information assets, ICT resources and technological assets, which may cause material damage to tangible and intangible assets of an organization, business interruption or reputational harm. The term 'cyber risk' also includes physical threats to the ICT resources within organization".

Given this concept's recency, the amplitude of risks it comprehends, and the high potential severity, the understanding, mitigation, reporting, risk management and insurance modeling related to cyber risk are still in early stages of development (Malavasi et al., 2021). There is no unique pricing method for cyber insurance, and a lot still needs to be developed regarding this issue (Eling & Zhu, 2018; Malavasi et al., 2021; Xu & Hua, 2019).

By way of example, Malavasi et al. (2021) found that no OLS-based technique would be able to correctly estimate relevant parameters for a cyber risk model. Thus, combining methods as peaks-over-threshold (POT) and Generalized Additive Models for Location Shape and Scale (GAMLSS) regression may better capture the complex and heterogeneous nature of cyber risk. This approach shows that time trends, as well as influence of factors like company size, business sector and contagion, vary concerning the type of cyber risk, both in terms of frequency and severity.

Xu & Hua (2019) propose a combination of stochastic processes (Markov and non-Markov), copulas and Monte-Carlo simulation to price cyber insurance. Fahrenwaldt et al. (2018) propose a network model based on Markov chains to the same end. Similarly, Antonio et al. (2021) use a Markov-based dynamic model with clustering structure to determine cyber insurance premiums. On another hand, Mukhopadhyay et al. (2013) propose a Copula-aided Bayesian Belief Network (CBBN) model for cyber-vulnerability assessment (C-VA) and expected loss computation. Then they use it as an input to compute the premium that a cyber risk insurer can charge following the concepts of collective risk modeling theory.

Among these emerging types of insurance is Parametric Insurance (Eabrasu, 2021; Lin & Kwon, 2020), object of our study.

2.4. Parametric insurance for climate related issues

In the literature, there is a growing number of instances where Parametric Insurance (PI) has been applied to address climate-related issues, particularly in recent years. Agriculture insurance is one of the most common applications of PI, with the initial parametric schemes primarily designed for this purpose (Horton, 2018). A review conducted by Jibril et al. (2022) examined the literature on weather index insurance for agricultural purposes between 2001 and 2020, analyzing 58 papers that met the review criteria. Their findings highlighted that rainfall and temperature-based indices were the most prevalent, while indices based on droughts, floods, vegetation, soil moisture, humidity, and sunshine hours were relatively underrepresented, despite their potential.

Kusuma, Jackson, & Noy (2018), for instance, developed a model to assess the applicability, feasibility, and estimated cost of implementing a weather-index insurance scheme based on droughts for rice production in Indonesia. They created district-specific indices based on the estimation of Panel Geographically Weighted Regressions models to reduce basis risk and calculated an actuarially robust and welfare-enhancing price for this scheme. It shows effectiveness in some districts, but not in all.

Another applicability of index-based insurance is regarding natural disasters and associated social matters. Linnerooth-Bayer et al. (2009) examined the costs, benefits and risks of public-private insurance programs that offer affordable economic security to vulnerable communities and governments by providing financial security against increasing severity and frequency of weather disasters such as droughts, floods, tropical cyclones, and other forms of weather extremes. As Lin & Kwon (2020) stated, PI can protect vulnerable populations in developing countries against natural disaster and weather risks where traditional insurance is too costly or infeasible, while reducing problems of moral hazard and adverse selection. As a matter of fact, there are 3 major regional parametric insurance schemes that address this issue: the Caribbean Catastrophe Risk Insurance Facility (CCRIF), the African Risk Capacity (ARC) and the Pacific Catastrophe Risk Assessment and Financing Initiative (PCRAFI) (Broberg, 2020; Horton, 2018).

Figueiredo, Martina, Stephenson, & Youngman (2018) proposed a generic probabilistic framework for parametric trigger modeling based on logistic regression and applied it to flood-related disasters in Jamaica, from 1998 to 2016, using gridded precipitation data as the hazard variable. The model has substantial skill at predicting the probability of loss occurrence on each day. They also demonstrated that the system can provide considerable utility to involved parties.

Regarding the energy generation applications, Han et al. (2019) studied the weather risks faced by wind power producers, especially in China, and discuss the feasibility of a wind-power generation index insurance, for which they establish a model. The simulation results show that wind power enterprises can effectively avoid economic losses caused by weather risks through weather index insurance.

Solar geoengineering (SG) entails using technology to modify the Earth's radiative balance to offset some of the climate changes caused by long-lived greenhouse gases. Horton et al. (2021) proposed the use of parametric insurance as a compensation mechanism for SG with the potential to ease disagreements about the technology, and to facilitate cooperative deployment. The plausibility of this mechanism is tested by exploring PCRAFI, a sovereign

risk pool providing parametric insurance coverage against tropical cyclones and earthquakes/tsunamis to Pacific Island countries since 2013.

Boyle et al. (2021) developed an irradiance-based weather derivative to hedge cloud risk for solar energy systems, i.e., a financial instrument tied to an underlying weather variable that act as PI for the contract holder. The design and evaluation of contracts are based on a linear optimization model (LEELO) outputting optimal sizes of solar photovoltaic, battery storage, and power-to-gas systems, as well as the operation of these systems for a given mine's load, irradiance, and technology costs. Their results indicate contracts are effective in cloudier climates with increasing utility for mines installing solar energy systems until the year 2030.

Regarding the applicability of this type of insurance, both Clarke (2016) and Cole, Stein, & Tobacman (2014) studied the demand for index insurance products, which is shown to be fundamentally different from the demand for indemnity insurance products. Enríquez et al. (2020) provided a report describing the characteristics, (dis)advantages, and potential markets for parametric insurance for renewable energy power producers. Their research focuses especially on Central America countries, where are already subjected to large fluctuations in precipitations (causing both floods and droughts), which tend to increase with climate change. The authors analyzed business opportunities, cost, willingness to pay, subsequent willingness to lend/invest, impact on interest rates, bank requirements, bundling feasibility, and insurance companies' willingness to offer parametric insurance.

According to this report, some of the PI main challenges for the renewable energy market are (i) the lack of familiarity with the product from both insurance companies, energy generators and regulators; (ii) premium costs and concerns about the value of parametric insurance relative to the costs of other types of insurance; (iii) inadequate network of local hydrometeorological stations or insufficiently reliable data from the stations; (iv) profitability in small countries' markets, and; (v) legal barriers to entry for transnational reinsurance companies, as this mechanism appears to be a fundamental support for local insurers to be able to provide PI (Enríquez et al., 2020).

The last three points should not be a concern for Brazil, as it is a large country with an energy matrix three times more renewable than the world energy matrix (Montoya et al., 2021), meaning that there is a large market for PI. Also, there is an well-established and resilient (re)insurance market in Brazil (Carvalho & Guimarães, 2023): only in the direct market, there are over 130 insurance companies in more than 100 lines of business (Carvalho & Bonetti, 2023), with the reinsurance companies operating in 19 different non-life lines of business up to 2021 (Song & Carvalho, 2022). Moreover, Brazil's National Institute of Meteorology (INMET) provides highly reliable data. Aguiar & Lobo (2020) showed that monthly rainfall data from Brazilian surface stations managed by INMET are highly correlated with NASA's Prediction of Worldwide Energy Resource online database, as coefficients are between 0.75 and 0.95 for almost all locations, with a p-value under 0.01. Also, simple linear models showed good fit for estimated (satellite) and observed (ground) rainfall relationship data. Therefore, these data may be useful to insurance companies in the developing of parametric insurance products (Rodrigues, 2022).

Regarding the first two points, Enríquez et al. (2020) proposed that insurers can conduct controlled experiments to assess various product specifications and pricing strategies before implementing parametric insurance as a new product line. Additionally, governments and development assistance organizations should consider offering short-term incentives to facilitate market development and assist in disseminating information about how parametric insurance works.

Studies on this subject have typically combined historical observations of a weather-index and the economic outcomes of the insurance product to create actuarial pricing models. The majority of the empirical literature has applied ordinary least square-based correlation or linear regression techniques (Jibril et al., 2022) to determine the insurance premiums. However, some research have shown that the use of more modern methodologies (e.g., neural networks and copulas) can potentially reduce the basis risk, defined as the variance of the policyholder's loss distribution given a specific value of the index (Lin & Kwon, 2020), and improve effectiveness of the model in comparison to simple regressions (Bokusheva, 2018; Cesarini et al., 2021; Pai et al., 2022).

Cesarini et al. (2021) introduce a methodology that leverages ML algorithms (neural network and support vector machines) to identify extreme flood and drought events in the Dominican Republic context. They utilize rainfall and soil moisture data spanning from 2000 to 2019. Their results demonstrate strong improvements compared to baseline logistic regression models, for both hazards.

Additionally, Bokusheva (2018) develops a copula-based design for weather index insurance, highlighting the superior suitability of copulas in modeling tail dependence compared to standard linear correlation. The author employs three Archimedean copulas to capture the left-tail dependence in the joint distribution of wheat yield data and cumulative precipitation. To handle relatively short time series, a hierarchical Bayesian model is applied for obtaining consistent estimates of tail dependence. The study shows that copula-based weather insurance contracts may provide significantly greater risk reduction compared to regression-based indemnification schemes.

Pai et al. (2022) propose a Bayesian spatial quantile regression model to mitigate the basis risk associated with earthquake parametric insurance. They incorporate spatial correlation to establish prior distributions for latent variables and apply the model to earthquake loss data from Yunnan Province spanning from 1992 to 2019. Their findings indicate that the loss ratio is more reasonable compared to existing earthquake insurance schemes, resulting in a reduction in basis risk.

In our research, we aim to evaluate the performance of the traditional OLS as well as spatial econometrics and copulas methodologies in the pricing of a parametric insurance for hydroelectric energy generation in Brazil, using a rainfall index as a key parameter.

3. METHODOLOGY

In this section, we outline the general methodology for the insurance pricing, as well as introduce two specific methods: spatial econometrics (3.2) and copulas (3.3).

3.1. The linear regression method

As stated by Han et al. (2019), in regions where the development of a weather index insurance was successful, the actuarial pricing method – specifically the classical convolution analysis method – is the most widely used, which can work simply based on historical data (Cummins, 1991; Frees, 2015; Omerašević & Selimović, 2020). This method is well-suited for our model because it allows us to anticipate low levels of energy generation. We can achieve this by using historical data on factors like reservoir water levels, river discharges, and their correlations with rainfall indexes.

This method assumes that the probability distribution of future loss is consistent with that of historical experience, and takes the expected value of compensation as the optimal estimate of pure premium (Han et al., 2019). Regarding the climate change and rain frequency, Wu et al. (2021) suggested that increasing drought risk should be a problem for South America in the future, varying its impact depending on the level of carbon emissions we experience. So, for an initial parametric scheme, the rainfall historical data should be enough, but as the climate situation increasingly changes, the model can be reviewed and improved. Kapphan, Calanca, & Holzkaemper (2012) examined the hedging effectiveness and profitability of weather-index insurance contracts that relied on historical data to be designed, and they showed that both hedging benefits and expected profits substantially increase for adjusted contracts, which suggests that a revision of the contracts estimations is encouraged from time to time.

The calculation of the risk premium, based on Han et al. (2019) and Kusuma et al. (2018), is as follows. First, a probability distribution is fitted on historical empirical data. Then, the model parameters are estimated. Finally, the expected payout value is weighted by the probabilities of occurrence, resulting in the risk premium (P), as shown in Equation (5).

$$P = e^{-r(T-t)}\left[\frac{1}{n}\sum_{i=1}^{n} L(I_i) \times \mathbb{P}(I_i)\right], \tag{5}$$

where I_i represents the weather index in the i-th year, $L(I_i)$ represents the economic loss in the i-th year, n represents the total number of observed years, $e^{-r(T-t)}$ represents the risk-free discount factor and $\mathbb{P}(I_i)$ represents the probability of occurrence of a certain level for the weather index in the i-th year.

Because the intended product is a short-term insurance, the risk-free discount factor can often be neglected in practical application, so the premium calculus is simplified as follows:

$$P_m = \frac{1}{M}\sum_{m=1}^{M}\left(S(I_{w,m}) \times \mathbb{P}(I_m)\right) \tag{6}$$

where M is the total number of months during the insurance term, $I_{w,m}$ represents the generation capacity of the power plant at the m-th month and $S(I_{w,m})$ represents the payout value at the m-th month. This equation represents a monthly pricing, and can be extended to incorporate the term established in the contract, by multiplying P_m by M.

The payout value, $S(I_{w,m})$, is a variable that combines the historical observed losses with the loss occurrence probability (that is, severity and frequency), as it is already common for insurance pricing (Frees, 2015). In our PI scheme, the frequency will be estimated by fitting a distribution to the chosen parameter, and the severity depends on the historical

generation levels associated with the index's levels and the on-grid price of energy, which is why the payout is expressed in terms of the generation capacity of the power plants ($I_{w,m}$).

In that way, following Kusuma et al. (2018), we can define the payout as:

$$S(I_{w,m}) = G_w \times (I_{w,m}) = G_w \times \begin{cases} 0 & R_{o,m} > R_{Tr} \\ \beta(R_{Tr} - R_{o,m}) & R_E < R_{o,m} \leq R_{Tr} \\ \beta(R_E - R_{o,m}) & R_{o,m} \leq R_E < R_{Tr} \end{cases} \quad (7)$$

where G_w is the on-grid power price, $R_{o,m}$ is the observed precipitation in each month m, R_{Tr} is the precipitation trigger, R_E is the precipitation exit threshold and β is the estimated coefficient that represents the energy variation in terms of rain variation. This means that the payout value increases as the observed precipitation levels fall further from the defined trigger, until reaching a specified exit threshold. Beyond this exit threshold, the payout value remains constant, serving as a maximum retention limit (MRL) value.

Given the trigger and exit thresholds, we can rewrite $\mathbb{P}(I_m)$ as:

$$\mathbb{P}(I_m) = \big(F(R_{Tr}) - F(R_E)\big) \quad (8)$$

where $F(R_{Tr}) = \mathbb{P}(R \leq R_{Tr})$ is the cumulative distribution function, which measures the probability of precipitation (R) being less than R_{Tr} and $F(R_E) = \mathbb{P}(R \leq R_E)$ does the same for R_E. Hence, the insurance monthly premium can be expressed as:

$$P_m = \frac{1}{M} \sum_{m=1}^{M} G_w \times \big(F(R_{Tr}) - F(R_E)\big) \times \begin{cases} 0 & R_{o,m} > R_{Tr} \\ \beta(R_{Tr} - R_{o,m}) & R_E < R_{o,m} \leq R_{Tr} \\ \beta(R_{Tr} - R_E) & R_{o,m} \leq R_E < R_{Tr} \end{cases} \quad (9)$$

To determine the trigger value, we adopt a similar approach to Kusuma et al. (2018). They used a cluster analysis involving a drought index and yield data to propose a parametric scheme for rice crops. The goal of the clustering model is to maximize the similarity of observations within each cluster while maximizing the difference between clusters. In our case, we follow a similar procedure by applying k-means clustering to the rainfall index and the power plant's energy generation data. We will explore various trigger levels to identify the one that optimizes the insurance design. Our starting points are the average precipitation of the lower generation cluster, the same as Kusuma et al. (2018), and the 2.5% precipitation quantile within the same cluster as the exit threshold.

To estimate the β coefficient, we develop an energy generation predictive model. To do so, as an innovation, we employ spatial econometrics to incorporate the strong interconnections between weather and location into the model. We subsequently compare the outcomes obtained from the spatial model to those from the conventional OLS method.

3.2. Spatial Econometrics

Spatial econometrics addresses the interrelationships between economic units in spatial contexts, encompassing geographic, economic, or social interaction spaces. It accounts for interdependence, spillover effects and heterogeneity that may exist within the data or econometric model, recognizing spatial autocorrelation and other effects (Anselin, 1988; Paelinck & Klaasen, 1979).

In spatial models, the spatial interactions are typically accounted for by a weighting matrix (Anselin, 1988; Kelejian & Piras, 2017; Moran, 1948). The w_{ij} element of this matrix describes the "closeness" between units i and j in terms of a distance measure. If $w_{ij} \neq 0$, unit j is said to be a neighbor of unit i. Units that are viewed as neighbors interact in a meaningful way (e.g. spillovers, externalities or geographic proximity issues) (Kelejian & Piras, 2017).

Denoting a n×n weighting matrix as

$$W = \begin{bmatrix} W_1 \\ \dots \\ W_n \end{bmatrix} = \begin{bmatrix} w_{11}\, w_{12}\ \dots\ w_{1j} \dots\ w_{1n-1}\, w_{1n} \\ \dots \\ w_{n1}\, w_{n2}\ \dots\ w_{nj} \dots\ w_{nn-1}\, w_{nj} \end{bmatrix} \quad (10)$$

then a general fixed-effects spatiotemporal model of panel data, with n observations in the cross-section and t periods of time, can be defined as (Anselin, 1988):

$$y_{it} = \rho W y_{it} + \alpha \iota_n + X_{it}\beta + W X_{it}\theta + u_{it} \quad (11)$$

$$u_{it} = \lambda W u_{it} + \mu_i + \tau_t + \nu_{it}, \quad \text{t=1,…,T} \quad (12)$$

where y_{it} is a n×1 vector of observations on each unit i being explained at time t, ι_n is a vector n×1 of 1's associated with the constant term (α), X_{it} is a n×k matrix of observations on k exogenous variables whose values vary over both cross-sectional units and time, W is the n×n nonnegative exogenous weighting matrix, as previously defined, representing the specific omitted effects of each locality, u_{it} a vector n×1 of disturbances, ν_{it}, μ_i and τ_t are n×1 vectors of iid white noise variables, where ν_{it} represents the stochastic errors and μ_i and τ_t may represent either fixed or random effects for the individuals and time. β and θ are k×1 parameter vectors, and α, ρ and λ are scalar parameters.

ρ determins the strength of spatial lag of the dependent variable, θ measures the influence of the neighboring values of independent variables and λ is responsible for filtering out the spatial dependence in the residual term, accounting for global effects.

This model can be seen as several stacked cross-sections, and it assumes the W matrix is invariant over time, meaning the panel is balanced.

There are several ways to construct a weighting matrix (Anselin, 1988). For this study, we consider the geographic distance between the units (i.e., hydroelectric powerplants) through georeferenced (by latitude and longitude) data and select the optimum weighting matrix, among k-nearest neighbors and Euclidian distance matrixes, by the AIC criterion, as recommended by Kubara & Kopczewska (2023).

Spatial models' specifications derive from the introduction of restrictions in the general spatial model parameters. For instance, the spatial autoregressive model (SAR) only has ρ as a remaining parameter, while the spatial error model (SEM) has λ, and the SARAR model combines both features (Kubara & Kopczewska, 2023). Models with θ are called spatial Durbin models (SDM and SDEM). The spatial models can be more easily estimated by starting from the traditional OLS model (a particular case of GLM) and testing for the different spatial effects (θ, ρ or λ) inclusion (Anselin, 1988).

We start by testing for the existence of spatial interaction in our data through the application of Lagrange Multipliers (LM) in the OLS residuals (Anselin, 1988; Florax et al., 2003). Figure 5 schematizes the LM procedure based on Florax et al. (2003).

Figure 5. Lagrange Multipliers tests procedure

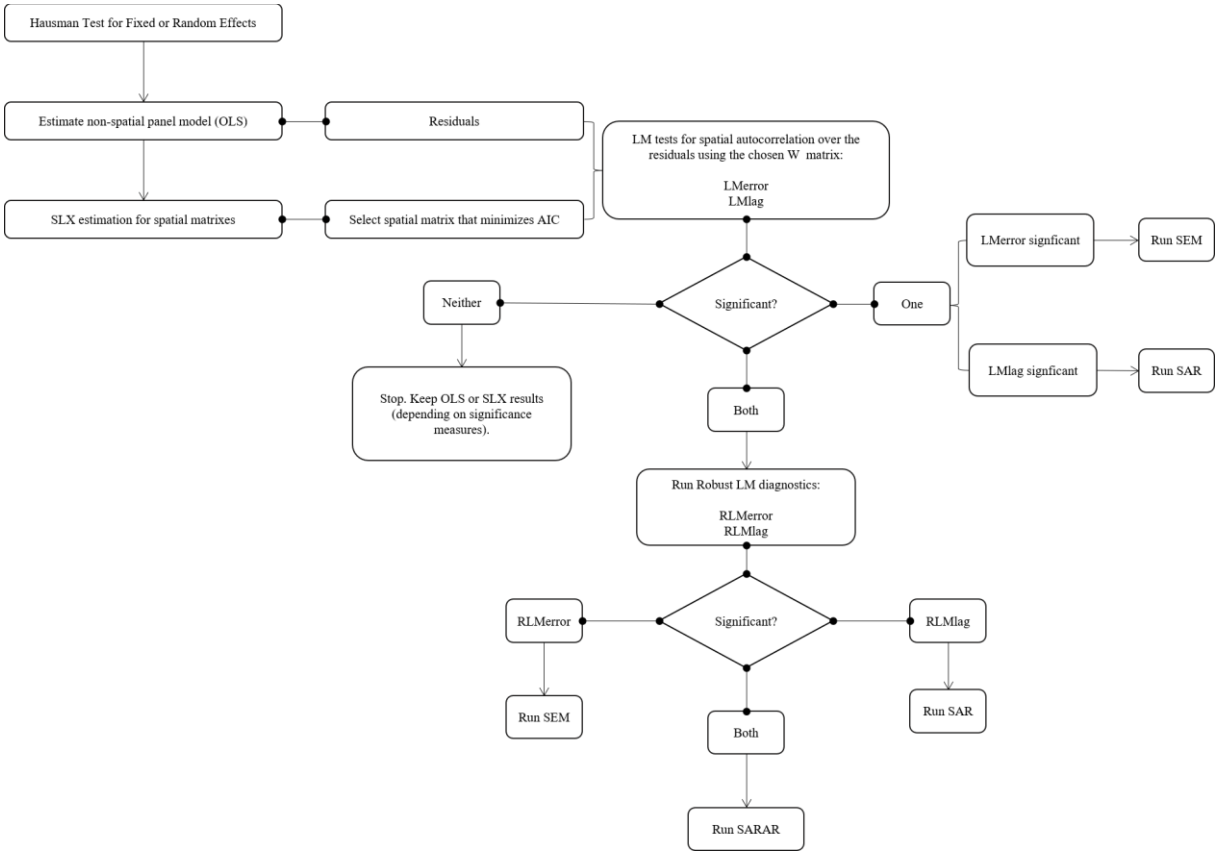

Source: own elaboration.

Based on the tests results, we estimate a model to predict the energy generation by the hydroelectric powerplants. Our initially proposed OLS model was as in Equation 13:

$$E_t = \beta_0 + \beta_1 V_t + \beta_2 A_t + \beta_3 R_t + \beta_4 T_t + \beta_5 H_t + \beta_6 WS_t + \beta_7 RG_t + u_t \quad (13)$$

where E is the generated energy, V is the reservoir's water volume, A is the affluent flow, R is the rain index value, T is the average temperature, H is the air relative humidity level, WS is the average wind speed, and RG indicates the Brazilian macroregion in which the powerplant is located. T, H and WS are used as controls for R.

As we evolved with the model testing, this proposal equation was shown not to be the best one, and our final model, as we will present in the results, can be expressed by Equation 14, in a fixed-effects, two-ways, SARAR form:

$$E_{it} = \rho W E_{it} + \beta_1 V_{it} + \beta_2 A_{it} + \beta_3 R\_3M_{it} + \beta_4 WS_{it} + \beta_5 H_{it} + \beta_6 V_{it} \times R\_3M_{it} + \beta_7 A_{it} \times R\_3M_{it} + \beta_8 WS_{it} \times H_{it} + u_{it} \quad (14)$$

$$u_{it} = \lambda W u_{it} + \mu_i + \tau_t + v_{it} \quad (15)$$

where μ_i represents the individual fixed effects and τ_t the time fixed effects. v_{it} are stochastic errors. R_3M is the average precipitation of the last 3 months. The detailed information regarding the data structure, modeling process and results are presented in section 4.

3.3. The Copulas models

As argued by Bokusheva (2018), the use of regression analysis introduces some restrictive assumptions on the joint distribution of the variables employed in the model. In particular, the use of regression models limits the scope of the analysis to a linear correlation dependence structure. Hence, it is implicitly assumed that the sensitivity of the energy generation variable to weather remains constant over its whole distribution, as it is captured

by the effect of weather on the energy generation conditional mean. Furthermore, linear correlation is inadequate for representing dependency in the tails of multivariate distributions, jeopardizing the assessment of extreme losses (Bokusheva, 2018).

By using copulas, we are able to overcome these issues. A copula links marginal distributions to form a joint distribution of random variables. A d-dimensional copula $C(u) = C(u_1, \ldots, u_d)$ is a multivariate distribution function on $[0, 1]^d$ with standard uniform marginal distributions (McNeil et al., 2005).

According to Sklar's theorem, any continuous multivariate distribution can be uniquely described by two parts: the marginal distributions $F_1, \ldots, F_d$ and the multivariate dependence structure captured by the copula C (Nelsen, 2006). That is, if F is a joint distribution function with marginal distributions $F_1, \ldots, F_d$, then there exists a copula C such that for all $(x_1, \ldots, x_d)$ in $\bar{R} = [-\infty, +\infty]$:

$$F(x_1, \ldots, x_d) = C(F_1(x_1), \ldots, F_d(x_d)) \tag{16}$$

Also, any joint probability density function $f(x_1, x_2)$ can be expressed as (Czado, 2019):

$$f(x_1, x_2) = \mathrm{c}_{12}(F_1(x_1), F_2(x_2)) \times f_1(x_1) \times f_2(x_2), \tag{17}$$

and any conditional density $f(x_1|x_2)$ can be expressed as (Czado, 2019):

$$f(x_1|x_2) = \mathrm{c}_{12}\big(F_1(x_1), F_2(x_2)\big) \times f_2(x_2), \tag{18}$$

where *c* is the copula density and *f* and F_i denote the probability density and cumulative marginal distribution functions, respectively.

There are many different types of copulas (organized in 'copula families'): copulas from elliptical family (e.g., Gaussian and t-Student copulas), Archimedean family (e.g., Clayton and Joe copulas) and extreme-value family (e.g., Tawn and Galambos copulas), among others. Given a data set, one way to choose the copula that best fits the data is using a model selection criterion, as AIC or BIC. Once the copula has been chosen, its parameters can be estimated using a two-step procedure: in the first step, the parameters of marginal distributions are obtained by fitting a parametric distribution to the empirical data. In the second step, the copula parameters are estimated by the maximum likelihood method (Bokusheva, 2018; Czado, 2019).

When $d > 2$, many of d-dimensional copulas do not have an explicit formula or computing their likelihood function isn´t feasible. To get through this, we can use a vine copula structure, where the joint probability density function $f(x_1, \ldots, x_d)$ is rewritten using conditional densities as:

$$f(x_1, \ldots, x_d) = f_{d|1\ldots(d-1)}(x_d|x_1, \ldots, x_{d-1}) \times f_{d-1|1\ldots(d-2)}(x_{d-1}|x_1, \ldots, x_{d-2}) \times \ldots \times f_1(x_1) \tag{19}$$

Note that the decomposition structure in Equation 18 is not unique: from the law of total probability, it is possible to decompose a bivariate distribution as a product of a conditional and a univariate distribution. From Equation 18, each conditional density can be expressed in terms of a copula density *c* so Equation 19 can be rewritten as (Joe, 1996):

$$f(x_1, \dots, x_d) = \prod_{j=1}^{d-1} \prod_{i=1}^{d-j} c_{i,(i+j)|(i+1),\dots,(i+j-1)}\left(F\left(x_i \middle| x_{i+1}, \dots, x_{i+j-1}\right), F\left(x_{i+j} \middle| x_{i+1}, x_{i+j-1}\right)\right) \times \prod_{k=1}^{d} f_k(x_k) \quad (20)$$

Our choice for vine copulas is based on the fact that they are very adequate to model conditional structures, while also being a flexible tool for multivariate non-Gaussian (asymmetric) distributions (B. Chang & Joe, 2019), which seems to be the case of our data, as we will describe in section 4.1.

Once we have modelled the variables' causal dependence structure (in the graphical sense) throughout the vine copulas, we will be able to assess the joint probability of occurrence of the variables. The variable(s) directly related to the energy generation will be chosen as index(es) for the PI, and the thresholds levels can be defined by observing the quantiles of this(these) variable(s) that directly relate to low levels of energy generation. The payout can still be set as in Equation 7, except for the beta coefficient, as this method does not provide coefficients. Instead, we use the copula parameters to weight the index's values. The probabilities of occurrence $F(R_{Tr})$ and $F(R_E)$ are given by the copula distribution itself.

4. RESULTS

In sections 4.1 and 4.2, we present a brief description of our database as well as some exploratory graphs that will base our further analyses. In section 4.3, we present the various estimated linear and spatial models, evaluating the best model choice. In section 4.4, we define the insurance thresholds, and in section 4.5 we present the insurance results with the spatial econometrics model. In section 4.6, we assess the variable's interdependencies through copulas, carrying out an endogeneity robustness check, and presenting a second approach for the parametric insurance design, with the copula models.

4.1. The data

We gathered the data for Brazilian powerplants energy generation and reservoirs levels from the National Electrical System Operator (ONS) official database, and the Standardized Precipitation Index (SPI) measures from the National Institute of Meteorology (INMET).

After treatment, the databases comprehend the generated energy by hydroelectric powerplants (in MWmed), the powerplants' location (state, region and coordinates) and identification variables, such as name, hydrographic basin, system and subsystem, alongside with a variable indicating if the powerplant operates as run-of-river or with water storage, and quantitative variables regarding water volume in the reservoirs (in meters), water flow (in m^3/s) and meteorological data, such as precipitation levels (mm), temperature (ºC), wind speed (m/s) and air relative humidity (%).

Our dataset is structured as a monthly panel spanning from January 2006 to December 2022, encompassing 151 powerplants. Originally, this panel was unbalanced, due to the fact that some powerplants were either under construction or not operational during the entire data collection period. To address this, we balanced the panel by assigning zero values for generation, water volume, and affluent flow on the dates when these powerplants did not exist or were non-operational.

Furthermore, to ensure that we did not lose observations during the model estimation, we applied a similar approach to powerplants with null volume, particularly those categorized as run-of-river powerplants, setting their volume to zero. As part of a robustness test, we conducted a comparison of the results obtained from OLS regressions using both the balanced and unbalanced datasets. The analysis revealed that the resulting coefficients did not exhibit significant differences between the two datasets (such results are presented in Annex 1). A balanced panel is best for the development of econometric models, particularly when dealing with spatial analysis, as it allows the neighborhood matrix to remain consistent across the entire panel. This stability reduces the overall complexity.

The data is originally available on an hourly basis, but we have aggregated it into monthly summaries. This approach aligns with the requirements of parametric insurance design, which considers monthly measurements for trigger events. Such a design is especially relevant in the context of energy generation, where issues typically arise after extended periods of insufficient rainfall, often spanning several days or even weeks.

To ensure data quality, we excluded the years prior to 2006 due to the limited coverage of INMET's meteorological meters, which were insufficient to adequately monitor all powerplant locations during that period. In the end, our panel comprises 30,804 month-powerplant observations. Descriptive statistics for our database can be found in Tables 1 to 7 and Figures 6 to 21.

Table 1. Time span of our data

Number of months	First date	Last Date
204	01/01/2006	31/12/2022

Source: own elaboration.

Table 2. Powerplants by year

Year	Number of Powerplants (unbalanced panel)	Number of Powerplants (balanced panel)
2006	107	151
2007	108	151
2008	110	151
2009	116	151
2010	123	151
2011	128	151
2012	130	151
2013	135	151
2014	137	151
2015	140	151
2016	144	151
2017	144	151
2018	146	151
2019	147	151
2020	148	151
2021	148	151
2022	151	151

Source: own elaboration.

Table 3. Powerplants by Brazilian geographic macroregions

Region	Number of powerplants
Center-West (CO)	22
North (N)	18
Northeast (NE)	09
South (S)	31
Southeast (SE)	70
Total	150

Note: The one missing powerplant is Itaipu 50 Hz, the Paraguayan portion of Itaipu. It is counted in the other metrics as usually Brazil buys a fraction of the generated energy from Paraguay.

Source: own elaboration.

Table 4. Powerplants by electricity subsystems

Region	Number of powerplants
North (N)	10
Northeast (NE)	08
South (S)	30
Southeast (SE)	103
Total	151

Source: own elaboration.

It is noteworthy that the region where a powerplant is located is not always the one (or the only one) where the generated energy is consumed. Powerplants located in the northern regions of Brazil (where Amazon Rainforest is located), for example, might produce electricity that is primarily directed to the densely populated southeast, which serves as the country's residential and industrial hub. This is made possible by Brazil's well-developed

electrical network infrastructure, which includes extensive long-distance transmission powerlines (Barroso et al., 2007; Cataia, 2019). Consequently, the number of power plants across different electric subsystems may diverge from the geopolitical macroregions due to this intricate distribution and transmission of energy.

Table 5. Ranking of powerplants' average monthly energy generation

Ranking	Powerplant name	Powerplant type	State and region	Basin name and subsystem	Generation (Mwmed)
1	Itaipu 60 HZ	Run-of-River	PR (S)	Paraná (SE)	3,490,762.0
2	Itaipu 50 HZ	Run-of-River	-	Paraná (SE)	2,949,235.0
3	Tucuruí	Storage water volume	PA (N)	Tocantins (N)	2,847,237.8
4	Belo Monte	Run-of-River	PA (N)	Amazonas (N)	1,888,693.7
5	Ilha Solteira	Storage water volume	SP (SE)	Paraná (SE)	1,203,226.2
6	Xingó	Run-of-River	AL (NE)	São Francisco (NE)	1,144,363.1
7	Santo Antônio	Run-of-River	RO (N)	Amazonas (SE)	1,071,824.2
8	Jirau	Run-of-River	RO (N)	Amazonas (SE)	1,051,988.1
9	São Simão	Storage water volume	MG (SE)	Paranaíba (SE)	841,826.4
10	Paulo Afonso IV	Run-of-River	BA (NE)	São Francisco (NE)	831,938.8
		...			
142	Batalha	Storage water volume	MG (SE)	Paranaíba (SE)	16,633.766
143	Santa Branca	Storage water volume	SP (SE)	Paraíba do Sul (SE)	16,608.905
144	Ourinhos	Run-of-River	SP (SE)	Paranapanema (SE)	16,541.247
145	Itutinga	Run-of-River	MG (SE)	Grande (SE)	16,079.630
146	Santa Clara (MG)	Run-of-River	MG (SE)	Mucuri (SE)	14,511.686
147	Barra do Braúna	Run-of-River	MG (SE)	Paraíba do Sul (SE)	13,784.478
148	Anta	Run-of-River	RJ (SE)	Paraíba do Sul (SE)	12,696.291
149	Camargos	Storage water volume	MG (SE)	Grande (SE)	12,353.470
150	Limoeiro	Run-of-River	SP (SE)	Grande (SE)	9,536.961
151	Jaguari	Storage water volume	SP (SE)	Paraíba do Sul (SE)	7,028.905

Note: Itaipu 60 Hz represents the Brazilian portion of Itaipu, while Itaipu 50 Hz represents the Paraguayan portion. These averages only take into account the periods when the powerplant was operational (thus its generation was greater than zero).

Source: own elaboration.

Table 6. 10 largest powerplants by monthly average energy generation and type

Ranking	Run-of-River				Storage Water Volume			
	Powerplant's name	State	Basin's name	Generation (Mwmed)	Powerplant's name	State	Basin's name	Generation (Mwmed)
1	Itaipu 60 HZ	PR	Paraná	3,490,762.0	Tucuruí	PA	Tocantins	2,847,237.8
2	Itaipu 50 HZ	-	Paraná	2,949,235.0	Ilha Solteira	SP	Paraná	1,203,226.2
3	Belo Monte	PA	Amazonas	1,888,693.7	São Simão	MG	Paranaíba	841,826.4
4	Xingó	AL	São Francisco	1,144,363.1	Salto Santiago	PR	Iguaçu	574,044.3
5	Santo Antônio	RO	Amazonas	1,071,824.2	Itumbiara	MG	Paranaíba	537,399.8
6	Jirau	RO	Amazonas	1,051,988.1	Água Vermelha	SP	Grande	524,462.0
7	Paulo Afonso IV	BA	São Francisco	831,938.8	Gov. Ney Braga	PR	Iguaçu	510,703.7
8	Porto Primavera	SP	Paraná	766,231.7	Marimbondo	MG	Grande	469,828.9
9	Jupiá	SP	Paraná	677,780.2	Gov. Bento Munhoz	PR	Iguaçu	463,135.1
10	Itá	SC	Uruguai	573,442.4	Luiz Gonzaga	PE	São Francisco	462,178.7

Note: Itaipu 60 Hz represents the Brazilian portion of Itaipu, while Itaipu 50 Hz represents the Paraguayan portion. These averages only take into account the periods when the powerplant was operational (thus its generation was greater than zero).

Source: own elaboration

Table 7. Descriptive statistics for the model's variables

Generation						
Min.	1st Qu.	Median	Mean	3rd Qu.	Max.	NAs
0	19,813	56,297	216,517	178,554	6,836,348	0
Useful Volume						
Min.	1st Qu.	Median	Mean	3rd Qu.	Max.	NAs
-8.294	0	0	22.32	45.23	194.01	0
Affluent flow						
Min.	1st Qu.	Median	Mean	3rd Qu.	Max.	NAs
-12.97	47.88	198.10	917.57	719.04	54,385.86	0
Precipitation						
Min.	1st Qu.	Median	Mean	3rd Qu.	Max.	NAs
0	224.6	748.5	1037.2	1563.7	9234.8	0
Temperature						
Min.	1st Qu.	Median	Mean	3rd Qu.	Max.	NAs
9.94	22.35	24.87	24.40	27.04	34.03	0
Wind Speed						
Min.	1st Qu.	Median	Mean	3rd Qu.	Max.	NAs
0.12	1.75	2.17	2.23	2.65	6.32	0
Humidity						
Min.	1st Qu.	Median	Mean	3rd Qu.	Max.	NAs
25.08	58.59	66.65	64.61	72.73	92.18	0

Note: Generation is the total generated energy in MWmed unit; Useful Volume refers to the available volume in the reservoir (in m^3) between the maximum normal operating level and the minimum normal operating level; Affluent Flow is the average water flow (in m^3/s) that reaches a hydroelectric facility or a hydraulic structure; Precipitation is the total amount of rain (mm); Temperature is the average temperature (°C); Wind Speed is the average wind speed (m/s); and Humidity is the average air relative humidity (%). The meteorological variables' values correspond to the result of the kriging technic later explained in section 4.2.

Source: own elaboration.

Figure 6. Histograms of the model's variables

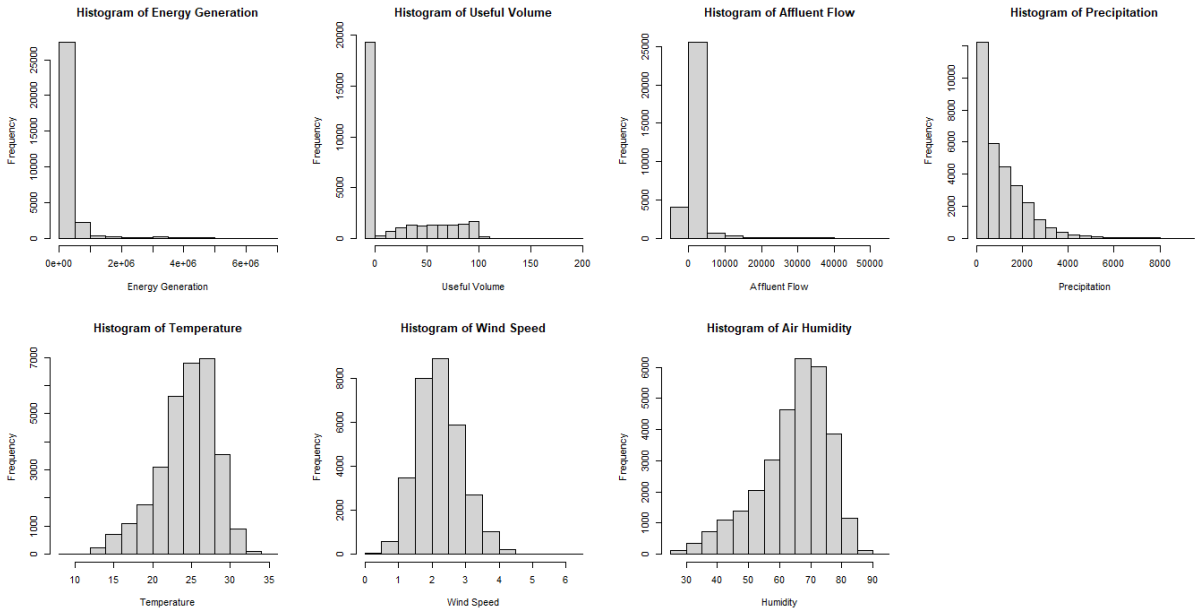

Source: own elaboration.

Figure 7. QQ-Plots of the model's quantitative variables

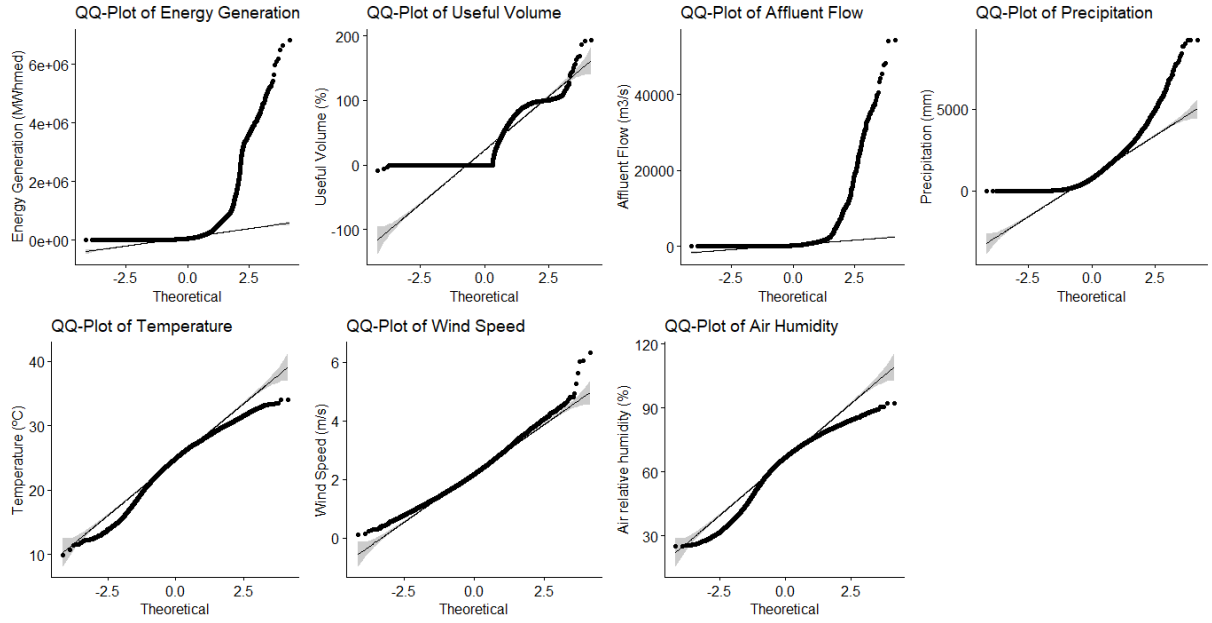

Source: own elaboration.

The histograms and qq-plots provide strong evidence that the data deviate from a Normal distribution, particularly in the case of generation, water volume, affluent flow and precipitation. These variables exhibit left-skewed distributions with heavy-tails. While temperature, wind speed and humidity show distributions that are relatively closer to a Gaussian shape, the qq-plots reveal non-normality even in these cases.

It is worth noting that climate data can significantly vary by region due to the vast expanse of Brazilian territory. To illustrate this regional variability, we have included histograms for precipitation, temperature, and energy generation specific to different regions in Figures 8 to 10.

Figure 8. Histograms of precipitation by region

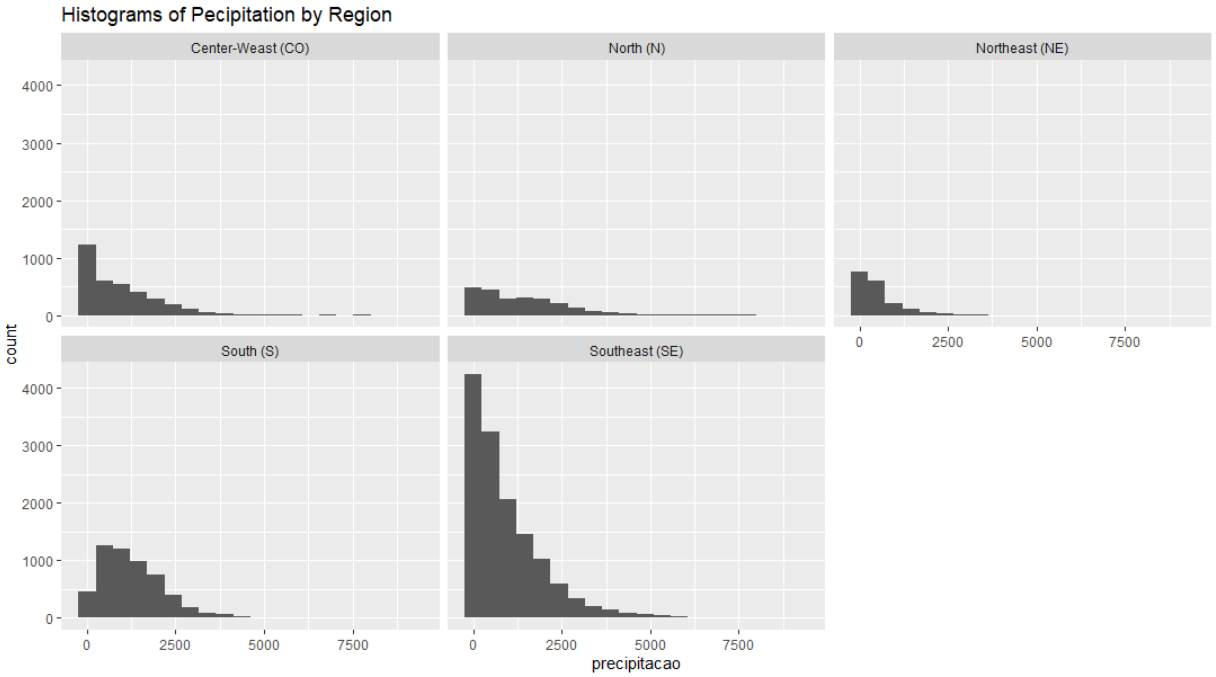

Source: own elaboration.

Figure 9. Histograms of temperature by region

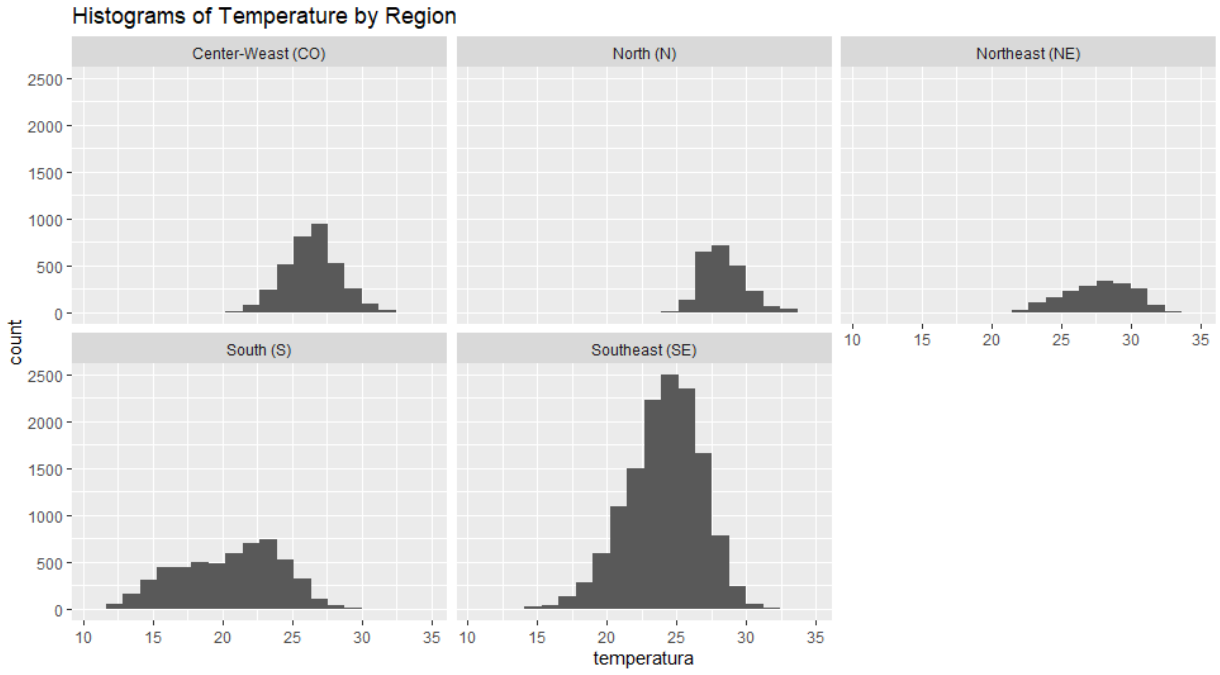

Source: own elaboration.

Figure 10. Histograms of energy generation by region

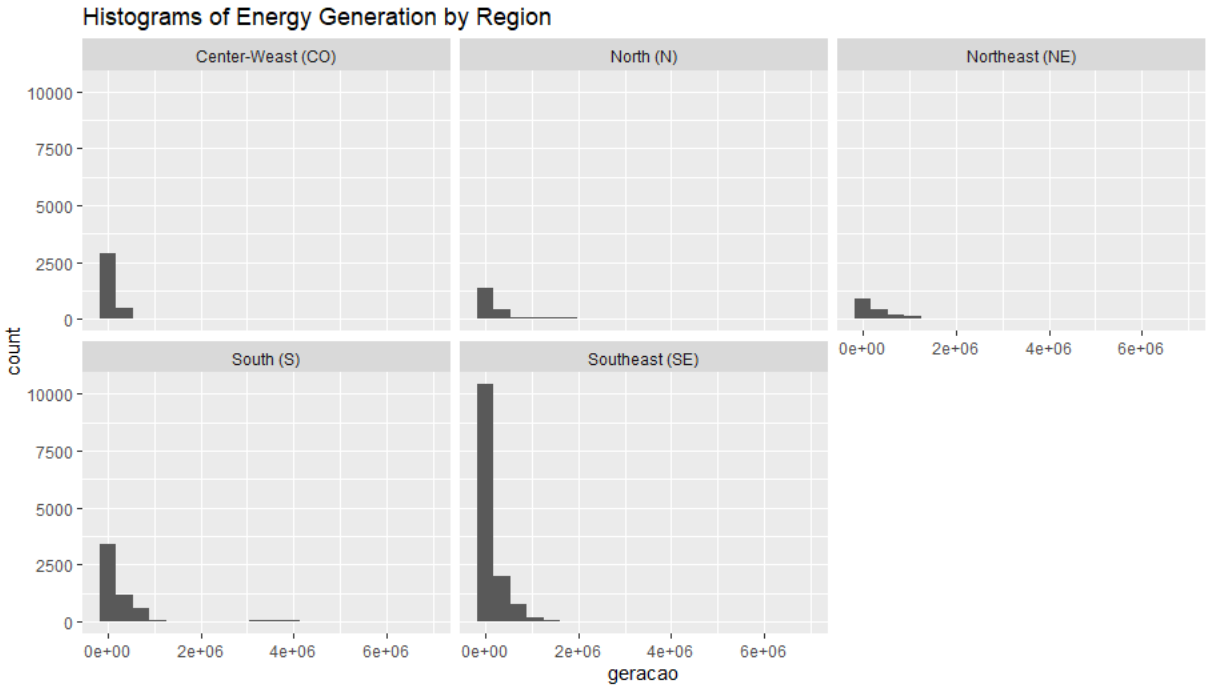

Source: own elaboration.

By examining the histograms, we verify typical climate characteristics specific to each region in Brazil. For instance, the North region stands out with its high precipitation levels and elevated temperatures. The Northeast region experiences the highest temperatures but comparatively lower precipitation. In contrast, the South region tends to have lower temperatures.

Regarding electricity generation, we observe the heaviest tails on South and North regions. This reflects the substantial power generation from major facilities like Itaipu, Tucuruí and Belo Monte, as shown in Tables 5 and 6.

Furthermore, our analysis extends to the examination of time series data, particularly focusing on key variables of interest such as generation and precipitation. This temporal analysis is visually depicted in Figures 11 to 21, providing insights into the behavior of these variables over time.

Figure 11. Energy generation time series

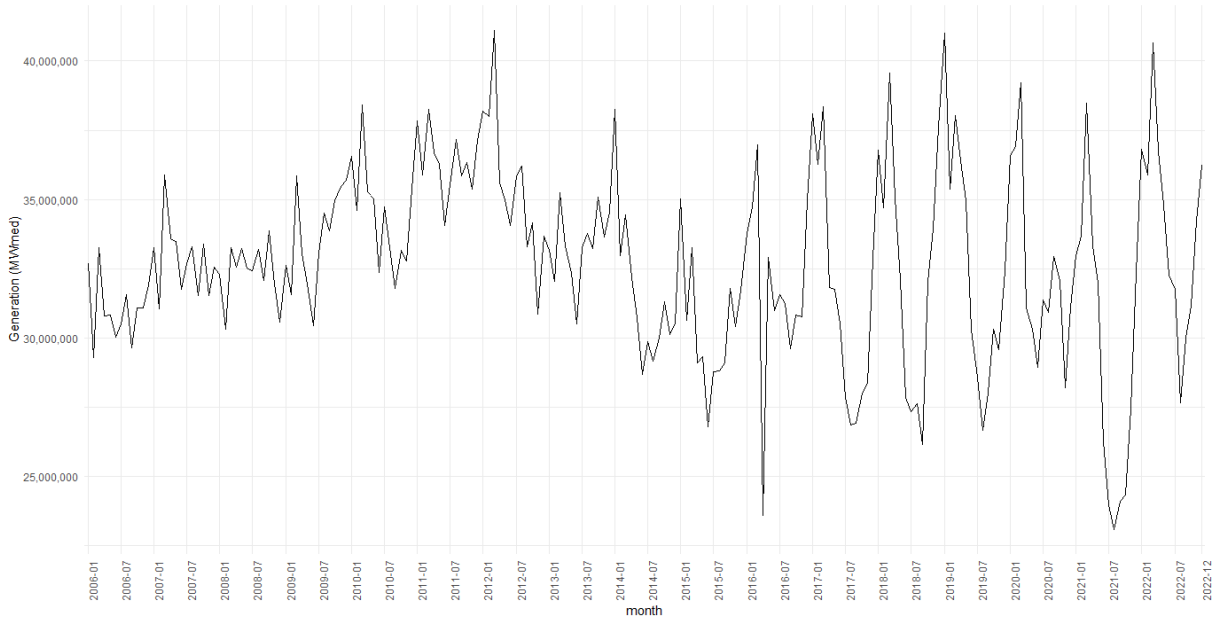

Note: the series is the sum of all energy generated in each month by all the powerplants

Source: own elaboration.

Figure 12. Precipitation time series

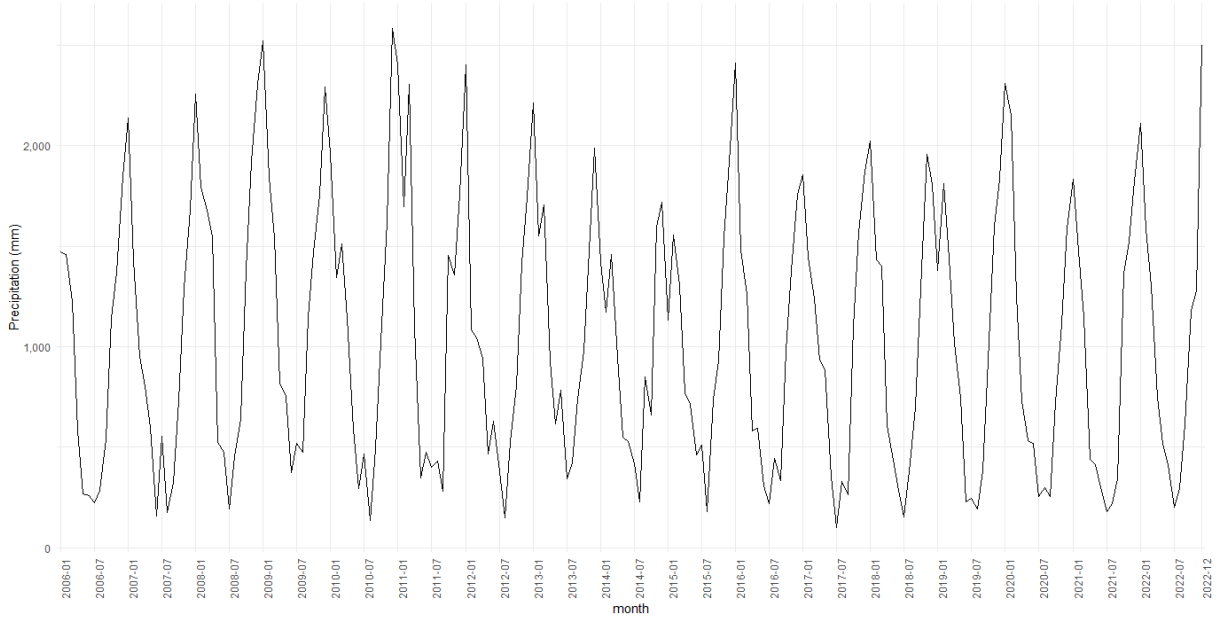

Note: the series is the average precipitation in each month taking all regions into account.

Source: own elaboration.

In Figure 11, we see a consistent upward trend for energy generation up until mid-2012. However, this positive trajectory was disrupted by a significant hydric crisis in Brazil, leading to an energy crisis in 2014, with extended periods of drought. This crisis caused a noticeable drop in energy generation. A similar pattern of reduced generation is visible in 2021, coinciding with yet another drought crisis. The impact of these droughts is further evident in Figure 12, where we observe that the peaks in precipitation are notably lower from 2013 to 2015 and again in 2021, accompanied by reduced valleys.

From 2016 to 2022, except for the 2021 crisis, energy generation stabilizes. During this period, its seasonality closely follows the seasonality of precipitation, as seen in Figure 12. Moreover, Figure 12 clearly shows the typical seasonality of pluviometry, characteristic of tropical and subtropical climates, with high levels of precipitation during the summer and lower levels during the winter. The amplitude of peaks and valleys in the series serves as a clear reflection of the two major droughts experienced in this timeframe, which occurred in 2014 and 2021.

Figure 13. Top 5 powerplants energy generation time series

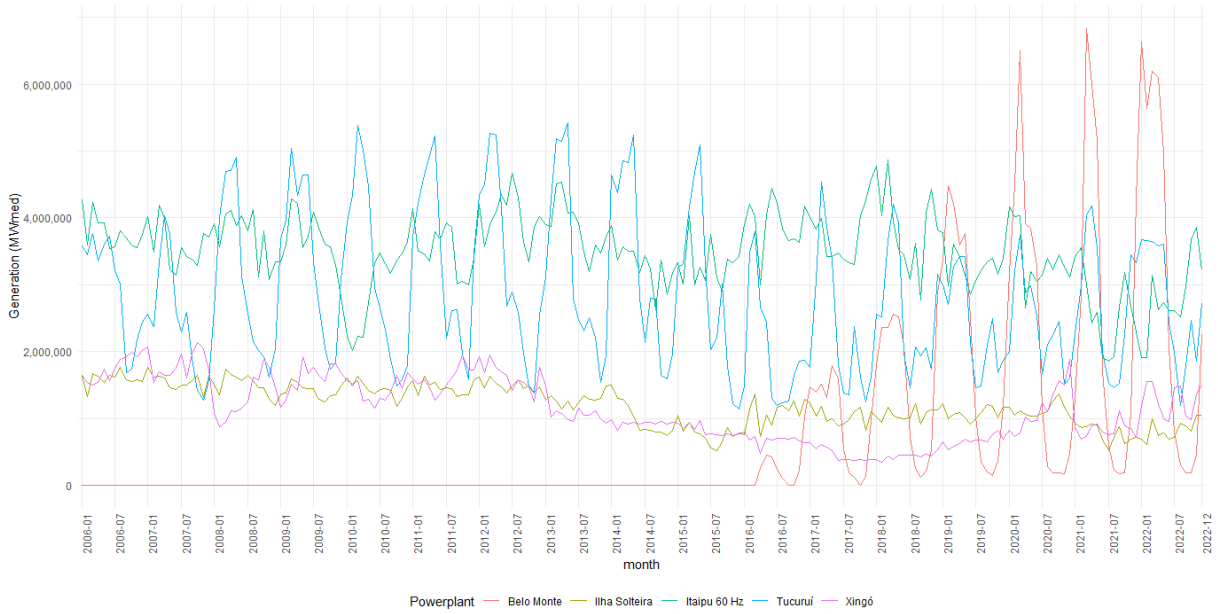

Source: own elaboration.

Figure 13 provides a compelling view of the time series for energy generation, highlighting the predominant contribution from the top 5 powerplants, notably Itaipu and Tucuruí initially, and later Belo Monte after 2016. It is noteworthy remarkable speed at which Belo Monte's generation capacity expanded once it became operational in 2016.

Furthermore, this shift in energy generation by Belo Monte dynamics is accompanied by a notable decline in production from Itaipu and, particularly, Tucuruí. This shift likely reflects changes in energy demand, with the new powerplant, Belo Monte, playing a significant role in supplying a substantial portion of the energy consumption, thereby impacting the generation patterns of Itaipu and Tucuruí.

Figure 14. Energy generation time series by region

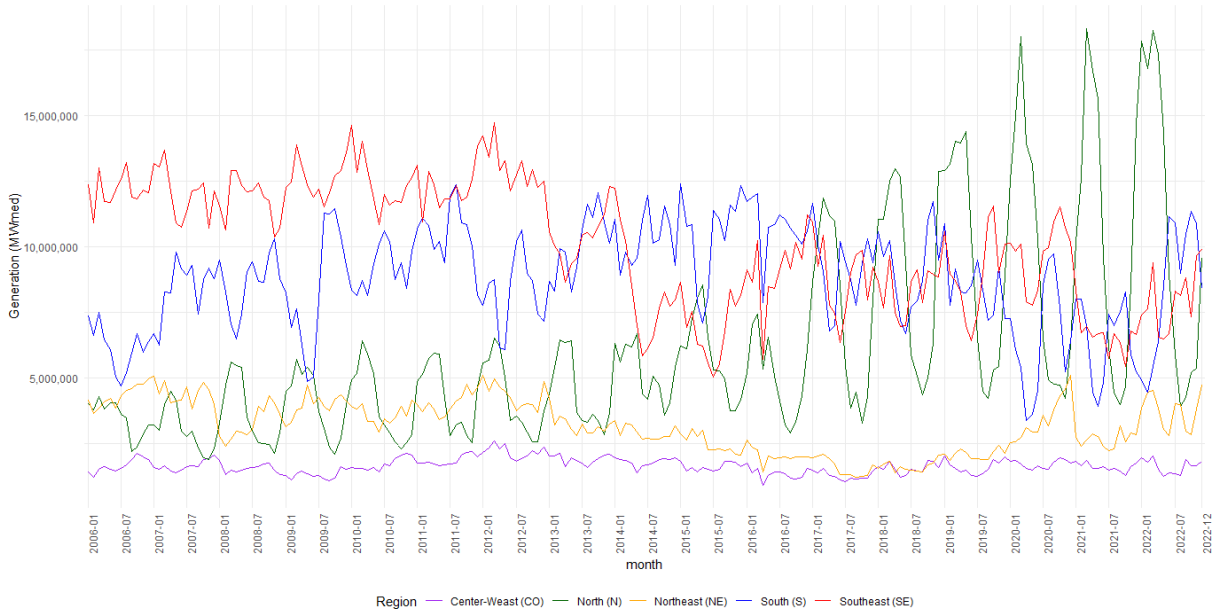

Note: the series are the sum of the energy generated in each month by all the powerplants in each region.

Source: own elaboration.

Figure 14 shows that regional energy generation patterns are also strongly influenced by the output of the major powerplants. Notably, none of the powerplants from the center-west region are among the top ten largest in terms of generation capacity. This absence in the top ranks is a contributing factor to the relatively lower levels of energy generation in the central-west region.

Figure 15. Precipitation time series by region

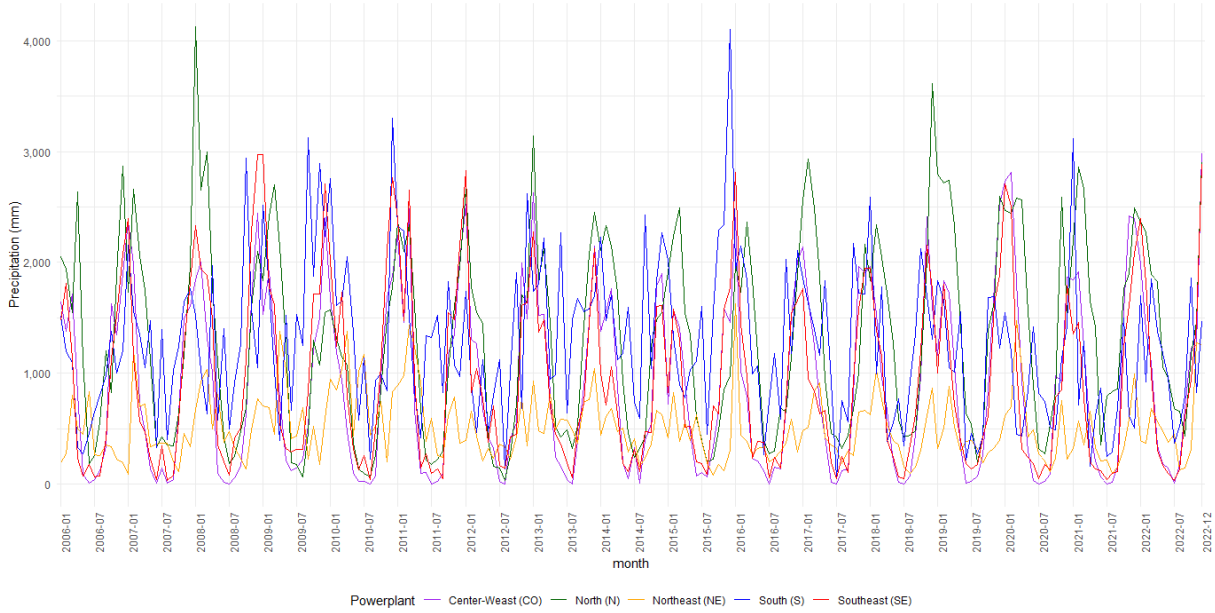

Note: the series are the average of precipitation in each region and month.

Source: own elaboration.

The series depicted in Figure 15 exhibit behavior similar to the overall time series shown in Figure 7. However, there are noticeable variations in precipitation levels, as well as

differences in the months when each region reaches its peak, owing to the distinct climatic conditions in these regions.

For a more comprehensive view, we present the interplay between energy generation and precipitation levels by region throughout time in Figures 16 to 21.

Figure 16. Generation x Precipitation - North

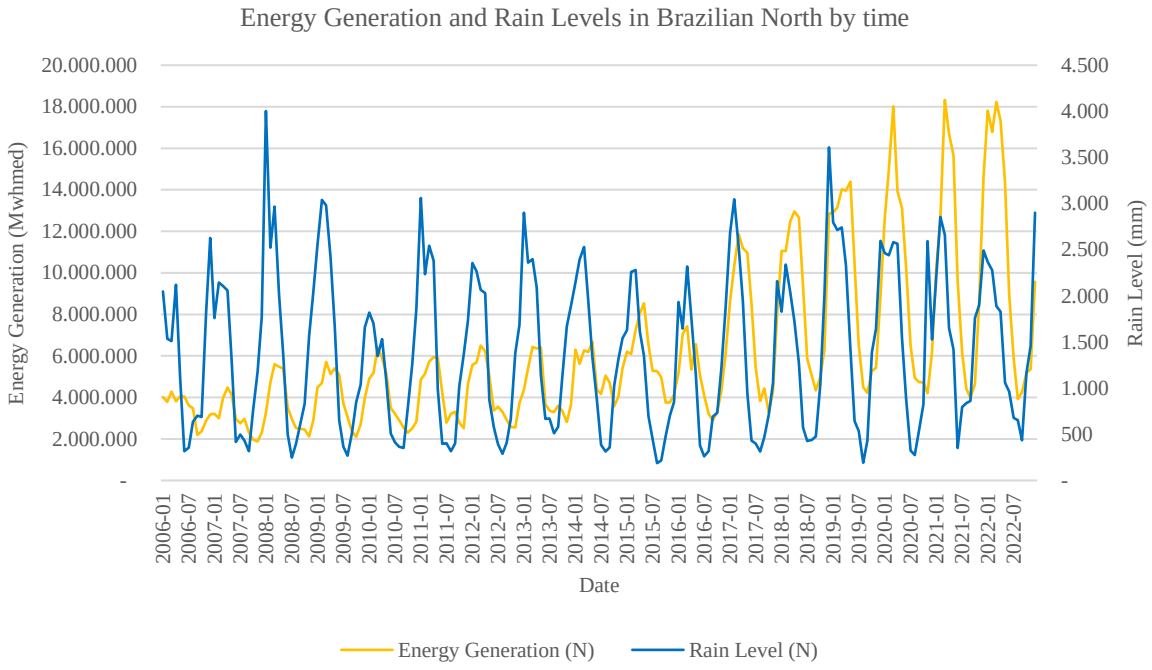

Source: own elaboration.

The northern region consistently experiences the highest levels of precipitation, even when comparing the lowest points in the precipitation levels to other regions. However, at the beginning of the time series, energy generation levels in this region were not particularly remarkable. This can be attributed to the relatively small number of powerplants, with Tucuruí being the sole significant contributor. It is noteworthy that Santo Antonio was inaugurated in 2012, followed by Jirau in 2014, and Belo Monte in 2016 (Castilho, 2019). The installation of these powerplants, particularly Belo Monte, catalyzed substantial growth in energy generation, to the extent that it even surpassed the generation levels of Itaipu.

Figure 17. Generation x Precipitation - Northeast

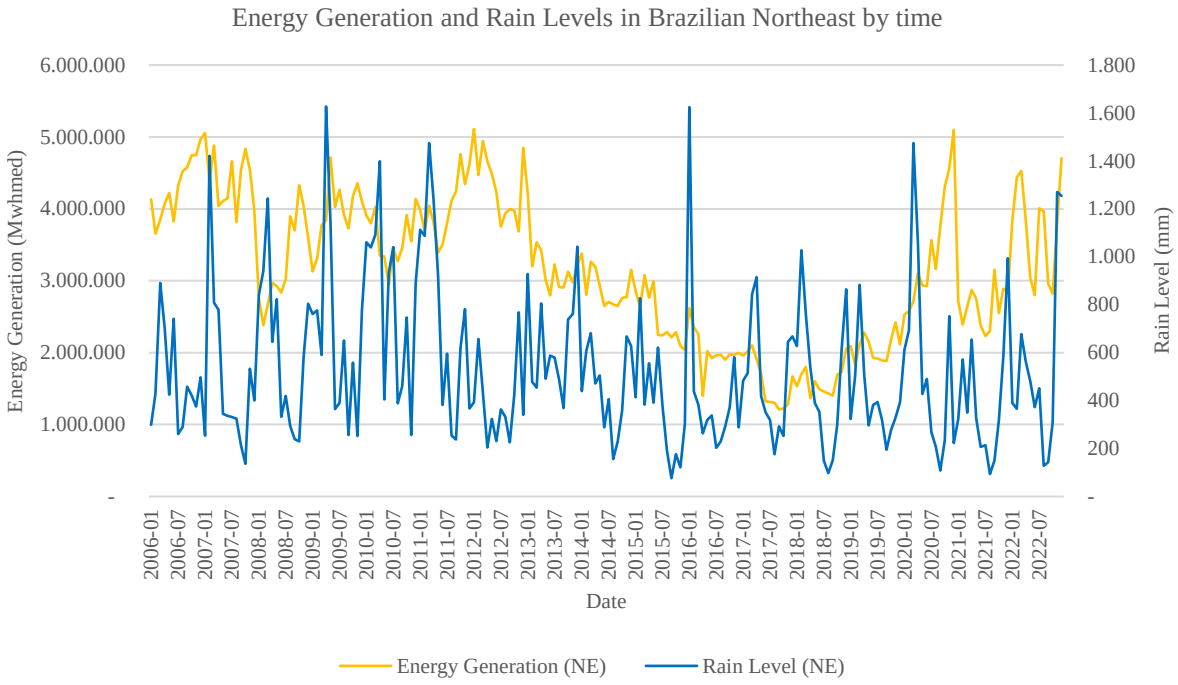

Source: own elaboration.

The northeast region of Brazil stands out as the driest among all the regions, characterized by scant rainfall and elevated temperatures. It is the region that has borne the brunt of hydric crises, as clearly shown in Figure 17, where both curves experience a notable decline. In response to these challenges, wind energy generation has gained prominence in this region. It is an efficient source of power and serves as a valuable complement to electricity generation during periods of drought, effectively diversifying the electricity matrix (de Jong et al., 2016; De Jong et al., 2013).

Figure 18. Generation x Precipitation - South

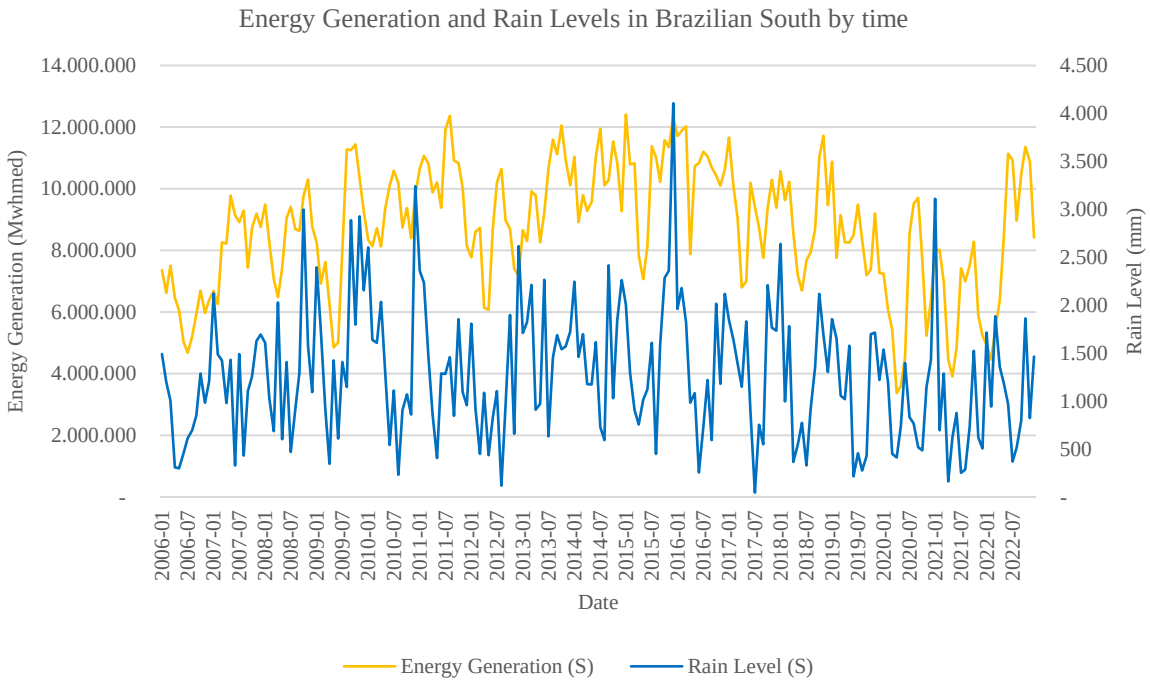

Source: own elaboration.

The southern region exhibits time series with higher volatility, marked by substantial energy generation levels, primarily driven by Itaipu, and moderate levels for precipitation. Like in other regions, the most significant peaks in precipitation are typically observed during the summer. However, this region also experiences smaller peaks during the spring months. Even during the winter months, when both precipitation and energy generation reach their lowest points, the energy generation levels in the south surpass those of northeast and central-west regions.

Since 2016, there is a trend of decreased energy generation, attributable to Belo Monte gradually compensating for a portion of the demand. However, this trend experienced an upturn in 2022, particularly in response to the hydric crisis. The lowest point in the generation curve was reached in July 2020, coinciding with the initial signs of the 2021 hydric crisis, which predominantly impacted the southern and southeastern regions during that period.

Figure 19. Generation x Precipitation - Southeast

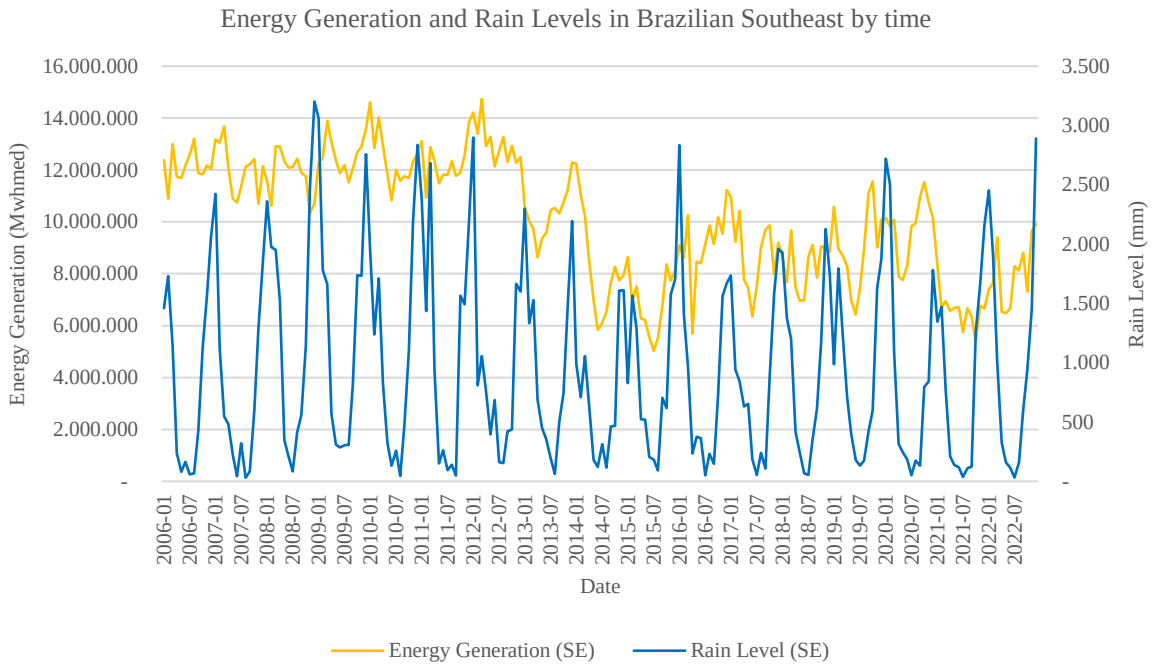

Source: own elaboration.

The southeastern region of Brazil boasts the highest concentration of powerplants, mirroring its status as the most densely populated area in the country, with approximately 45% of the Brazilian population residing there. Moreover, this region serves as the industrial hub, particularly in São Paulo. Consequently, the cumulative energy generation in the southeast is substantial, and its electrical subsystem also receives energy from powerplants situated in other regions, including the south and even the north.

During both energy crises (2014-2016 and 2020-2021), the energy generation series registers significant declines. The precipitation series, on the other hand, reflects the characteristic climate seasonality but is notably less volatile compared to regions like the northeast or the south. It is worth noting that this series exhibits lower peaks during periods of hydric crises.

Figure 20. Generation x Precipitation – Center-west

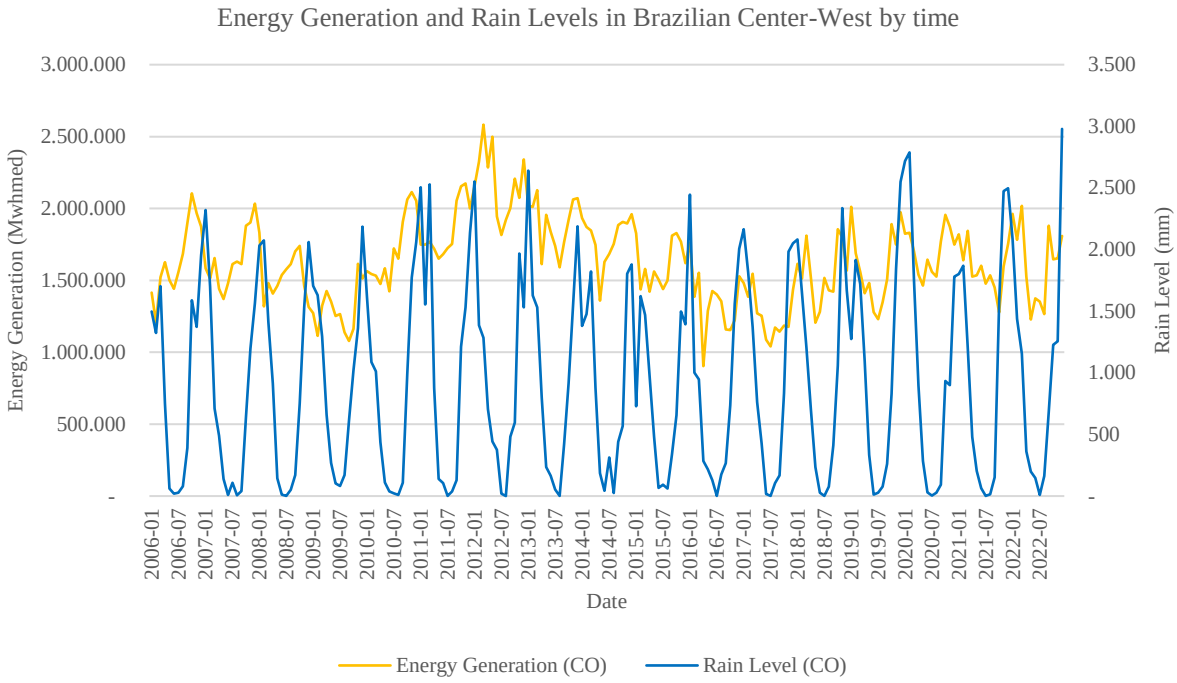

Source: own elaboration.

The central-west region displays relatively modest levels of energy generation. As the least populated area in Brazil, it lacks an independent electrical subsystem. Most of its powerplants primarily supply energy to the southeast region, while some also contribute to the electrical subsystems of the north and south, given its shared hydrographic basins with these three regions.

Precipitation levels in the central-west region closely resemble those of the southeast. However, it is important to note that part of the region is covered by the Amazon Rainforest, where the climate conditions are more akin to those in the north.

Figure 21. Generation x Precipitation - Brazil

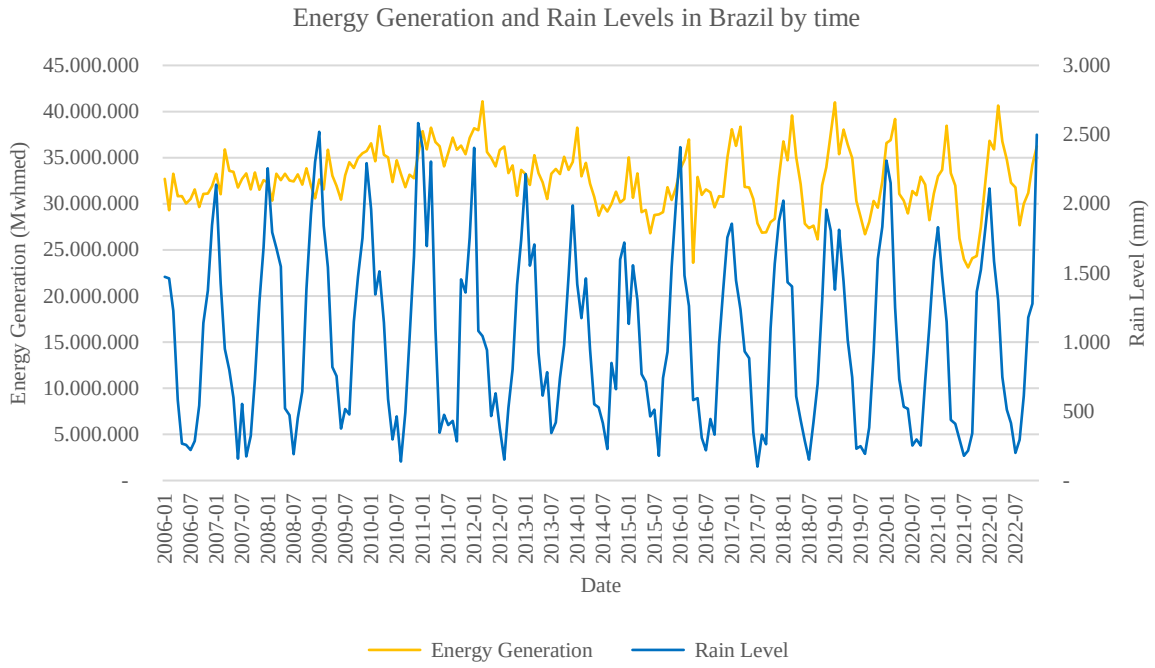

Source: own elaboration.

The nationwide time series for Brazil serves as a synthesis of the regional data. The hydric and energy crises of 2014 and 2021 are clearly discernible in the country-wide time series. What is particularly noteworthy is the close alignment between energy generation and precipitation, as they tend to move together. In periods of increased rainfall, energy generation surges, while in times of drought, the energy generation diminishes. This correlation is fundamental to the parametric design we advocate, and it holds great significance for a nation that heavily relies on hydroelectric energy.

4.2. Spatial exploratory analysis

In addition to traditional descriptive statistics, we perform an exploratory analysis to delve into the data's spatial characteristics. Figure 22 provides a visual representation of the geographical distribution, illustrating the positions of hydroelectric powerplants marked in blue points and INMET's meteorological meters pinpointed in red points.

Figure 22. Map of Brazilian hydro powerplants (blue) and meteorological meters (red)

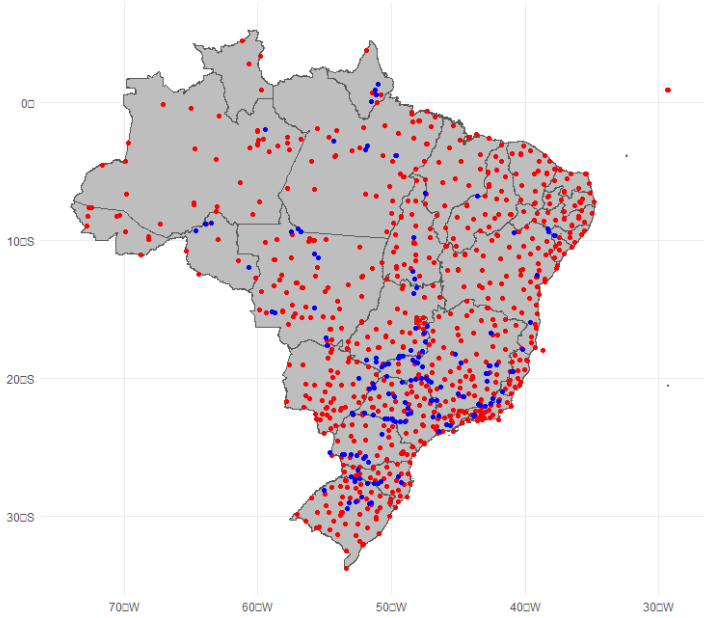

Source: own elaboration.

The map illustrates that there are sufficient meteorological meters in close proximity to each powerplant to enable obtaining accurate precipitation measurements for insurance purposes. To assign the corresponding meteorological measures to each powerplant for the model (given that the data from powerplants' generation, water volume and water flow originates from a distinct database than the meteorological data), we employed a kriging technique.

Our choice of kriging parameters (e.g., distribution to be fitted and the fitting method) was based on a thorough graphical analysis of the kriging plots. For computational efficiency and due to the relatively close proximity of most meteorological meters to one another, we applied the kriging technique using only the three nearest meters to interpolate the data. This method was executed separately for each time period (month) and the results were subsequently organized and stacked in the panel structure.

As an illustrative example of the kriging analysis, Figure 23 displays the fitted data for December 2022.

Figure 23. Kriging models fitness to meteorological data – December 2022

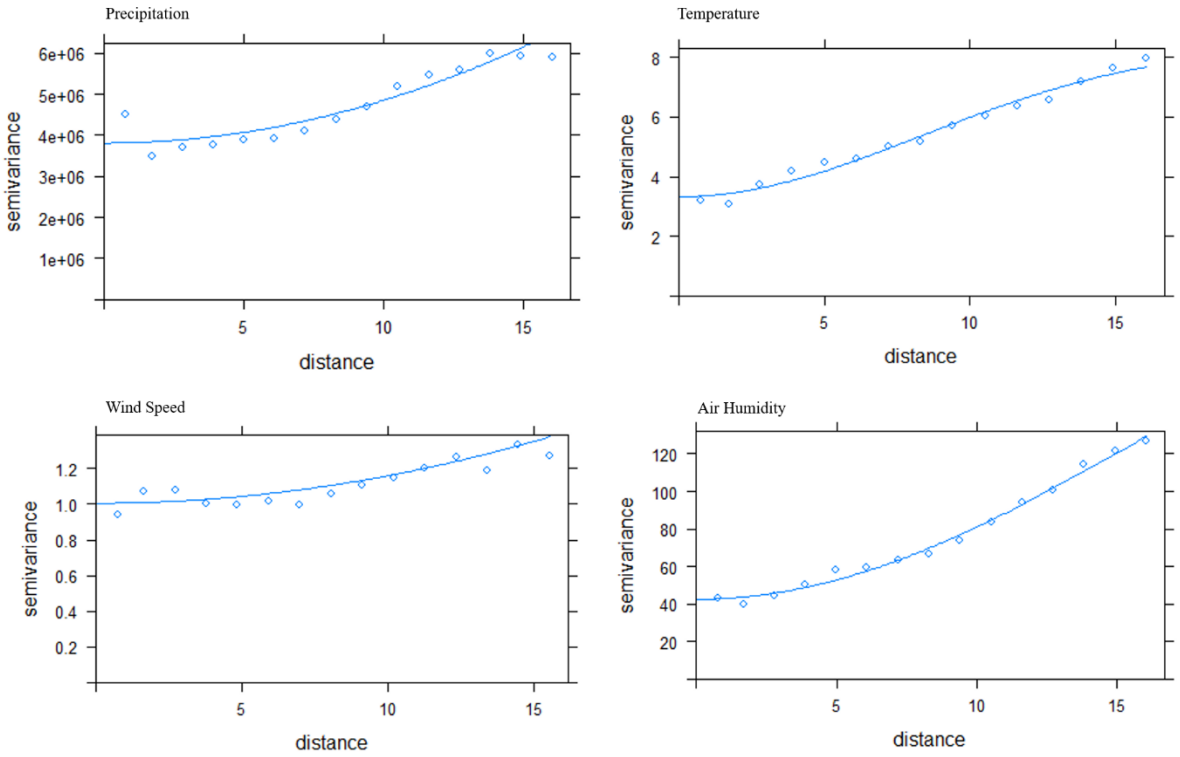

Source: own elaboration.

In general, the kriging technique proved to be effective in interpolating the data, particularly when dealing with shorter distances. All the statistics presented up to this point pertain to the kriged database. In Figure 24, we provide histograms comparing the original INMET's database with the data post-kriging, which has been merged with the locations of the powerplants.

Figure 24. Histograms of meteorological data – original and kriged

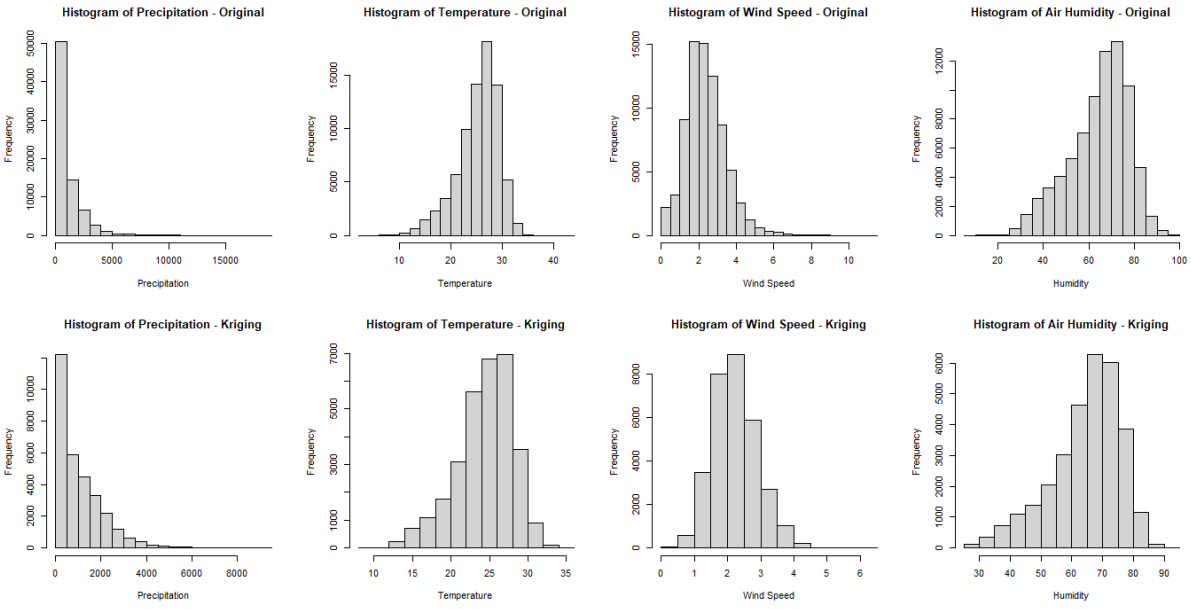

Source: own elaboration.

As expected, the distributions exhibit minimal deviation from the original data, providing us with confidence in utilizing this dataset for the model. Figure 25 offers a visual representation of the precipitation levels at each geographical point, encompassing both meteorological meters and powerplants locations on the map.

Figure 25. Map of precipitation

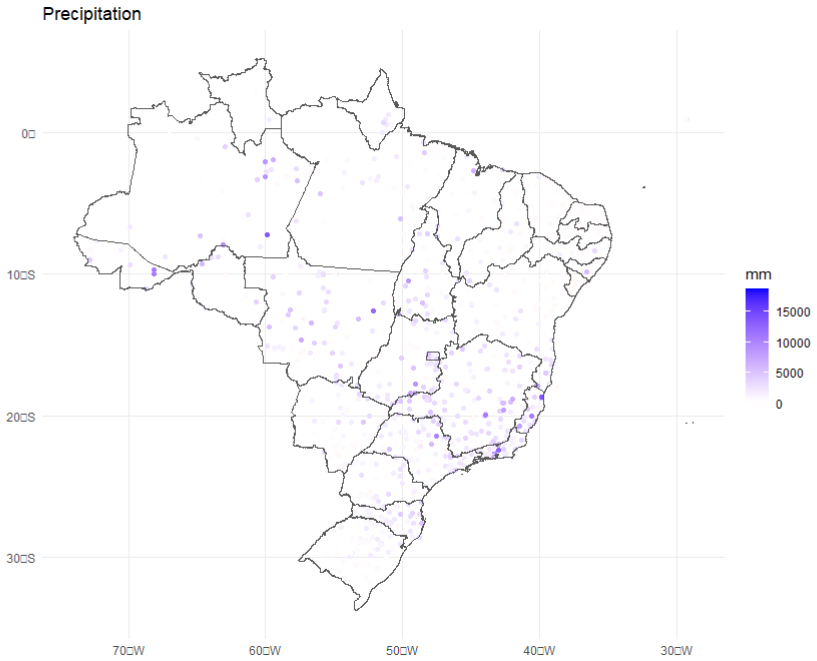

Source: own elaboration.

Figure 26 shows a theoretical expansion of this interpolation as a heat map.

Figure 26. Heat map of precipitation

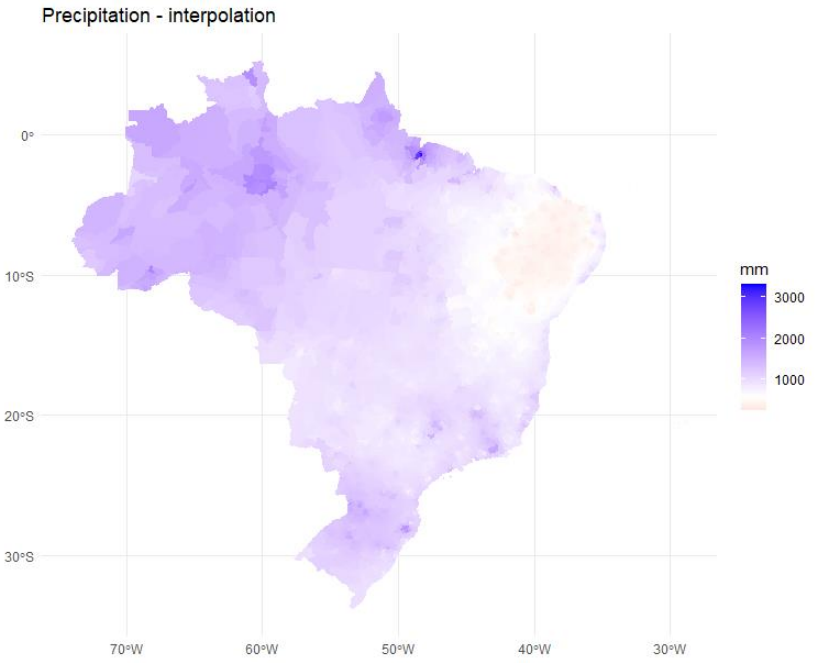

Source: own elaboration.

Finally, we examine the correlations between variables, which serve as additional information to guide the selection of variables to include in the model. Tables 8 to 10 display these correlations.

Table 8. List of Variables

Variable	Generic Code
Generation	Y
Upstream Level	X1
Downstream Level	X2
Useful Volume	X3
Affluent flow	X4
Effluent Flow	X5
Turbine Flow	X6
Spilled Flow	X7
Transferred Flow	X8
Natural Flow	X9
Artificial Flow	X10
Incremental Flow	X11
Net Evaporation Flow	X12
Consumptive Use Flow	X13
Precipitation	X14
Temperature	X15
Wind Speed	X16
Humidity	X17
month_dummy	X18
year_dummy	X19
Average Precipitation in the Last 3 Months	X20

Note: Generation is the generated energy in MWmed unit; Upstream Level is the water level (in meters) immediately upstream of a hydroelectric facility; Downstream Level is the water level (in meters) immediately downstream of a hydroelectric facility; Useful Volume refers to the available percentual of the reservoir's volume between the maximum normal operating level and the minimum normal operating level; Affluent Flow means the water flow (in m^3/s) that reaches a hydroelectric facility or a hydraulic structure; Effluent Flow is the water flow (in m^3/s) that leaves a hydroelectric plant or hydraulic structure; Turbine Flow is the water flow (in m^3/s) that passes through the turbines of a hydroelectric plant; Spilled Flow (in m^3/s) is the water flow released by a reservoir through surface spillways and/or bottom spillways; Natural Flow is the flow (in m^3/s) that would occur in a section of the river if there were not upstream, anthropic actions in the basin, such as the regularization of reservoirs, flow transfers and abstraction for various purposes; Incremental Flow is the flow (in m^3/s) resulting from the difference in natural flows between two completed sections of a watercourse; Net evaporation flow is the difference between actual evaporation from the reservoir lake and estimated actual evapotranspiration for that area under natural conditions and; Consumptive use flow is the water flow (in m^3/s) destined to the set of activities in which its use causes a decrease in available water resources, such as irrigation, animal husbandry and urban, rural and industrial supplies; Precipitation is the total amount of rain (mm); Temperature is the average temperature (°C); Wind Speed is the average wind speed (m/s); Humidity is the average air relative humidity (%); month_dummy is a dummy variable indicating the month of each observation, as year_dummy is the year for each observation; and Average Precipitation in the Last 3 Months is the average precipitation for each locality considering the observation's month and the previous two months.

Source: own elaboration.

Table 9. Pearson's Correlations

	Y	X1	X2	X3	X4	X5	X6	X7	X8	X9	X10	X11	X12	X13	X14	X15	X16	X17	X18	X19	X20
Y	1.0000	-0.0773	-0.1320	0.0641	0.6877	0.6813	0.6609	0.2256	0.1620	0.6744	0.6123	0.4583	0.1889	0.5450	0.0367	0.0660	0.1191	0.0049	-0.0148	-0.0058	0.0495
X1	-0.0773	1.0000	0.8795	0.4155	-0.1375	-0.1350	-0.1151	-0.0909	-0.0561	-0.1348	-0.0736	-0.1059	0.0482	-0.0505	-0.0460	-0.2716	0.0498	-0.1514	0.0088	0.1220	-0.0563
X2	-0.1320	0.8795	1.0000	0.3625	-0.1405	-0.1385	-0.1000	-0.0803	-0.0428	-0.1394	-0.1094	-0.1009	0.0536	-0.0461	-0.0369	-0.2041	-0.0072	-0.1824	0.0122	0.1636	-0.0473
X3	0.0641	0.4155	0.3625	1.0000	-0.0287	-0.0250	-0.0103	-0.0166	-0.0413	-0.0282	-0.0890	0.0226	0.1802	-0.0133	-0.0291	-0.0984	0.0405	-0.0460	-0.0544	-0.0157	0.0197
X4	0.6877	-0.1375	-0.1405	-0.0287	1.0000	0.9851	0.7982	0.7439	0.2134	0.9795	0.4983	0.7556	0.1067	0.4112	0.1000	0.1184	-0.0176	0.0700	-0.0686	0.0341	0.1357
X5	0.6813	-0.1350	-0.1385	-0.0250	0.9851	1.0000	0.8120	0.7441	0.0974	0.9625	0.4956	0.7175	0.1153	0.4275	0.0885	0.1175	-0.0065	0.0548	-0.0547	0.0266	0.1245
X6	0.6609	-0.1151	-0.1000	-0.0103	0.7982	0.8120	1.0000	0.3152	0.0247	0.7767	0.4171	0.5417	0.1414	0.5004	0.0646	0.1308	-0.0105	0.0064	-0.0237	0.0973	0.0891
X7	0.2256	-0.0909	-0.0803	-0.0166	0.7439	0.7441	0.3152	1.0000	0.1622	0.7271	0.1543	0.6623	-0.0090	0.0395	0.0920	0.0589	-0.0773	0.1025	-0.0696	0.0127	0.1290
X8	0.1620	-0.0561	-0.0428	-0.0413	0.2134	0.0974	0.0247	0.1622	1.0000	0.2035	0.1178	0.3450	-0.0178	-0.0080	0.0141	0.0508	-0.0691	0.0358	-0.0281	0.0685	0.0173
X9	0.6744	-0.1348	-0.1394	-0.0282	0.9795	0.9625	0.7767	0.7271	0.2035	1.0000	0.5424	0.7400	0.1095	0.3726	0.1184	0.1238	-0.0331	0.0976	-0.1081	0.0366	0.1607
X10	0.6123	-0.0736	-0.1094	-0.0890	0.4983	0.4956	0.4171	0.1543	0.1178	0.5424	1.0000	0.2061	0.2012	0.5866	0.0300	0.0228	0.1136	0.0183	-0.0452	-0.0123	0.0445
X11	0.4583	-0.1059	-0.1009	0.0226	0.7556	0.7175	0.5417	0.6623	0.3450	0.7400	0.2061	1.0000	0.0185	0.1393	0.0998	0.0861	-0.1068	0.1081	-0.0692	0.0525	0.1328
X12	0.1889	0.0482	0.0536	0.1802	0.1067	0.1153	0.1414	-0.0090	-0.0178	0.1095	0.2012	0.0185	1.0000	0.3827	-0.1182	0.0483	0.0574	-0.1855	-0.0109	0.0140	-0.1201
X13	0.5450	-0.0505	-0.0461	-0.0133	0.4112	0.4275	0.5004	0.0395	-0.0080	0.3726	0.5866	0.1393	0.3827	1.0000	-0.0969	0.0412	0.1378	-0.1762	0.0320	0.0594	-0.1069
X14	0.0367	-0.0460	-0.0369	-0.0291	0.1000	0.0885	0.0646	0.0920	0.0141	0.1184	0.0300	0.0998	-0.1182	-0.0969	1.0000	-0.0098	-0.1053	0.5870	-0.0649	-0.0305	0.7966
X15	0.0660	-0.2716	-0.2041	-0.0984	0.1184	0.1175	0.1308	0.0589	0.0508	0.1238	0.0228	0.0861	0.0483	0.0412	-0.0098	1.0000	-0.2236	-0.3400	-0.0192	0.0617	-0.0046
X16	0.1191	0.0498	-0.0072	0.0405	-0.0176	-0.0065	-0.0105	-0.0773	-0.0691	-0.0331	0.1136	-0.1068	0.0574	0.1378	-0.1053	-0.2236	1.0000	-0.2081	0.2026	-0.2367	-0.1819
X17	0.0049	-0.1514	-0.1824	-0.0460	0.0700	0.0548	0.0064	0.1025	0.0358	0.0976	0.0183	0.1081	-0.1855	-0.1762	0.5870	-0.3400	-0.2081	1.0000	-0.2265	-0.0820	0.6218
X18	-0.0148	0.0088	0.0122	-0.0544	-0.0686	-0.0547	-0.0237	-0.0696	-0.0281	-0.1081	-0.0452	-0.0692	-0.0109	0.0320	-0.0649	-0.0192	0.2026	-0.2265	1.0000	0.0000	-0.3377
X19	-0.0058	0.1220	0.1636	-0.0157	0.0341	0.0266	0.0973	0.0127	0.0685	0.0366	-0.0123	0.0525	0.0140	0.0594	-0.0305	0.0617	-0.2367	-0.0820	0.0000	1.0000	-0.0372
X20	0.0495	-0.0563	-0.0473	0.0197	0.1357	0.1245	0.0891	0.1290	0.0173	0.1607	0.0445	0.1328	-0.1201	-0.1069	0.7966	-0.0046	-0.1819	0.6218	-0.3377	-0.0372	1.0000

Source: own elaboration.

Table 10. Pearson's Correlation: Selected Model Variables

	Y	X3	X4	X14	X15	X16	X17	X20
Y	1,0000	0,0641	0,6877	0,0367	0,0660	0,1191	0,0049	0,0495
X3	0,0641	1,0000	-0,0287	-0,0291	-0,0984	0,0405	-0,0460	0,0197
X4	0,6877	-0,0287	1,0000	0,1000	0,1184	-0,0176	0,0700	0,1357
X14	0,0367	-0,0291	0,1000	1,0000	-0,0098	-0,1053	0,5870	0,7966
X15	0,0660	-0,0984	0,1184	-0,0098	1,0000	-0,2236	-0,3400	-0,0046
X16	0,1191	0,0405	-0,0176	-0,1053	-0,2236	1,0000	-0,2081	-0,1819
X17	0,0049	-0,0460	0,0700	0,5870	-0,3400	-0,2081	1,0000	0,6218
X20	0,0495	0,0197	0,1357	0,7966	-0,0046	-0,1819	0,6218	1,0000

Source: own elaboration.

Although Effluent Flow and Turbine Flow exhibit strong correlations with Energy Generation, they were excluded from consideration due to their high correlation with Affluent Flow. Essentially, when we have information about the water flow reaching the powerplant, it becomes redundant to also know the water flow reaching the turbines and subsequently exiting the system. This is especially true when there is a high degree of correlation between these flows, making Affluent Flow the more informative variable. Furthermore, among these three variables, Affluent Flow demonstrates the highest correlation with energy generation.

We kept both precipitation measures to assess which one yields superior results for the model.

4.3. The spatial model estimation

We started the modeling process by testing Equation 13 against some variations (i.e., inclusion/removal of variables and interactions). We then selected the best OLS fit by the adjusted R-squared value. Throughout these tests, we conducted the Hausman Test, which consistently favored fixed-effects, with a highly significant p-value (<0.01).

All models discussed in this section were estimated using Maximum Likelihood estimators. The chosen OLS model is represented by Equation 21:

$$E_{it} = \beta_0 + \beta_1 V_{it} + \beta_2 A_{it} + \beta_3 R_{3M\,it} + \beta_4 WS_{it} + \beta_5 H_{it} + \beta_6 V_{it} \times R_{3M\,it} + \beta_7 A_{it} \times R_{3M\,it} + \beta_8 WS_{it} \times H_{it} + \mu_i + \tau_t + v_{it} \quad (21)$$

where E is the generated energy, V is the reservoir's water volume, A is the affluent flow, R_3M is the average precipitation in the last 3 months, WS is the average wind speed and H is the air relative humidity level, μ and τ are fixed effects for individuals and time, respectively, and v_{it} is the disturbance term.

We found that the inclusion of a moving precipitation average increased the model's performance when compared to using only the monthly precipitation (R_{it}). We incorporated H and WS as control variables for precipitation, considering that their interaction might be related to air monsoons, which correlate with rainfall patterns. Temperature, on the other hand, exhibited little or no significance in most models, prompting its exclusion.

Table 11 presents the model coefficients, standard errors, and significance indicators. It also includes some of the other models we tested, offering a basis for comparison.

Table 11. OLS results

	OLS 1	**OLS 2**	**OLS 3**	**OLS 4**	**OLS 5**	**OLS 6**	**OLS 7**
Formula	V+A+R+T+WS+H	V*R+A*R+WS+H*R	V+A*R+WS*H	V+A*R+WS*H*R+T	V*R_3M+A*R_3M+WS*H*R_3M+T	V*R_3M+A*R_3M+WS*H	V*R_3M+A*R_3M+WS*H+T
V	1592.9494***	1628.1***	1587.3***	1577.8***	1574.3***	1602.6***	1573.4***
	(60.381)	(67.3430)	(59.918)	(60.2990)	(74.22)	(73.568)	(74.245)
A	63.3813***	73.873***	73.667***	73.922***	88.256***	87.791***	87.8600***
	(0.5567)	(0.8797)	(0.87944)	(0.8826)	(1.0863)	(1.0809)	(1.0811)
R	7.1098***	22.3710*	11.359***	-94.01**			
	(1.3977)	(9.7036)	(1.3771)	(34.3860)			
R_3M					-166.22***	16.065***	18.13***
					(35.86)	(1.9687)	(2.0935)
T	-912.3535°			-1833.6***	-1412.6000**		-1455.7**
	(492.118)			(521.3800)	(526.02)		(502.43)
WS	7593.9173***	8057***	53166***	42634***	30345*	54884***	55018***
	(2214.2409)	(2189.5000)	(9919)	(11695)	(12373)	(9840.5)	(9839.4)
H	-177.955	-199.1600	1455.8***	1090*	658.58	1533.9***	1347.1***
	(158.0674)	(146.6700)	(387.99)	(462.21)	(494.89)	(387.82)	(393.1)
V*R		-0.0398					
		(0.0314)					
A*R		-0.0050***	-0.0050***	-0.0051***			
		(0.0003)	(0.0003)	(0.0003)			
V*R_3M					-0.0778*	-0.0806*	-0.0764*
					(0.0372)	(0.0372)	(0.0372)
A*R_3M					-0.0106***	-0.0103***	-0.0104***
					(0.0004)	(0.0004)	(0.0004)
WS*H			-699.53***	-611.03**	-433.24***	-706.18***	-715.96***
			(149.78)	(187.38)	(200.84)	(149.11)	(149.13)
WS*R				58.242***			

	OLS 1	OLS 2	OLS 3	OLS 4	OLS 5	OLS 6	OLS 7
				(14.351)			
H*R		-0.1264		1.3734**			
		(0.1274)		(0.45)			
WS*R_3M					80.91*		
					(15.561)		
H*R_3M					2.3975***		
					(0.4766)		
WS*H*R				-0.7523***			
				(0.1882)			
WS*H*R_3M					-1.0481***		
					(0.2066)		
Adjusted R^2	0.31839	0.32351	0.32396	0.32457	**0.3344**	0.33371	0.33387
AIC	833,318	833,087.8	833,066.4	833,042.3	**832,591.7**	832,619.9	832,613.4
BIC	834,635	834,421.4	834,391.7	834,401	833,958.7	**833,953.5**	833,955.4
n	151	151	151	151	151	151	151
t	204	204	204	204	204	204	204

Note: The standard errors are shown between parentheses. The models include a μ and τ vectors for spatial and temporal fixed-effects.

Statistical significance: *** p<0.001; ** p<0.01; * p<0.05; ° p<0.1.

Source: own elaboration.

None of the models exhibited statistical significance for R_3M when it was already included in the model along with R. Consequently, we faced the decision of selecting between these two variables for the final model and the insurance index. The models featuring R_3M presented best fit, hence we opted for this variable as the index. It better captures the dynamics of drought crises since it considers a more extended time frame. Additionally, R_3M exhibits significant interaction with volume, while R does not. This is likely because storage powerplants take longer to manifest the effects of drought, as they possess larger water reserves, and the water usage can be adjusted according to the energy demand to prevent rapid depletion of these reserves.

Models 5 (by adjusted R-squared and AIC criterion) and 6 (by BIC criterion) were considered the best. The discrepancy in the statistical measures between them is negligible, prompting our decision in favor of Model 6 for the sake of simplicity and ease of interpretation. In this selected model (Model 6), the precipitation index interacts solely with A and V, rendering it a more straightforward and direct measure for the PI. The interaction of WS and H can be attributed to the influence of air monsoons, but the inclusion of a temporally lagged precipitation measure would add complexity to the interpretation. The inclusion of temperature does not yield improvements to this model, as shown in model 7. Besides, the BIC criterion is particularly suited for large samples, as it is the case of our dataset.

As expected, the positive coefficients for water volume, affluent flow and precipitation signify a direct, proportional relationship with generation. In other words, higher levels of rain or increased water flow/volume correspond to higher energy generation, while a lack of rain or reduced water flow/volume results in decreased energy output. The negative signs for the interactions indicate that they slightly reduce the individual effects of the variables, which is also true for wind speed and humidity.

The decision not to transform the variables into logarithmic form was based on the presence of zero values in many of them, which would make impossible the application of logarithmic functions without prior treatment. With the OLS chosen, we conducted LM tests on the model residuals to assess spatial dependency.

We crafted four different weighting matrices: k-nearest neighbors for 3 and 5 neighbors, and inverse distance for 15 and 30 kilometers. All matrices were binary in style. The results for LM tests for all the weighting matrices are presented in Table 12.

Table 12. LM Tests

	3-knn Matrix	**5-knn Matrix**	**15 km Dist. Matrix**	**30 km Dist. Matrix**
LMlag	129.38	110.3	4.2512	4.3012
p-value	<0.001	<0.001	0.03922	0.03809
LMerror	64.79	65.75	3.3725	3.4198
p-value	<0.001	<0.001	0.06629	0.06442
RLMlag	83.945	50.624	2.7931	2.7747
p-value	<0.001	<0.001	0.09467	0.09576
RLMerror	19.354	6.0691	1.9144	1.8933
p-value	<0.001	0.01376	0.1665	0.1688

Source: own elaboration.

From Table 9, we infer that the SAR model (LMlag and RLMlag) appears to be more suitable for all matrices. For the distance matrixes, the SEM model (LMerror and RLMerror) does not exhibit significance in the robust LM tests. For the 5-knn matrix, although both are significant in all tests at a 5% significance level, SAR yields a smaller p-value. Meanwhile,

for the 3-knn matrix, both SAR and SEM are significant at the 1% significance level, possibly indicating a SARAR model.

Since the LM tests indicated the existence of spatial effects, we estimated SLX models, with the same variables as the OLS, to determine the most suitable weighting matrix. The results are presented in Table 13.

Table 13. SLX models' results for different W matrices

	3-knn Matrix	**5-knn Matrix**	**15 km Dist. Matrix**	**30 km Dist. Matrix**
Useful Volume	1525.2***	1537.8***	1584.7***	1584.5
	(74.125)	(74.224)	(73.746)	(73.765)
Affluent Flow	88.185***	87.987***	87.736***	87.739
	(1.0801)	(1.0812)	(1.0809)	(1.0809)
Average 3-months Precipitation	16.065***	19.982***	16.247***	16.276
	(1.9687)	(2.1961)	(1.9836)	(1.9849)
Wind	52983***	50749***	55150***	55063
	(9932.2)	(9978.8)	(9855.5)	(9856.7)
Humidity	1734.8***	1739.8***	1601.7***	1601.2
	(392.03)	(392.74)	(388.72)	(388.78)
Useful Volume * Average 3-months Precipitation	-0.0694°	-0.0711°	-0.0813*	-0.0815
	(0.0372)	(0.0372)	(0.0373)	(0.0373)
Affluent Flow * Average 3-months Precipitation	-0.0105***	-0.0104***	-0.0103***	-0.0103
	(0.0004)	(0.0004)	(0.0004)	(0.0004)
Wind Speed*Humidity	-725.46***	-703.35***	-724.85***	-723.48
	(149.16)	(149.45)	(149.35)	(149.36)
Laged Useful Volume	188.64***	141.93***	9.0193***	8.6544
	(33.316)	(24.578)	(2.283)	(2.2738)
Laged Affluent Flow	2.8154***	1.5791***	0.0185	0.0199
	(0.3299)	(0.259)	(0.024)	(0.024)
Laged Average 3-months Precipitation	-3.7288***	-1.4725*	0.0108	0.0109
	(0.8463)	(0.5911)	(0.017)	(0.017)
Laged Wind Speed	3438.6**	3274***	59.287*	60.045
	(1092.4)	(734.79)	(24.386)	(24.35)
Laged Humidity	-85.037	-67.011	-2.6189	-2.6784
	(74.541)	(50.295)	(1.8238)	(1.8216)
AIC	**832,177.2**	832,214.7	832,303.1	832,303.8
BIC	**832,293.9**	832,331.4	832,419.8	832,420.5
n	151	151	151	151
t	204	204	204	204

Note: The standard errors are shown between parentheses. The models include a μ and τ vectors for spatial and temporal fixed effects. Statistical significance: *** p<0.001; ** p<0.01; * p<0.05; ° p<0.1.

Source: own elaboration.

The significance of lagged variables from the SLX models, particularly in the case of knn-type matrices, could be attributed to the spatial proximity of powerplants within the same basin. This suggests that the energy generation of a powerplant may not only be explained by

its own water flow/volume levels but also by the levels of its nearest neighbors, as they share common watercourses and meteorological conditions.

From Table 13, the weighting matrix using the 3 nearest neighbors is the most suitable, given its lower AIC and BIC. We then proceeded to test the spatial models using this particular W matrix. As shown in Table 12, both SAR and SEM exhibit significance for this matrix. Therefore, we tested both of them, in addition to SARAR, which combines the spatial lag and error. The results and comparison of the models are presented in Table 14.

Table 14. Results for different model structures estimation

	OLS	**SLX**	**SAR**	**SEM**	**SARAR**
Useful Volume	1602.6***	1525.2***	1600***	1605.1***	1613.4***
	(73.568)	(74.125)	(75.127)	(75.342)	(74.99)
Affluent Flow	87.791***	88.185***	88.961***	88.751***	89.061***
	(1.0809)	(1.0801)	(1.0742)	(1.0758)	(1.0743)
Average 3-months Precipitation	11.3590***	16.065***	20.704***	20.805***	20.604***
	(1.3771)	(1.9687)	(2.3001)	(2.3048)	(2.2967)
Wind Speed	54884***	52983***	38915***	38985***	3844***
	(9840.5)	(9932.2)	(10333)	(10352)	(10319)
Humidity	1533.9***	1734.8***	1762.8***	1791.1***	1755.5***
	(387.82)	(392.03)	(407.05)	(407.77)	(406.59)
Useful Volume* Average 3-months Precipitation	-0.0806*	-0.0694°	-0.068°	-0.0707°	-0.0701°
	(0.0372)	(0.0372)	(0.037)	(0.0371)	(0.037)
Affluent Flow* Average 3-months Precipitation	-0.0103***	-0.0105***	-0.0106***	-0.01056***	-0.0106***
	(0.0004)	(0.0004)	(0.0003)	(0.0003)	(0.0003)
Wind Speed*Humidity	-706.18***	-725.46***	-688.6***	-682.53***	-688.13***
	(149.11)	(149.16)	(154.35)	(154.62)	(154.17)
Laged Water Volume		188.64***			
		(33.316)			
Laged Affluent Flow		2.8154***			
		(0.3299)			
Laged Average 3-months Precipitation		-3.7288***			
		(0.8463)			
Laged Wind Speed		3438.6**			
		(1092.4)			
Laged Humidity		-85.037			
		(74.541)			
ρ			0.0267945***		0.0345518***
			(0.0021289)		(0.0044424)
λ				0.0151150***	-0.0133444*
				(0.002443)	(0.0054031)
AIC	832,619.9	832,177.2	831,693.1	831,868.8	**831,671.8**
BIC	833,953.5	832,293.9	831776.4	831,952.2	**831,763.5**
n	151	151	151	151	151

t	204	204	204	204	204
Hausman Test – Fixed x random Effects	Fixed Effects p<0.001	Fixed Effects p<0.001	Fixed Effects p<0.001	Fixed Effects p<0.001	Fixed Effects p<0.001
Haussman Test – Fixed Effects x Pooling	Fixed Effects p<0.001	Fixed Effects p<0.001	Fixed Effects p<0.001	Fixed Effects p<0.001	Fixed Effects p<0.001

Note: The standard errors are shown between parentheses. The models include a μ and τ vectors for spatial and temporal fixed effects. The SARAR model returned null log-likelihood, so we could not calculate its AIC nor its BIC. Statistical significance: *** p<0.001; ** p<0.01; * p<0.05; ° p<0.1.

The fixed-effects SARAR is the most suitable model, with smaller AIC and BIC values, for explaining and predicting the powerplant's energy generation. The chosen model, therefore, can be expressed as in Equation 22:

$$E_{it} = \rho W E_{it} + \beta_1 V_{it} + \beta_2 A_{it} + \beta_3 R_{3M\,it} + \beta_4 WS_{it} + \beta_5 H_{it} + \beta_6 V_{it} \times R_{3M\,it} + \beta_7 A_{it} \times R_{3M\,it} + \beta_8 WS_{it} \times H_{it} + \mu + \tau + \lambda W u_{it} + \mu_i + \tau_t + v_{it} \quad (22)$$

The presence of a ρ term, associated with the W matrix, implies that the powerplant's energy generation can be explained not only by its own measurements of water flow/volume and the regional meteorological conditions, but also by the energy generated by its neighboring powerplants. This suggests that the conditions of a powerplant are closely related to those of its nearest neighbors, often sharing the same basin and, as a result, experiencing similar watercourses and meteorological conditions. The positive sign of ρ further indicates that variations in energy generation typically occur in the same direction for a powerplant and its neighbors.

The interpretation of the λ term suggests the existence of random shock effects on neighboring powerplants, which negatively affect the energy generation of the observed powerplant but are not captured by the variables in the model. One such effect could be the MRE mechanism. Given the highly interconnected nature of the Brazilian electrical system, with minimum energy generation targets established for each powerplant and periodically revised by ONS, a powerplant's energy generation is also contingent on the energy demand and the generated levels by all other suppliers in the electrical system. This is an omitted variable to the model, which the λ term helps capture.

In addition to the model's coefficients, it is important to assess the direct and indirect effects of the variables when dealing with a SARAR model. The interpretation of the coefficients in this case is not straightforward due to the spillovers between the terms in the data generation process (Kelejian & Piras, 2017; LeSage & Pace, 2009). Table 15 presents such effects.

Table 15. Direct, Indirect and Total Effects for SARAR model

	Direct	**Indirect**	**Total**
Useful Volume	1613.44	57.72	1671.16
Affluent Flow	89.06	3.19	92.25
Average 3-months Precipitation	20.60	0.74	21.34
Wind Speed	38440.31	1375.17	39815.49
Humidity	1755.51	62.80	1818.31
Useful Volume* Average 3-months Precipitation	-0.07	0.00	-0.07
Affluent Flow* Average 3-months Precipitation	-0.01	0.00	-0.01
Wind Speed* Humidity	-688.14	-24.62	-712.76

Source: own elaboration.

In Table 15, the total effects encompass the coefficients derived from the SARAR model presented in Table 14, augmented by the spillovers' effects. These total effects are further divided into direct and indirect effects. Direct effects pertain to the impact that a change in a specific variable (x_{it}) has on the predicted energy generation (y_{it}), for the same powerplant. In contrast, indirect effects denote the influence that this change in x_{it} has on the energy generation y_{jt}, for neighboring powerplants, where i and j represent neighboring units.

For instance, *ceteris paribus*, an increase of 1 meter in the useful volume of a powerplant's reservoir yields a direct effect of 1,613.44 MWmed increase in that powerplant's energy generation. This change also induces a 57.72 MWmed increase for the three nearest neighboring powerplants energy generation, cumulatively resulting in a 1,671.16 increase in energy generation for the entire system.

We will use the direct effect coefficients to estimate the insurance payout, as they serve as predictors for a powerplant's expected energy generation.

4.4. Defining the Insurance Trigger

Following Kusuma et al. (2018), we employ a clustering technique to identify instances in which both E and R_3M were low levels. We compute the average R_3M and designated it as the initial trigger (other scenarios will be assessed further in this section). Additionally, the 2.5% quantile of R_3M within the lower cluster was designated as the exit threshold, meaning the maximum indemnity limit. The chosen technique was the k-means clustering, a widely employed and well-established clustering algorithms (Hair Jr et al., 2014).

As each powerplant exhibits unique characteristics, we cannot define a one-size-fits-all trigger that applies to all of them. Therefore, this aspect of the insurance contract must be tailored to each powerplant individually. We will present the calculations for the two largest energy generators from each region, one representing a run-of-river powerplant and another with water storage. The selected powerplants are: Itaipu and Salto Santiago (South), Belo Monte and Tucuruí (North), Xingó and Luiz Gonzaga (Northeast) and Porto Primavera and Ilha Solteira (Southeast).

For all these powerplants, we conducted data clustering into three groups. This number was determined as optimal based on a scree plot analysis, the results of which are displayed in Figure 27.

Figure 27. Scree Plots

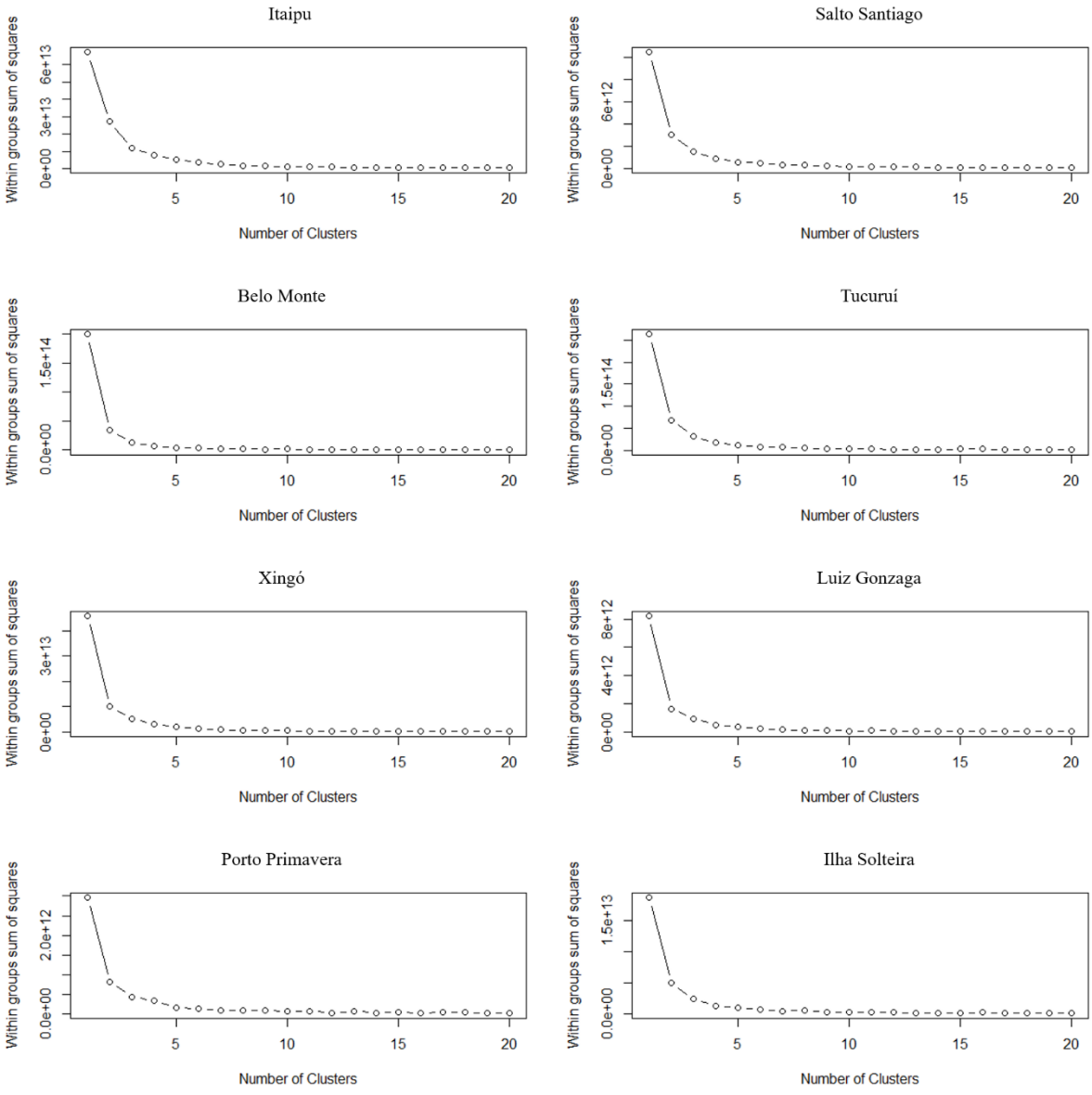

Source: own elaboration.

When we clustered the energy generation based solely on precipitation, the resulting clusters did not exhibit a well-ordered structure concerning generation values, as one can see on Figure 28. This discrepancy is likely due to the fact that low levels of rainfall do not always immediately translate to low levels of energy generation. Powerplants typically maintain water reserves for weather drought periods, which means it may require an extended period of low rainfall levels to jeopardize their generation capacity, especially for larger powerplants. Consequently, low levels of precipitation can still be associated with some instances of medium or high energy generation, as illustrated in Figure 28.

Figure 28. Energy Generation x Average Precipitation Clusters

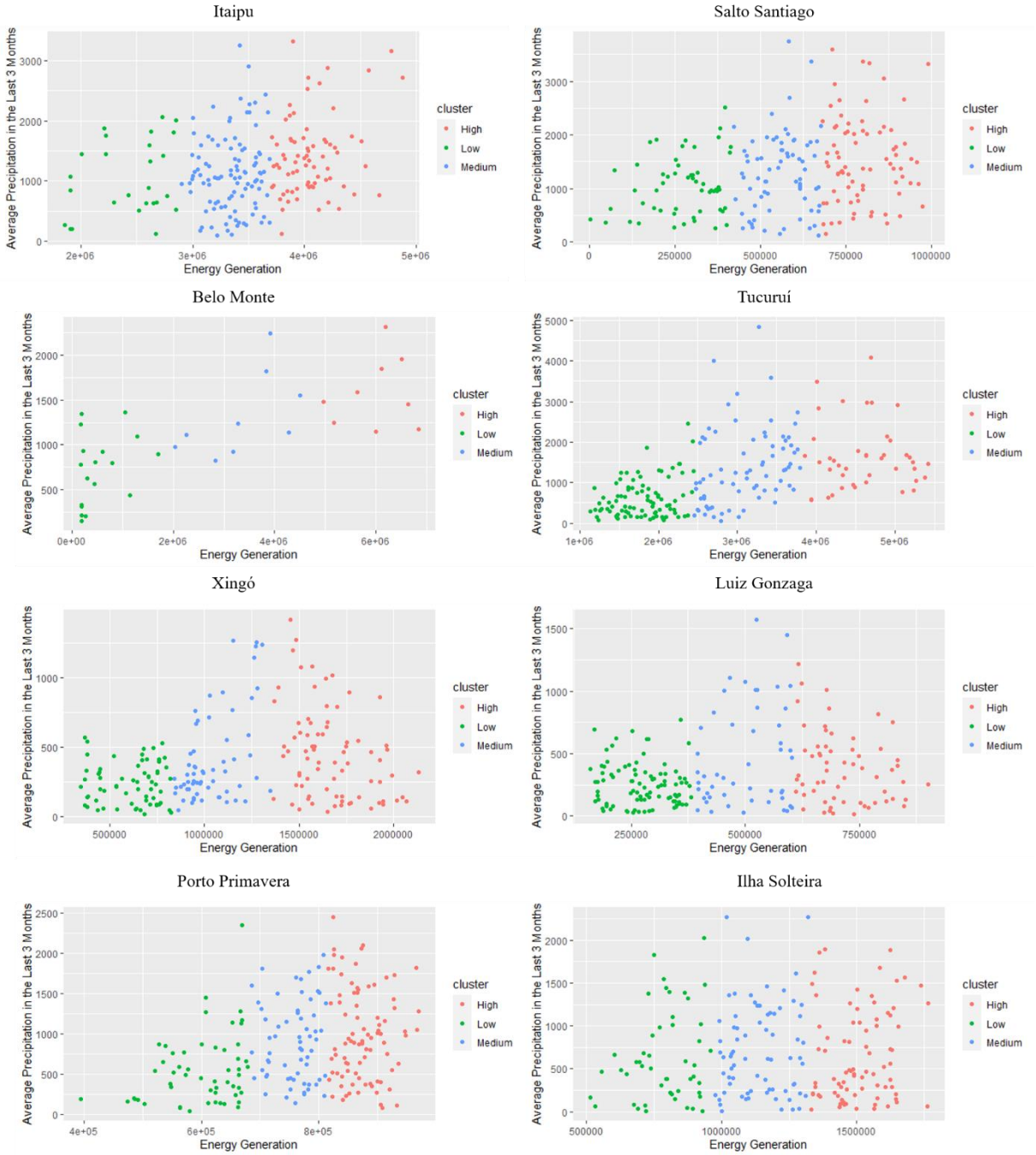

Note: for Belo Monte, it was considered only the data from January 2020 forward, when the series gains stationarity, so that there is no bias from the early years when the energy generation levels were lower.

Source: own elaboration.

Belo Monte stands as an exception, where the variables display a more distinct correlation and low levels of R_3M consistently correspond to low levels of energy generation.

Relying the parametric insurance scheme solely on the precipitation index would result in the insurance being triggered more frequently than necessary. To address this issue, we decided to set the trigger not only on precipitation, but as a combination of precipitation and water flow (for run-of-river powerplants) or precipitation and water volume (for water storage powerplants). These variables exhibit stronger correlations with energy generation and

interact with the R_3M variable in the econometric model. This adjustment led to a redefined cluster structure, now in a 3-D perspective, as depicted in Figure 29.

Figure 29. Clusters in a 3-D Perspective

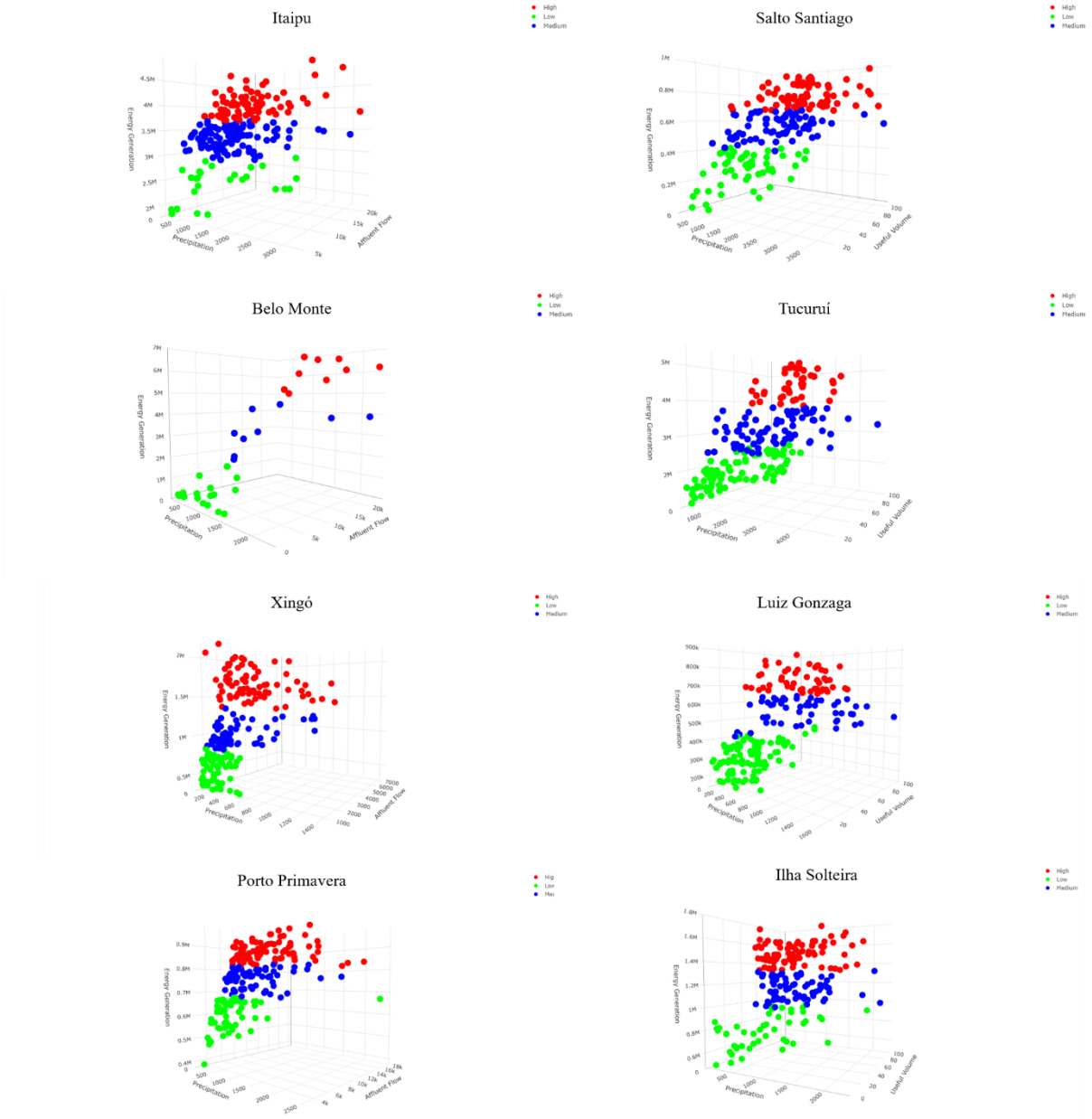

Note: for Belo Monte, it was considered only the data from January 2020 forward, when the series gains stationarity, so that there is no bias from the early years when the energy generation levels were lower.

Source: own elaboration.

An inquiry may arise concerning the need for two triggering indexes, prompting a consideration of utilizing either Affluent Flow or Useful Volume as the sole trigger. When examining Affluent Flow, there is an evident structure in the observations that is substantial enough to allow a PI mechanism triggered solely by this variable. In contrast, when focusing on Useful Volume, the data exhibits even greater dispersion than with the average precipitation, rendering it unfeasible to use solely this variable. Therefore, for water storage-type powerplants, a combination of both volume and rainfall levels is imperative. These results are presented in Figure 30.

Figure 30. Energy Generation x Affluent Flow/Useful Volume

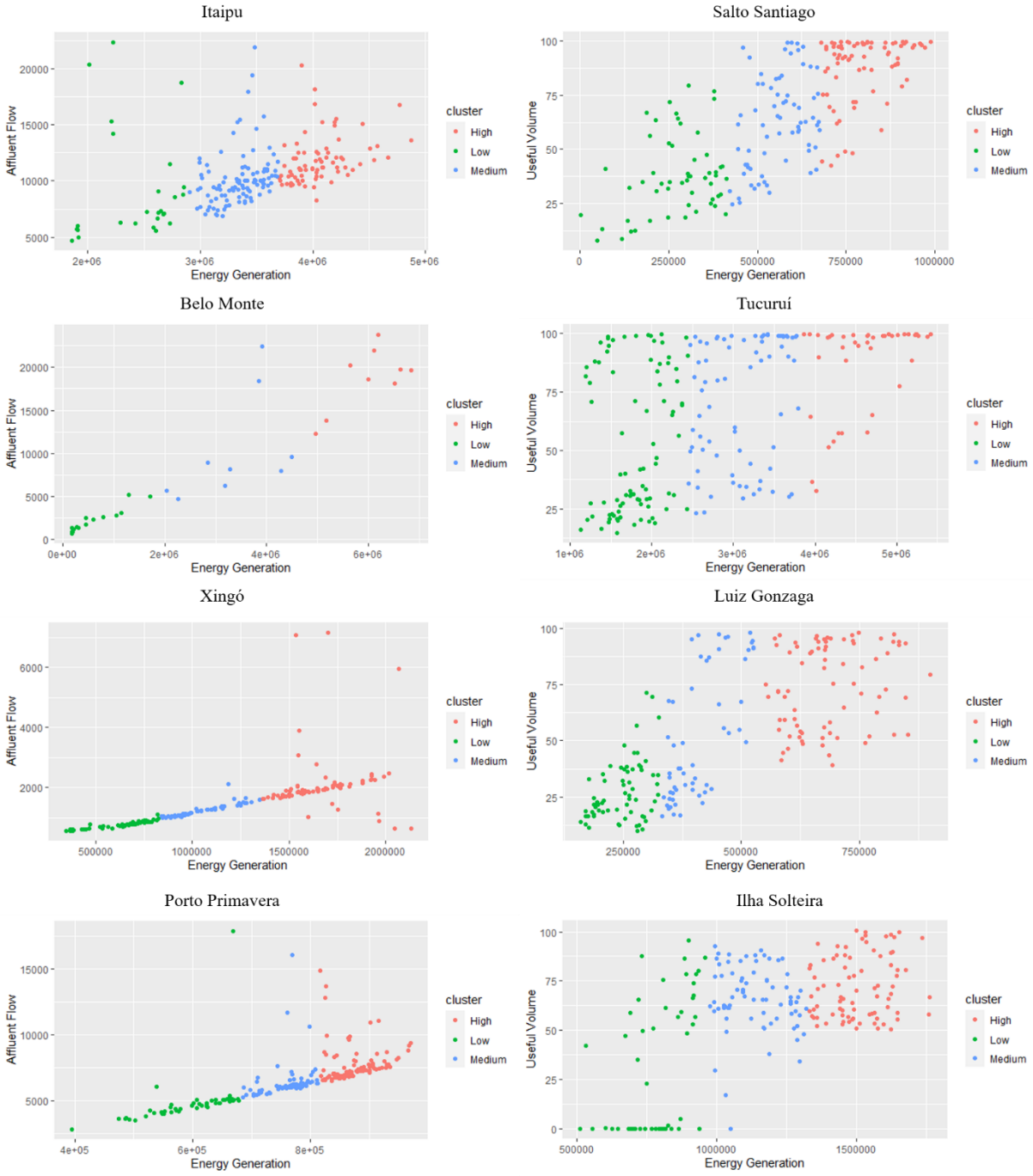

Note: for Belo Monte, it was considered only the data from January 2020 forward, when the series gains stationarity, so that there is no bias from the early years when the energy generation levels were lower.

Source: own elaboration.

For the sake of standardization, and given the variables interactions in the SARAR model, we will employ the bivariate trigger for all powerplants, although it is worth noting that the results of an affluent flow trigger for the run-of-river powerplants could also be assessed. Utilizing the 3-D lower clusters, the defined trigger and exit thresholds for each simulated scenario, as outlined in Table 16.

Table 16. Triggers and Exit Thresholds

	R_3M Trigger					R_3M Exit Threshold		
Powerplant	Average	Median	35% Quantile	30% Quantile	1st Quartile	5% Quantile	2.5% Quantile	1% Quantile
Itaipu	1046.11	858.50	642.69	634.24	642.69	195.76	165.50	138.41
Salto Santiago	1046.37	973.85	719.08	623.11	589.21	322.70	291.88	264.90
Belo Monte	722.89	789.96	555.17	452.48	356.65	199.06	175.88	161.97
Tucuruí	608.42	466.80	322.84	290.47	243.72	119.84	93.06	74.84
Xingó	242.67	230.26	152.81	130.72	106.29	47.10	46.13	34.34
Luiz Gonzaga	266.31	267.59	178.13	158.40	131.17	37.52	34.38	30.76
Porto Primavera	540.72	464.62	272.85	260.94	186.96	83.67	77.35	56.86
Ilha Solteira	631.62	505.96	368.34	267.07	223.40	33.77	12.00	6.94
	A/V Trigger					A/V Exit Threshold		
Powerplant	Average	Median	35% Quantile	30% Quantile	1st Quartile	5% Quantile	2.5% Quantile	1% Quantile
Itaipu	9160.68	7146.32	6282.79	6212.97	6282.79	5107.42	4849.49	4752.89
Salto Santiago	37.82	35.49	30.76	28.56	24.54	12.36	9.76	8.25
Belo Monte	1964.42	1399.96	1107.74	934.07	871.16	818.85	751.87	711.69
Tucuruí	53.10	41.11	30.07	28.04	26.26	19.06	16.87	15.87
Xingó	732.81	745.03	696.37	648.41	609.81	562.17	556.47	554.07
Luiz Gonzaga	27.17	23.34	19.00	18.42	17.14	11.63	11.01	10.35
Porto Primavera	4845.22	4723.92	4216.74	4352.28	4213.87	3582.68	3538.91	3201.40
Ilha Solteira	32.49	22.84	0.00	0.00	0.00	0.00	0.00	0.00

Source: own elaboration.

Ilha Solteira presents a great deal of zeros in its volume data. However, these zeros are, most likely, measurement errors, as there is energy generation in all months, besides this being the largest hydroelectric plant in the state of São Paulo, with large reservoirs that would hardly ever be at zero capacity.

To calculate the payout and premium with 2 triggers, we redefine Equation 7 as:

$$S(I_{w,m}) = G_w \times (I_{w,m})$$

$$= G_w \times \begin{cases} 0 & R\_3M_{o,m} > R\_3M_{Tr}\ or\ A_{o,m} > A_{Tr} \\ \alpha(R\_3M_{Tr} - R\_3M_{o,m}) + \beta(A_{Tr} - A_{o,m}) + \phi(R\_3M_{Tr} - R\_3M_{o,m})(A_{Tr} - A_{o,m}) & R\_3M_E < R\_3M_{o,m} < R\_3M_{Tr}\ and\ A_E < A_{o,m} < A_{Tr} \\ \alpha(R\_3M_E - R\_3M_{o,m}) + \beta(A_E - A_{o,m}) + \phi(R\_3M_E - R\_3M_{o,m})(A_E - A_{o,m}) & R\_3M_{o,m} < R\_3M_E\ and\ A_{o,m} < A_E\ and\ R\_3M_{o,m} < R\_3M_{Tr}\ and\ A_{o,m} < A_{Tr} \\ \alpha(R\_3M_E - R\_3M_{o,m}) + \beta(A_{Tr} - A_{o,m}) + \phi(R\_3M_E - R\_3M_{o,m})(A_{Tr} - A_{o,m}) & R\_3M_{o,m} < R\_3M_E\ and\ R\_3M_{o,m} < R\_3M_{Tr}\ and\ A_{o,m} < A_{Tr} \\ \alpha(R\_3M_{Tr} - R\_3M_{o,m}) + \beta(A_E - A_{o,m}) + \phi(R\_3M_{Tr} - R\_3M_{o,m})(A_E - A_{o,m}) & A_{o,m} < A_E\ and\ R\_3M_{o,m} < R\_3M_{Tr}\ and\ A_{o,m} < A_{Tr} \end{cases} \quad (23)$$

where $R\_3M_{o,m}$ is the observed precipitation at each month m, R_3M_{Tr} is the precipitation trigger, R_3M_E is the precipitation exit threshold, $A_{o,m}$ is the observed affluent flow at each month m, A_{Tr} is the affluent flow trigger and A_E is the affluent flow exit threshold. α, β and ϕ are the direct effects coefficients estimated for the SARAR model for R_3M, A and their interaction, respectively. In the case of water storage powerplants, A is replaced by V (useful volume). The precipitation measure R_3M is the average precipitation in the last 3 months.

And Equation 9 as:

$$P_m = \frac{1}{M}\sum_{m=1}^{M} \mathbb{P}(I_i) \times S\left(I_{w,m}\right) = \frac{1}{M}\sum_{m=1}^{M} \left(F(R_{Tr}) - F(R_E)\right) \times \left(F(A_{Tr}) - F(A_E)\right) \times S\left(I_{w,m}\right) \quad (24)$$

It is important to point out that, when we simply multiply $\left(F(R_{Tr}) - F(R_E)\right)$ and $\left(F(A_{Tr}) - F(A_E)\right)$, we are treating these variables as independent, which may not be entirely accurate, as shown in Table 9 and evident in the econometric model, where they interact. Ideally, the most appropriate approach would be to assess their joint distribution. However, to simplify the calculations, we will assume their independence here.

4.5. Results with spatial econometrics and clusters

For simplification purposes, we assume a constant on-grid energy price (G_w) of 260,46 R$/MWh, which is the current generation energy tariff for residential consumers in Brazil[3]. Since the tariff is stated in MWh, we need to multiply the MWmed energy generation data by the number of productive hours on each month to obtain the corresponding MWh measurement. We utilize the measure from the powerplants' latest official reports. In cases where this information is not explicitly stated, we assume it to be 95% of the total amount of hours in a month, accounting for a small allocation of hours for maintenance purposes.

To determine $F(R\_3M_{Tr})$, $F(R\_3M_E)$, $F(A_{Tr})$ (or $F(V_{Tr})$) and $F(A_E)$ (or $F(V_E)$), we estimate the distributions of R_3M, A and V for the measurements of each powerplant. The best-fit results, chosen based on the BIC, are presented in Table 17 and depicted in Figures 31 to 46.

[3] https://www.enel.com.br/pt-saopaulo/Para_Voce/tarifa-energia-eletrica.html

Table 17. Distributions and Frequency Probabilities

Distributions with best fit			$F(R\_3M_{Tr})$					$F(R\_3M_E)$		
Powerplant	R_3M	A/V	Average	Median	35% Quantile	30% Quantile	1st Quartile	5% Quantile	2.5% Quantile	1% Quantile
Itaipu	Weibull	Gamma	0.4442	0.3305	0.2051	0.2005	0.2051	0.0229	0.0166	0.0118
Salto Santiago	Weibull	Weibull	0.4078	0.3678	0.2301	0.1818	0.1655	0.0576	0.0481	0.0403
Belo Monte	Weibull	Student-t	0.2860	0.3329	0.1771	0.1197	0.0749	0.0230	0.0178	0.0150
Tucuruí	Gamma	Weibull	0.3402	0.2494	0.1554	0.1347	0.1057	0.0375	0.0255	0.0182
Xingó	Gamma	Student-t	0.4122	0.3905	0.2460	0.2031	0.1558	0.0503	0.0488	0.0316
Luiz Gonzaga	Gamma	Weibull	0.4991	0.5012	0.3419	0.3027	0.2467	0.0527	0.0470	0.0405
Porto Primavera	Weibull	Student-t	0.3435	0.2821	0.1334	0.1249	0.0759	0.0220	0.0194	0.0120
Ilha Solteira	Weibull	Normal	0.5817	0.4886	0.3691	0.2702	0.2251	0.0269	0.0080	0.0042
Distributions with best fit			$F(A_{Tr})$ **or** $F(V_{Tr})$					$F(A_E)$ **or** $F(V_E)$		
Powerplant	R_3M	A/V	Average	Median	35% Quantile	30% Quantile	1st Quartile	5% Quantile	2.5% Quantile	1% Quantile
Itaipu	Weibull	Gamma	0.3269	0.1017	0.0470	0.0437	0.0470	0.0110	0.0074	0.0063
Salto Santiago	Weibull	Weibull	0.1529	0.1306	0.0909	0.0751	0.0506	0.0082	0.0044	0.0028
Belo Monte	Weibull	Student-t	0.5631	0.3937	0.2537	0.1555	0.1201	0.0922	0.0600	0.0435
Tucuruí	Gamma	Weibull	0.3459	0.2030	0.1002	0.0851	0.0729	0.0340	0.0253	0.0218
Xingó	Gamma	Student-t	0.1391	0.1523	0.1024	0.0617	0.0366	0.0158	0.0141	0.0134
Luiz Gonzaga	Gamma	Weibull	0.1996	0.1530	0.1056	0.0998	0.0874	0.0423	0.0381	0.0339
Porto Primavera	Weibull	Student-t	0.1633	0.1346	0.0446	0.1249	0.0443	0.0037	0.0029	0.0003
Ilha Solteira	Weibull	Normal	0.1509	0.0822	0.0127	0.0127	0.0127	0.0127	0.0127	0.0127

Source: own elaboration.

It is noteworthy that, aside from Ilha Solteira's water volume, all best-fitted distributions are heavy-tailed. This is in accordance with the histograms presented in Figure 24, which show that, generally, the explicatory variables data is right-skewed. Figures 31 to 46 show the distributions adjustment to the data, recalling that our interest relies mainly on the left tails, where the triggers are localized.

Figure 31. Average 3-months Precipitation – Weibull Fit - Itaipu

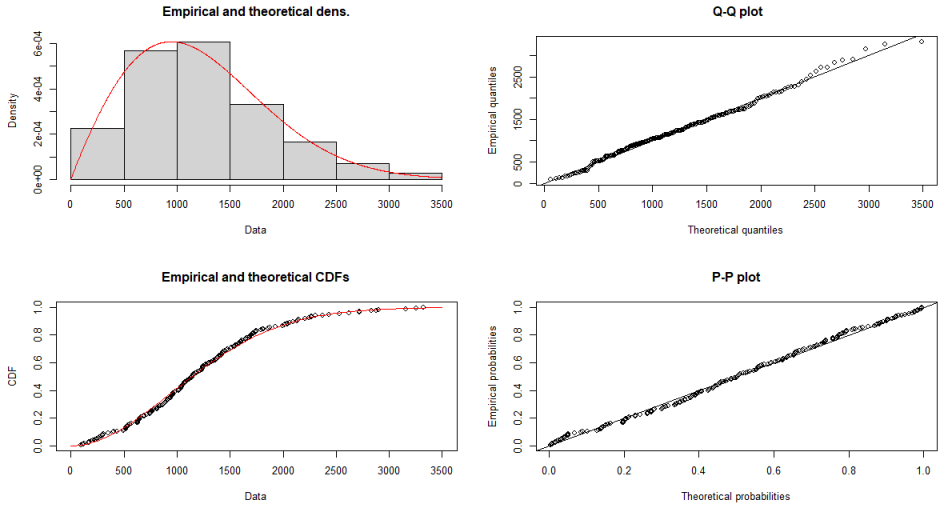

Source: own elaboration.

Figure 32. Affluent Flow – Gamma Fit - Itaipu

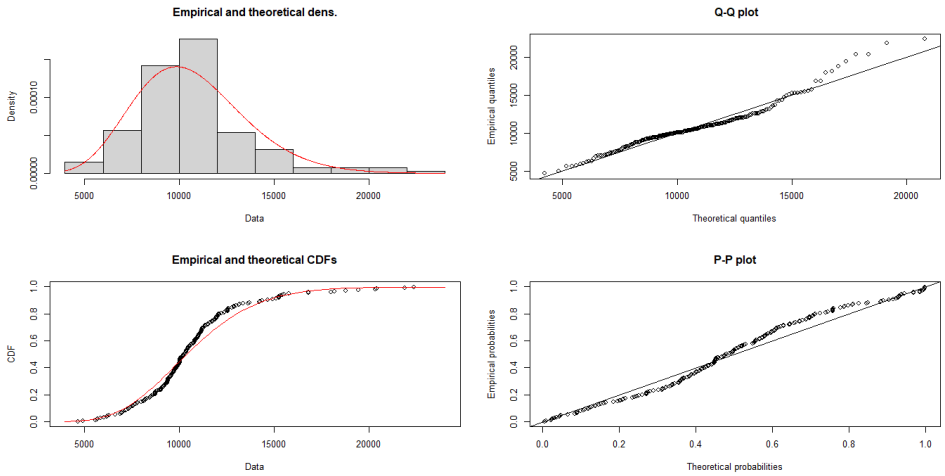

Source: own elaboration.

Figure 33. Average 3-months Precipitation – Weibull Fit – Salto Santiago

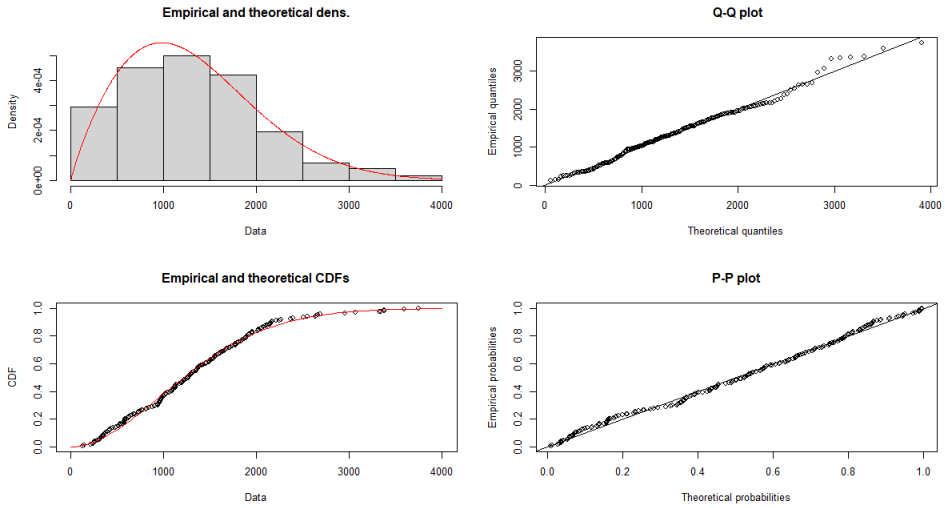

Source: own elaboration.

Figure 34. Useful Volume – Weibull Fit – Salto Santiago

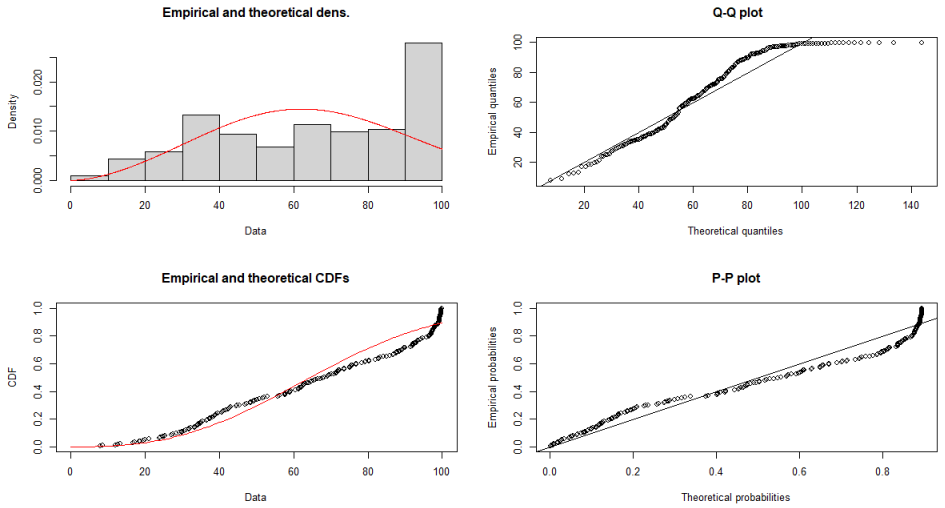

Source: own elaboration.

Figure 35. Average 3-months Precipitation – Weibull Fit – Belo Monte

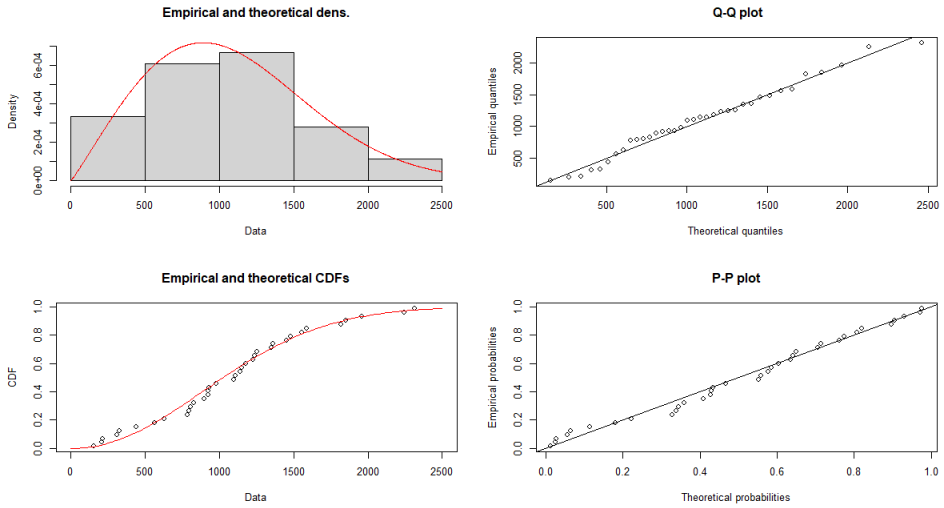

Source: own elaboration.

Figure 36. Affluent Flow – Student-t Fit – Belo Monte

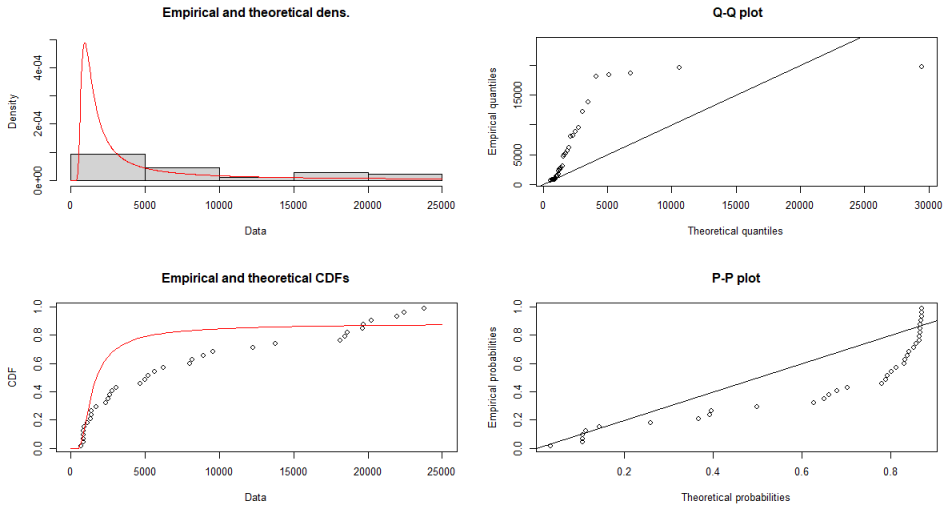

Source: own elaboration.

Figure 37. Average 3-months Precipitation – Gamma Fit - Tucuruí

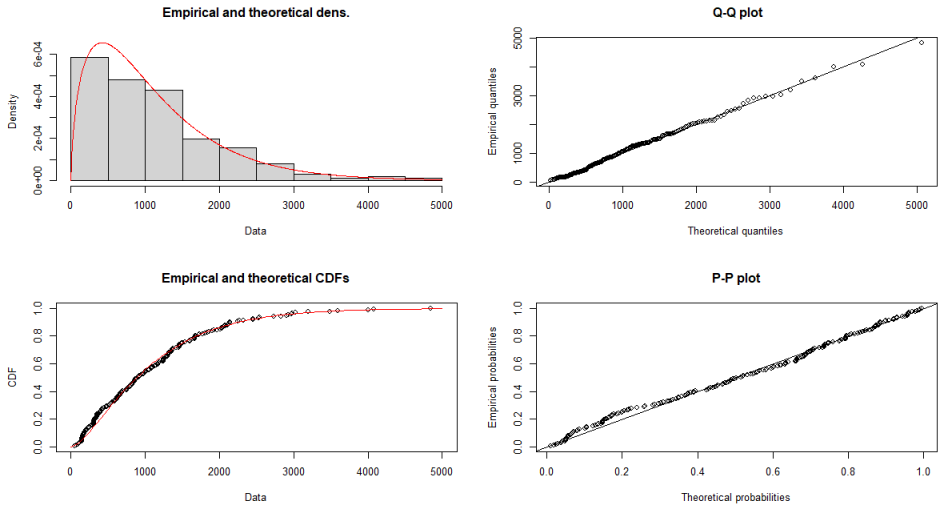

Source: own elaboration.

Figure 38. Useful Volume – Weibull Fit - Tucuruí

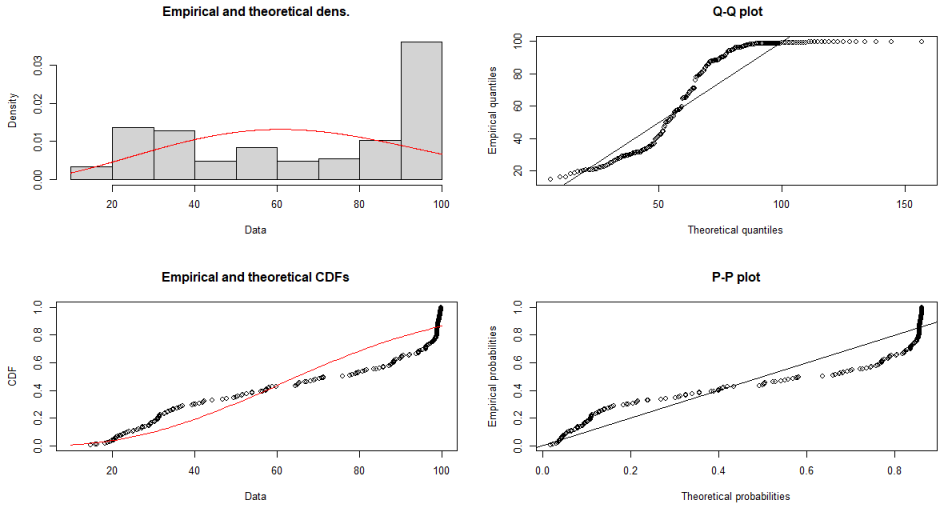

Source: own elaboration.

Figure 39. Average 3-months Precipitation – Gamma Fit - Xingó

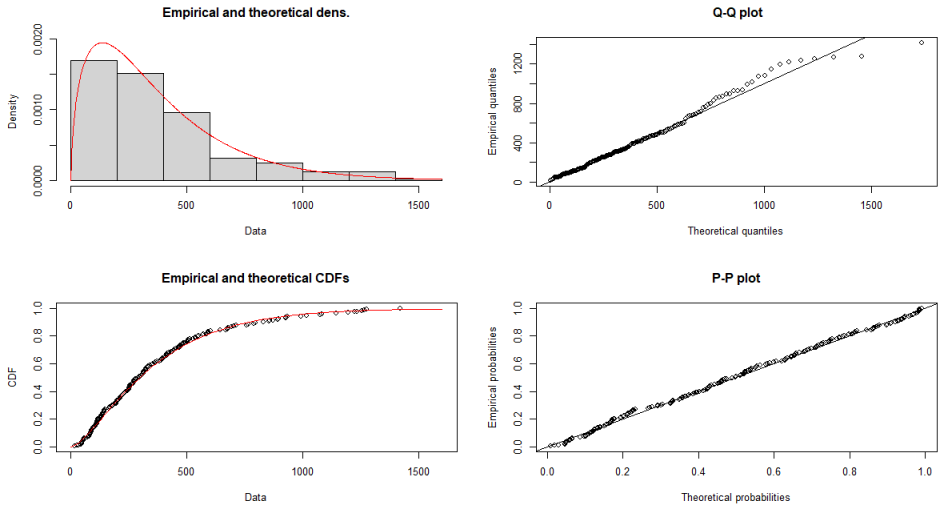

Source: own elaboration.

Figure 40. Affluent Flow – Student-t Fit - Xingó

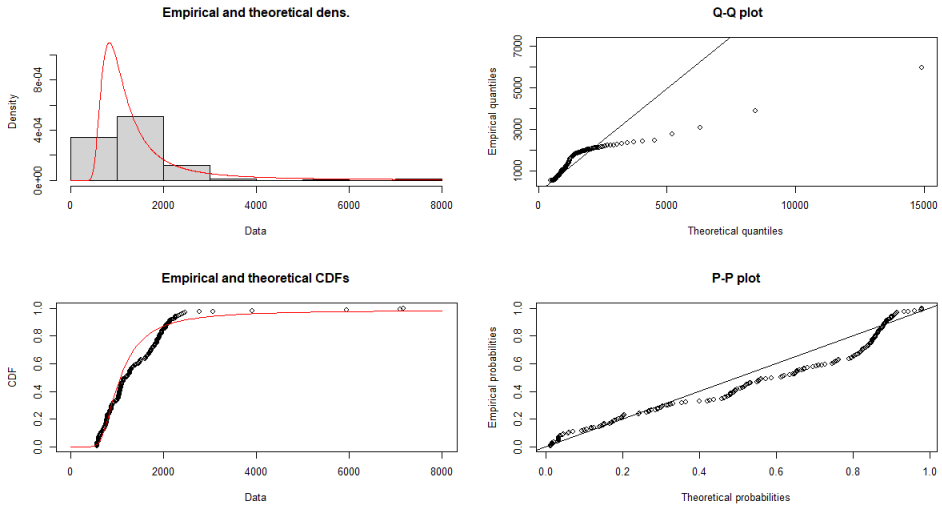

Source: own elaboration.

Figure 41. Average 3-months Precipitation – Gamma Fit – Luiz Gonzaga

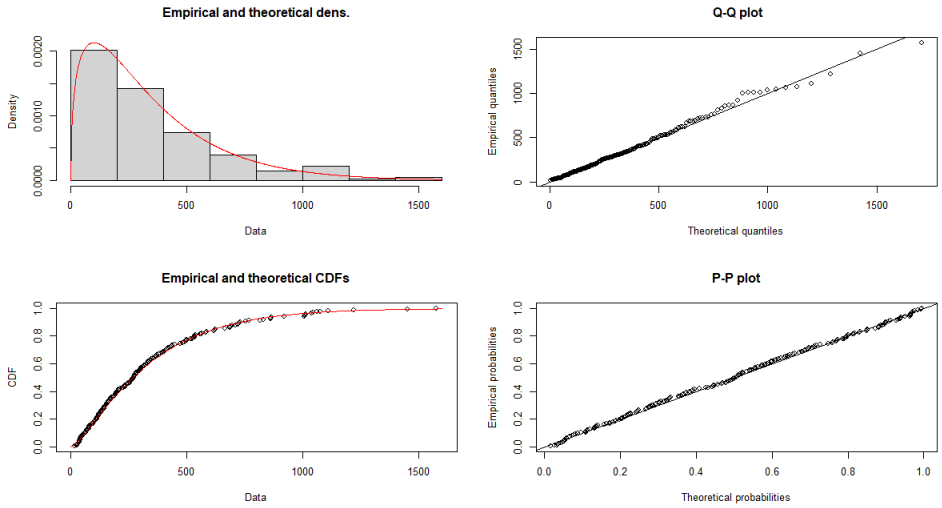

Source: own elaboration.

Figure 42. Useful Volume – Weibull Fit – Luiz Gonzaga

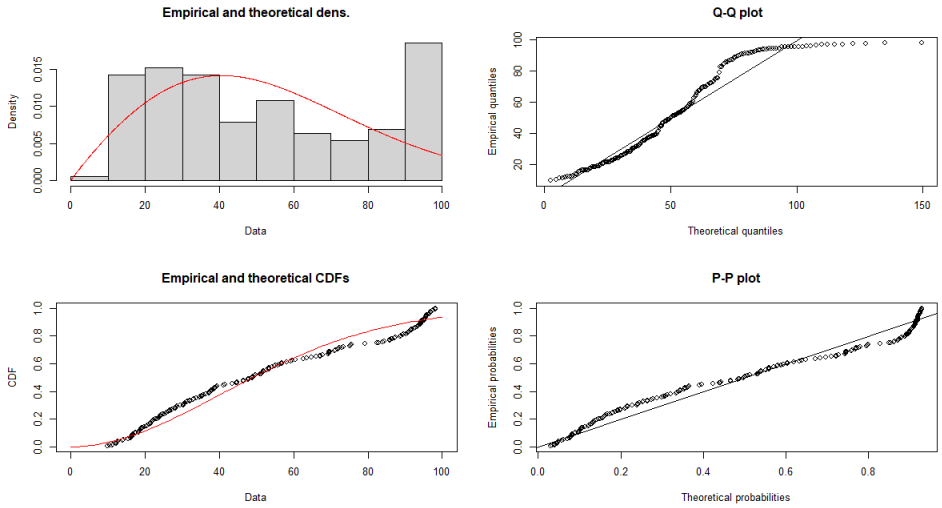

Source: own elaboration.

Figure 43. Average 3-months Precipitation – Weibull Fit – Porto Primavera

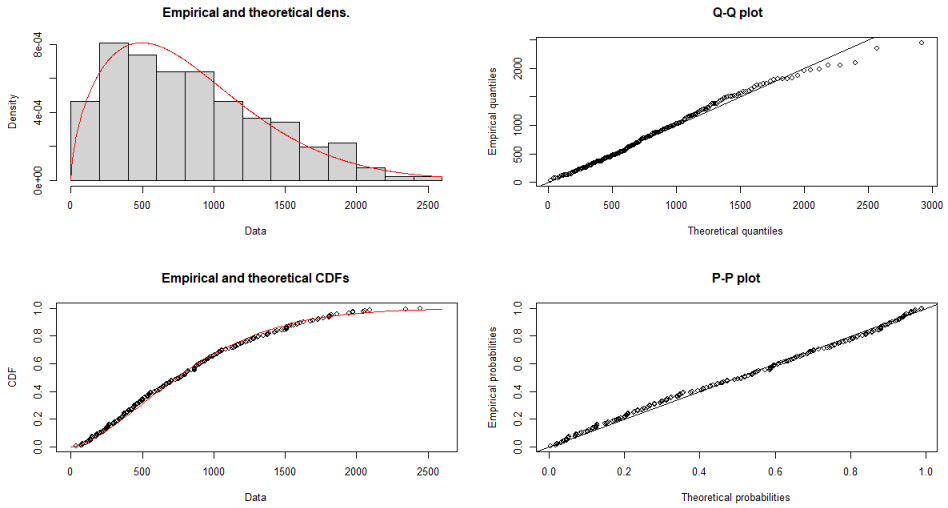

Source: own elaboration.

Figure 44. Affluent Flow – Student-t Fit – Porto Primavera

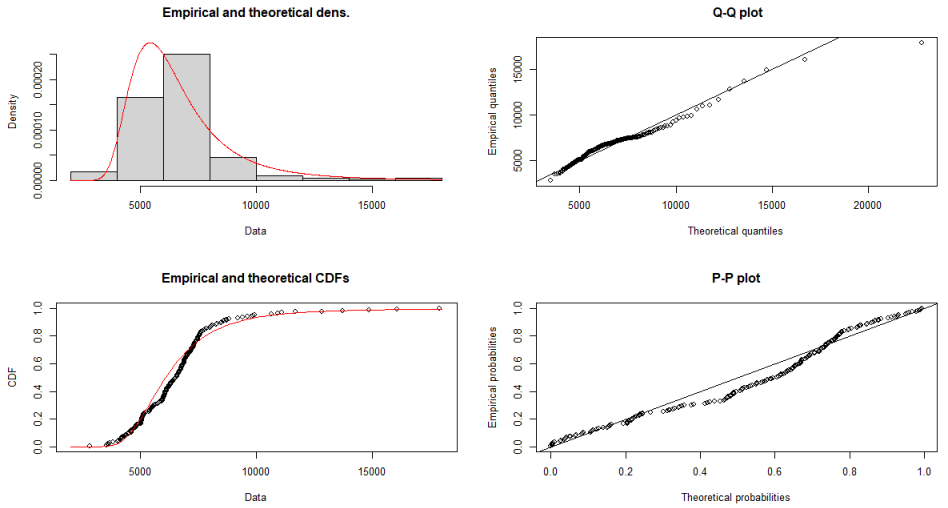

Source: own elaboration.

Figure 45. Average 3-months Precipitation – Weibull Fit – Ilha Solteira

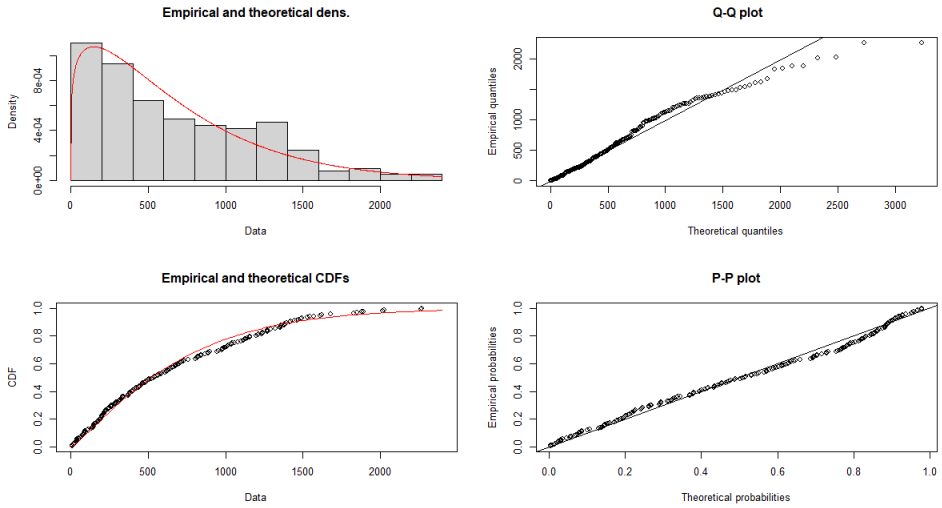

Source: own elaboration.

Figure 46. Useful Volume – Normal Fit – Ilha Solteira

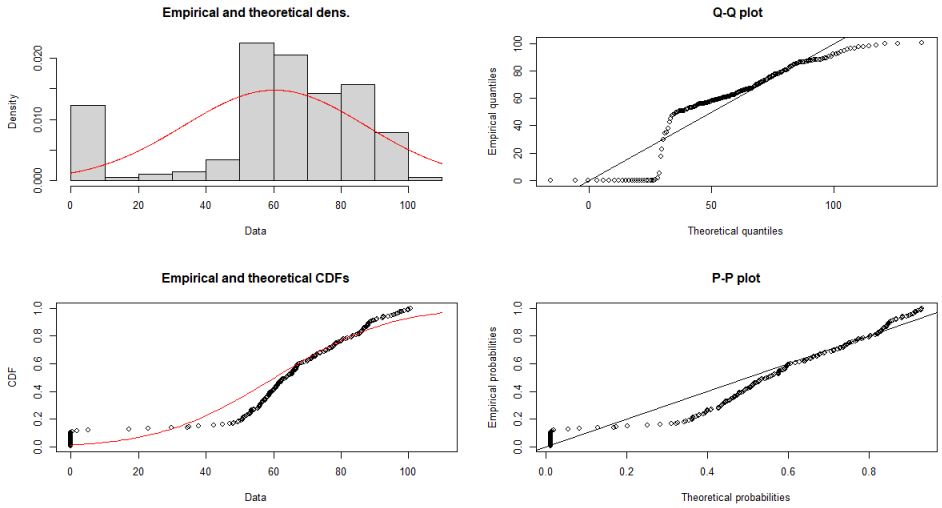

Source: own elaboration.

Based on these premises and following Equations 23 and 24, we can compute the total indemnity amount that an insurance company would have paid if the powerplants had such a contract throughout the analyzed period, as well as the received premiums. An illustration of these calculations is presented on Table 18, specifically for Itaipu.

Table 18. Payout and Premium Calculation for Itaipu

Month	Precipitation	Affluent Flow	Bellow Triggers?	Bellow Exit(s)?	Predicted "loss" of generation (Mwmed)	Productive Hours	Energy Tariff	Payout	Probability	Premium
m	R_3M_o	A_o	$R\_3M_o < R\_3M_{Tr}$ and $A_o < A_{Tr}$	$R\_3M_o < R\_3M_E$ or $A_o < A_E$	$(I_{w.m})$	97.25%[4] of the hours in the month	G_w	$S(I_{w.m})$	$\mathbb{P}(I_i)$	$S(I_{w.m}) \times \mathbb{P}(I_i)$
2006-01	1553.57	11911.99	No	No	0.00	706.8	260.46	R$ 0.00	0.0295906	R$ 0.00
2006-02	1469.76	11030.25	No	No	0.00	638.4	260.46	R$ 0.00	0.0295906	R$ 0.00
.....										
2021-04	761.92	6238.02	Yes	No	82005.69	700.2	260.46	R$ 14.955.713.947,83	0.0295906	R$ 442.547.993,36
2021-05	630.31	5869.04	Yes	No	115540.85	706.8	260.46	R$ 21.270.275.671,89	0.0295906	R$ 629.399.428,85
2021-06	205.31	5704.03	Yes	No	132485.49	700.2	260.46	R$ 24.161.920.715,38	0.0295906	R$ 714.964.833,21
2021-07	263.81	4688.48	Yes	Yes	203147.29	706.8	260.46	R$ 37.398.019.269,18	0.0295906	R$ 1.106.628.439,19
2021-08	192.58	4946.10	Yes	No	195018.35	706.8	260.46	R$ 35.901.538.162,72	0.0295906	R$ 1.062.346.720,98
2021-09	120.36	6992.60	Yes	Yes	219447.13	700.2	260.46	R$ 40.021.471.648,84	0.0295906	R$ 1.184.257.871,69
2021-10	535.37	8743.67	No	No	0.00	706.8	260.46	R$ 0,00	0.0295906	R$ 0,00
2021-11	644.19	7104.32	Yes	No	8065.02	700.2	260.46	R$ 1.470.850.270,90	0.0295906	R$ 43.523.287,37
2021-12	638.17	6297.71	Yes	No	78246.37	706.8	260.46	R$ 14.404.618.263,83	0.0295906	R$ 426.240.761,89
2022-01	838.21	5664.86	Yes	No	132056.41	706.8	260.46	R$ 24.310.677.171,13	0.0295906	R$ 719.366.620,46

Source: own elaboration.

[4] Retrieved from Itaipu's 2022 Report (Itaipu Binacional, 2022)

The calculations in Table 18 were conducted using the Itaipu's lower cluster medians as triggers and the 2.5% quantiles as exit thresholds. This scenario was determined to be the most favorable in terms of feasibility for both the insurer and the powerplant. With these parameters, 4.4% of the observed months would have qualified for indemnification, a reasonable proportion for insurance contracts covering extreme losses. The total payout would have amounted to R$ 213,895,085,121.69, with the majority of claims concentrated in the year 2021, which indeed witnessed the most severe drought of Itaipu's history. Hence, the insurance would effectively fulfill its intended purpose of mitigating high-cost systemic risks.

Given the substantial magnitude of the payouts, which aligns with the characteristic of covering extreme losses, it becomes imperative for such an operation to be backed by a reinsurance company. The monthly actuarially fair premium (risk premium), as defined in Equation 24, would be:

$$P_m = \frac{1}{M}\sum_{m=1}^{M} \mathbb{P}(I_i) \times S(I_{w,m}) = \frac{0{,}029590563 \times \text{R\$ } 213{,}895{,}085{,}121.69}{204}$$
$$= \text{R\$ } 31{,}025{,}862.53 \qquad (25)$$

or R$ 372,310,350.41 annually. This value must be adjusted to account for the insurer's loadings, commissions and tax obligations, resulting in the actual commercial premium. Only to provide an example, if these loadings amounted to 70%, the resulting annual commercial premium would be R$ 632,927,595.70, which represents only 4% of Itaipu's annual operational earnings[5] (Itaipu Binacional, 2022), therefore making it a viable (and useful) contract for both parties. It offers low frequency, high severity coverage with an affordable premium[6].

We reiterate the concern regarding the assumption of independence between R_3M and A. The expected claim probability for the claims was of 2.96% (as indicated in Table 18), yet the actual claims occurred with a frequency of 4.4%. This underscores that the independence assumption led to an underestimation of the actual claim frequency.

Results for the other powerplants were computed using the same methodology applied to Itaipu and are summarized in Table 19. Detailed results considering the other triggers and thresholds are available upon request.

[5] Considering a R$ 5.00 per dollar exchange rate.

[6] We intended to evaluate the proportion of the insurance premium over the operational revenue for other powerplants as well. However, this information was not available for other powerplants, as most are not publicly traded companies, and some are part of energetic conglomerates that only provide information for the Holding Company.

Table 19. Insurance Design Results

Powerplant	Chosen Triggers	Chosen Exit thresholds	Expected Frequency ($\mathbb{P}(I_i)$)	Claims Frequency	Total Payout	Annual Risk Premium	Loss ratio	Payouts during droughts of 2014-2016 or 2021-2022?
Itaipu	Median	2,5% Quantile	3.0%	4.4%	R$ 213,895,085,121.69	R$ 372,310,350.41	3,379.5%	Yes
Salto Santiago	35% Quantile	2,5% Quantile	1.6%	4.9%	R$ 977,802,834,915.26	R$ 906,490,705.94	6,345.1%	Yes
Belo Monte	Median	2,5% Quantile	10.5%	2.9%	R$ 42,900,183,589.93	R$ 265,345,353.84	951.0%	Yes
Tucuruí	30% Quantile	2,5% Quantile	0.7%	3.9%	R$ 138,481,582,463.52	R$ 53,192,874.73	1,5314.0%	Yes
Xingó	35% Quantile	2,5% Quantile	1.7%	3.9%	R$ 14,305,445,807.28	R$ 841,496,812.19	5,737.9%	No
Luiz Gonzaga	30% Quantile	2,5% Quantile	1.6%	5.9%	R$ 293,992,187,415.39	R$ 272,668,571.27	6,342.4%	Yes
Porto Primavera	35% Quantile	2,5% Quantile	0.5%	3.4%	R$ 65,118,491,029.56	R$ 18,217,030.36	21,027.0%	Yes
Ilha Solteira	Median	2,5% Quantile	3.2%	4.9%	R$ 1,377,013,860,716.78	R$ 2,602,104,207.31	3,112.9%	Yes

Note: for Itaipu, we used a 97.25% proportion for operational hours (Itaipu Binacional, 2022) and for Porto Primavera, 96.2% (PWC, 2023). For the other powerplants, this information was not available, so we used 95%.

Source: own elaboration.

The triggers were chosen in order to standardize the claims frequency level among the different powerplants. The exit threshold choice did not show expressive variations on the payout or premium amounts, so we kept the intermediate level (2.5) as exit for all powerplants.

Belo Monte stands out with the lower frequency, even when utilizing the highest of its proposed triggers (from table 17). This is due to its historical series comprehending mostly drought periods (from 2020-2022), so the generated lower cluster corresponds to extremely low levels of precipitation and affluent flow, hence it is very unlikely to activate the insurance. For the same reason, it is the only powerplant to present a lower frequency than the expected, as its history through droughts implies that it would reach low levels of precipitation and affluent flow very often. Given that, these parameters must be revisited when additional data is available.

Given the high proportion of zero volume measurements for Ilha Solteira, the payout and premium values are much higher than on other powerplants.

The resulting loss ratios are very elevated, but can be mitigated with mechanisms like loadings, deductibles and, most of all, reinsurance. Also, these numbers reflect a 16 years period, with the claims concentrated on sparse windows of successive claims. Therefore, during most of the period there is no claims, so the received premiums must be financially applicated and the yields can also serve as part of the loss ratio mitigation.

Furthermore, these results show that this product might not be solely sustainable, especially because it is individualized and would hardly constitute a policies portfolio, as there is a limited number of buyers (powerplants). However, when incorporated in the aggregate portfolio of the insurer, other products can compensate the loss ratio, while the elevated premium revenues can be used for yields and funding other projects of the insurer (while always maintaining provisions for the claims, of course).

Table 19 illustrates that Parametric Insurance (PI) can be a practical option for alleviating hydrological risk in energy generation, particularly during drought crises. It is important to note that the design of this insurance product must be tailored to each powerplant's unique characteristics. Furthermore, the substantial loss ratio, premiums and payouts associated with this product make it more suitable for offerings backed by reinsurance companies.

As for differences in results between run-of-river and water storage powerplants, a more detailed analysis of these variations may require further examination. The water storage powerplants needed lower quantiles as triggers to present a claims ratio near the level achieved with the median for Itaipu. Utilizing the median as trigger for these powerplants resulted in frequencies around 15% or higher, therefore unfeasible for an extreme losses insurance. These distinctions may arise from the distinct operational and hydrological characteristics of the two types of powerplants, necessitating specific insurance contract designs for each category.

Two main questions could arise from this modelling:

1. How about possible endogeneity in the model? Can we assure that generation is indeed dependent on the other variables, or it can serve as an explanatory variable for the others as well? In other words, what is the direction of the correlation?
2. Can we assess the joint distribution of the variables, in order to better estimate the frequency and avoid typical problems caused by linear models given that all marginal probability distributions are heavy-tailed?

These questions can be answered using a different type of modeling: through copulas.

4.6. Assessing the interdependence among the variables through copulas

As previously explained, copulas are mathematical functions that link the joint distribution of random variables with their marginal distributions. In particular, vine copulas are structures that decompose multidimensional copulas into a product of two-dimensional copulas and marginal distributions.

In the context of multidimensional copulas or any typical joint multivariate statistical function, it is possible to break it down into conditional copulas. These conditional copulas are structures that enable the derivation of the joint distribution of two variables, X and Y, conditioned on a set of random variables Z_i. This means that they allow obtaining the copula density $c(X, Y|Z_i)$. A situation with a relevant interpretation for this study is the case in which c is an independent copula. If $c(X, Y|Z_i)$ is an independent copula, then it can be said that X is exogenous to Z_i and, therefore, Y can be (partially) explained by Z_i (this set contains explanatory variables for Y, which are independent of X).

In this section, we delve into the examination of the dependency structure of the variables presented in Table 10. To streamline our analysis, the powerplants were categorized into two distinct groups: run-of-river and water storage powerplants.

The variables were labeled as in Table 20:

Table 20. Labels for Copula Structures

Variable	Copula Label
Energy Generation	1
Useful Volume	2
Affluent flow	2
Average Precipitation in the Last 3 Months	3
Temperature	4
Wind Speed	5
Humidity	6

Note: The useful volume was used only when the powerplant is classified as water storage type, and the affluent flow when it is classified as run-of-river.

Source: own elaboration.

4.6.1. Run-of-River Powerplants

We conducted an analysis of the dependence between the six variables for the same set of powerplants as studied in the previous section: Itaipu, Belo Monte, Xingó and Porto Primavera. The results for these powerplants were remarkably similar. For the sake of discussion and to avoid redundancy, we will take Itaipu as the reference case.

Table 21 presents the structure of the most suitable vine copula (determined by the lowest BIC value) for Itaipu. Additionally, it includes the most well-fitted copula (as obtained through maximum likelihood estimation) for each variable pair at every edge of the vine copula. The table also provides dependence measures, including Kendall's tau, lower tail coefficients, and upper tail coefficients. The notation $(a, b|c, d)$ indicates that variables a and b are conditioned on variables c and d:

Table 21. Vine Copula for Itaipu

Tree	Edge	Copula		Dependence measures		
		Family	Parameters	Kendall´s tau	Upper tail	Lower tail
1	(2,1)	TawnII180*	3.07/0.64	0.47		0.56
	(6,2)	Frank	3.45	0.34		
	(3,4)	Frank	1.66	0.18		
	(6,3)	Gaussian	0.55	0.37		
	(6,5)	TawnII90*	-2.13/0.24	-0.18		
2	(6,1|2)	Independent	-	0.00		
	(3,2|6)	Frank	1.04	0.11		
	(6,4|3)	Clayton90*	-0.75	-0.27		
	(5,3|6)	Joe	1.11	0.06	0.14	
3	(3,1|6,2)	Independent	-	0.00		
	(4,2|3,6)	Gumbel	1.26	0.21	0.26	
	(5,4|6,3)	Frank	-2.23	-0.24		
4	(4,1|3,6,2)	Independent	-	0.00		
	(5,2|4,3,6)	Independent	-	0.00		
5	(5,1|4,3,6,2)	Frank	-1.65	-0.18		

Note: * means the copula is rotated to the degrees presented in the family's name.

Source: own elaboration.

The results in Table 21 can be also represented by a tree structure. The tree structure for Itaipu is shown in Figure 48.

Figure 47. Vine Copula Tree for Itaipu

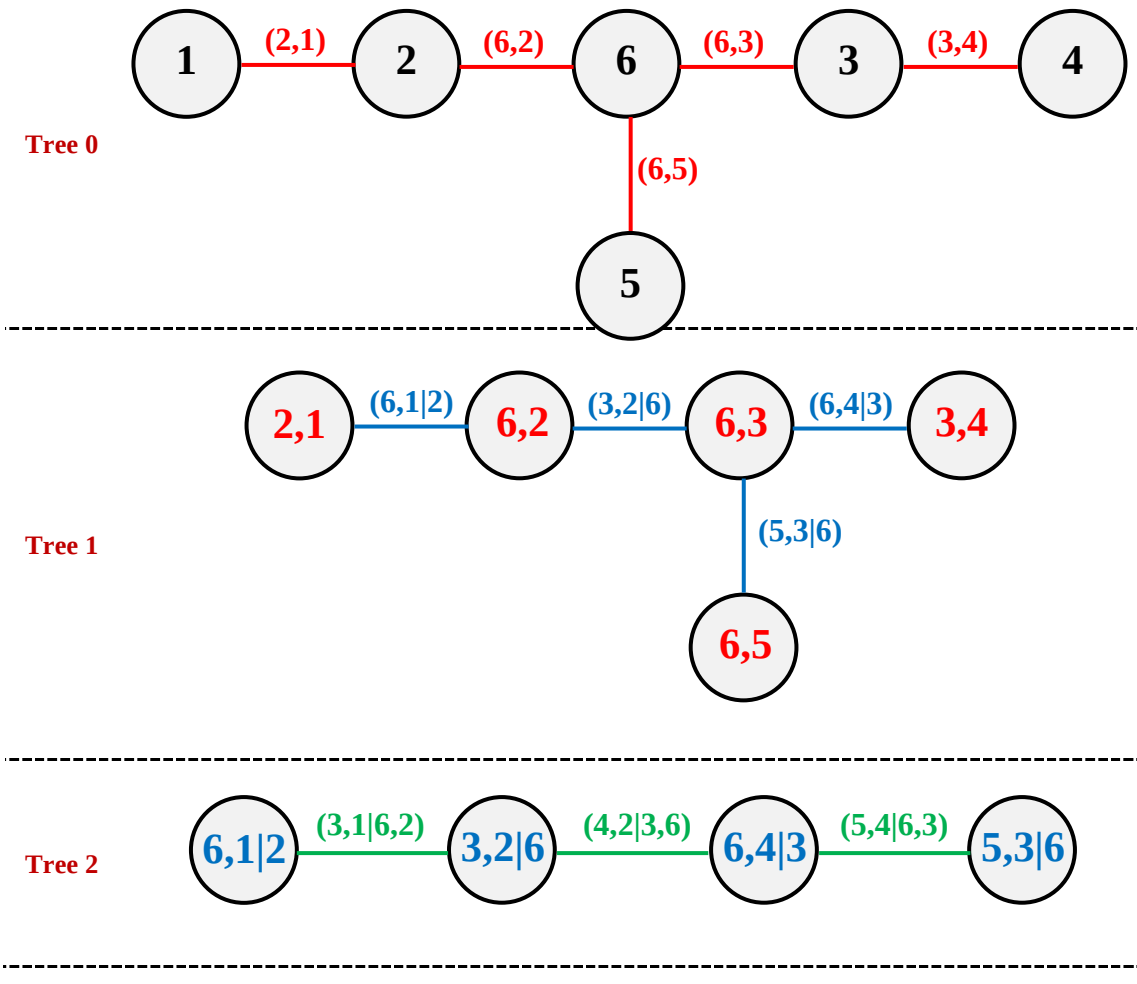

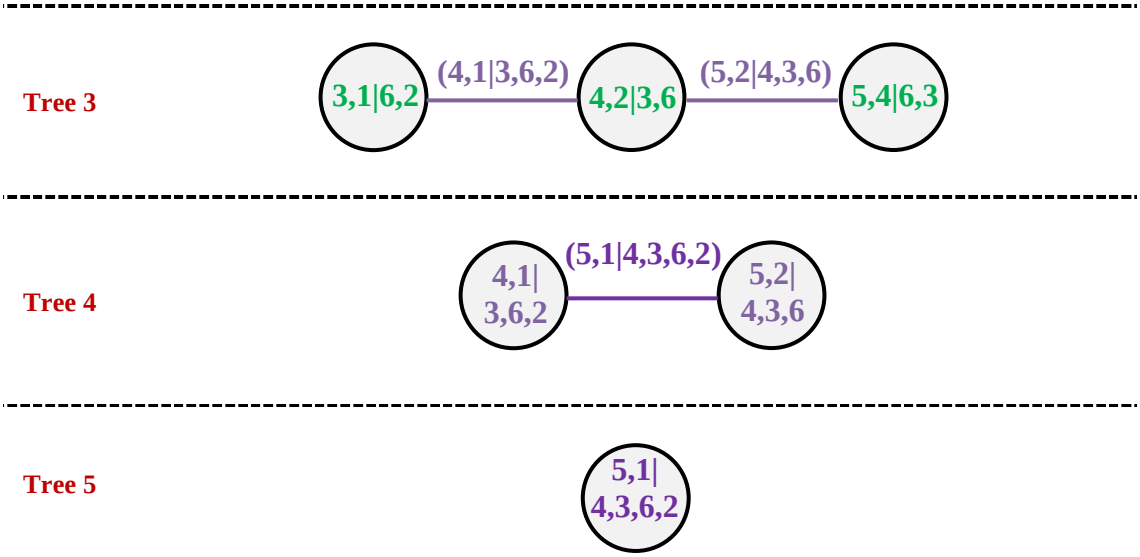

Source: own elaboration

Let f_{123456} be the joint density of the six analyzed variables and f_i, with $1 \leq i \leq 6$, their marginal univariate densities. Figure 47 displays the optimal decomposition, so that the Equation 20 can be rewritten as:

$$f_{123456} = f_1 \cdot f_2 \cdot f_3 \cdot f_4 \cdot f_5 \cdot f_6 \cdot c_{21} \cdot c_{62} \cdot c_{63} \cdot c_{65} \cdot c_{34} \cdot c_{61|2} \cdot c_{32|6} \cdot c_{64|3} \cdot c_{53|6} \cdot c_{31|62} \cdot c_{42|36} \cdot c_{54|63} \cdot c_{41|362} \cdot c_{52|436} \cdot c_{51|4362} \quad (26)$$

Furthermore, in the first tree (Tree 1), the strongest correlation (0.47) is observed between energy generation and affluent flow, represented by the pair (2,1). For this same pair, a strong lower tail dependence (0.56) is noticeable, indicating that low flow values correlate with low generation values, which is consistent with the proposed Itaipu model.

In the subsequent trees, we have highlighted specific cells. They reveal that energy generation is independent of humidity given affluent flow $(6,1|2)$, just as energy generation and precipitation are also independent given afluent flow and humidity $(3,1|6,2)$. Likewise, energy generation is independent of temperature given the affluent flow, precipitation, and humidity $(4,1|3,6,2)$.

In other words, these results mean that: (i) given the affluent flow, humidity is exogenous to it and exhibits no correlation with energy generation. This suggests that either humidity influences the affluent flow value, or variations in humidity have no direct impact on the energy generation processes; (ii) precipitation is exogenous to affluent flow and humidity, and it does not correlate with energy generation. Th precipitation serves as an explanatory variable for changes in affluent flow and/or in humidity, but does not directly explain the variation in energy generation directly; and (iii) temperature is exogenous to affluent flow, precipitation and humidity, and it is also not correlated with energy generation.

These findings can be summarized in the network structure in the Figure 49. The direction of each arrow indicates the causal inference (in the graphical sense), while its width represents the strength of dependence (indicated by the respective Kendall's tau value) among the six analyzed variables.

Figure 48. Network representing Itaipu's Vine Copula

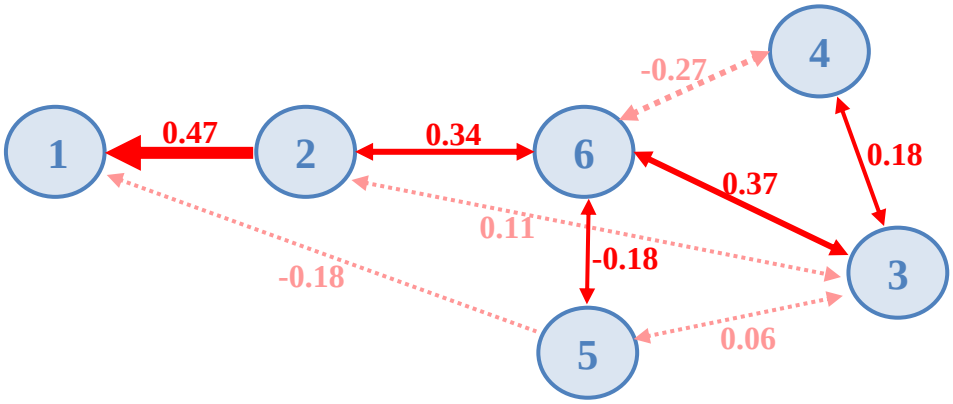

Source: own elaboration

Arrows in solid lines indicate the unconditional dependency relationship, while dotted lines indicate conditional dependencies. In Figure 49, becomes evident that meteorological factors (precipitation, temperature, wind speed and humidity, indicated by the numbers 3, 4, 5 and 6 respectively) are clearly associated, but the nature of this association is diffuse, and it is challenging to determine causal relationships among them. Also, these meteorological factors collectively impact the affluent flow which, in turn, influences variations in energy generation. Thus, as a result, the focus should be on understanding the relationship between the pair (2,1) to derive the required quantiles to price the insurance.

These findings align with the spatial econometrics estimated model and cluster analysis. Temperature is exogenous to the model and was not included in the SARAR equation. Affluent Flow exhibits the highest correlation with energy generation and could serve as a single trigger for the run-of-river powerplants. The relationship between Affluent Flow and R_3M can be conditioned on humidity, explaining the underestimation of frequency in the previous model.

As previously explained in this section, the conclusions drawn for Itaipu hold for the other run-of-river powerplants under analysis. Table 22 shows the same information previously shown, but this time for Belo Monte:

Table 22. Vine Copula for Belo Monte

Tree	Edge	Copula		Dependence measures		
		Family	Parameters	Kendall´s tau	Upper tail	Lower tail
1	(2,5)	Tawn90*	-20.0/0.11	-0.11		
	(2,1)	Surv.Gumbel	4.31	0.77		0.83
	(4,2)	Gumbel270*	-2.13	-0.53		
	(4,3)	Gumbel270*	-2.07	-0.52		
	(6,4)	Clayton90*	-2.59	-0.56		
2	(1,5|2)	Independent	-	0.00		
	(4,1|2)	Independent	-	0.00		
	(6,2|4)	Independent	-	0.00		
	(6,3|4)	Independent	-	0.00		
3	(4,5|1,2)	Independent	-	0.00		
	(6,1|4,2)	Independent	-	0.00		
	(3,2|6,4)	Independent	-	0.00		
4	(6,5|4,1,2)	TawnII180*	8.75/0.19	0.18		0.19
	(3,1|6,4,2)	Independent	-	0.00		
5	(3,5|6,4,1,2)	Independent	-	0.00		

Note: * means the copula is rotated to the degrees presented in the family's name.

Source: own elaboration.

What is noteworthy for Belo Monte is the emergence of predominantly independent copulas in all trees after the first one. The significant relations here are primarily direct, rather than conditional. This characteristic might result from the limited number of observations available. It also shows why this was the only powerplant to present the possibility of designing a PI indexed solely on precipitation, as indicated in Figure 28.

Despite this unique feature, the findings echo the same principles already discussed in the analysis of Itaipu. The strongest correlation (0.77) is observed between energy generation and affluent flow, represented by the pair (2,1). Moreover, there is a robust dependence (0.83) in the lower tail, meaning that low affluent flow values are related to low energy generation values, which is consistent with the expectations for run-of-river powerplants. Table 22 also enables the construction of a network structure, similar to the one developed for Itaipu.

Figure 49. Network representing Belo Monte's Vine Copula

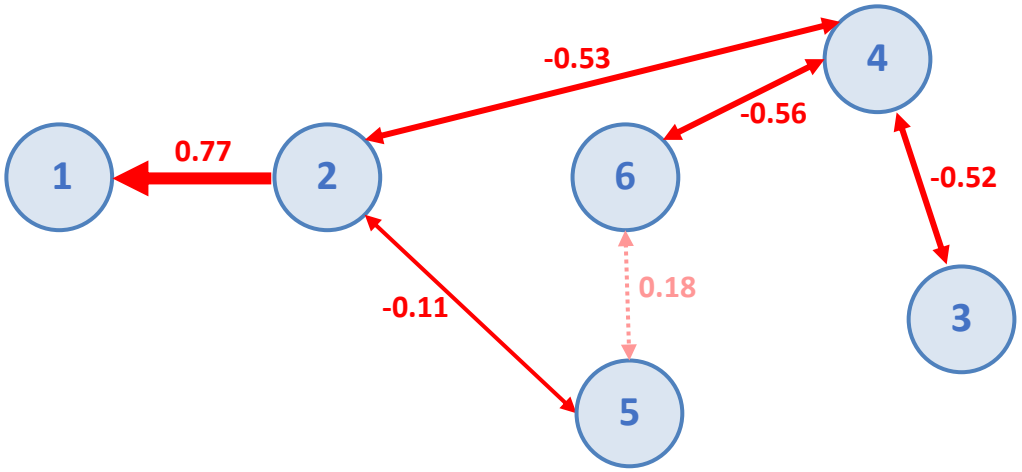

Source: own elaboration.

This network presented in Figure 49 also highlights the diffuse dependence between meteorological factors (3, 4, 5 and 6) and their impact on the affluent flow. Consequently, this impact on the affluent flow leads to variations in the amount of generated energy. This supports the strategy of focusing only on the relationship (2,1) to derive the necessary quantiles for insurance pricing.

A consistent pattern of behavior is observed for the other run-of-river powerplants. For Xingó, there is a strong correlation (0.88) between energy generation and affluent flow, along with a significant dependence parameter of 0.88 in the lower tail. Similar results are observed for Porto Primavera, with a correlation of 0.72 between energy generation and affluent flow, and a lower tail dependence parameter of 0.79. Figures 50 and 51 depict the networks for Xingó and Porto Primavera.

Figure 50. Network representing Xingó's Vine Copula

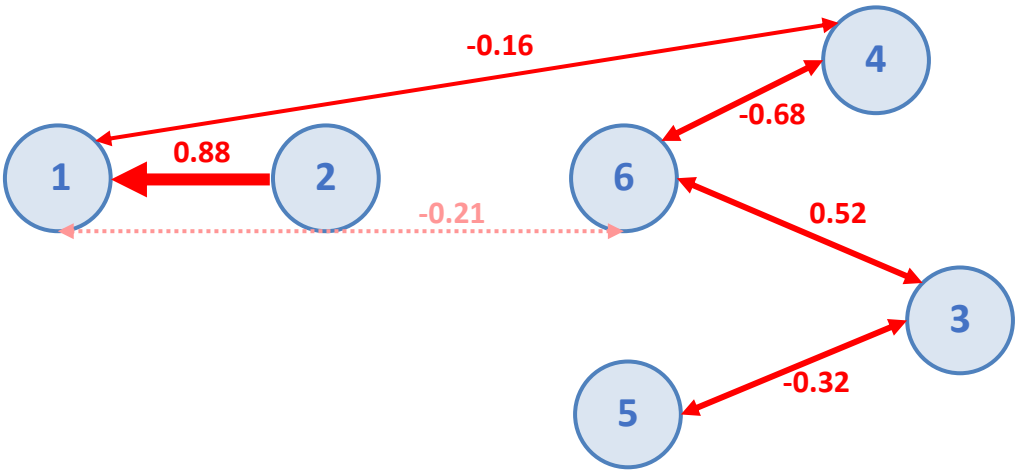

Source: own elaboration.

Figure 51. Network representing Porto Primavera's Vine Copula

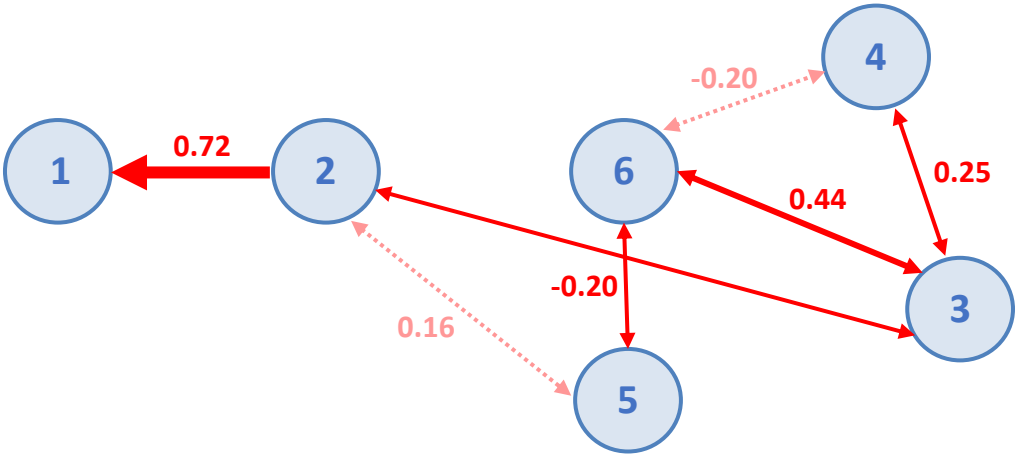

Source: own elaboration.

4.6.2. Water Storage Powerplants

Similar to the previous section, the dependence structure among the six variables will be analyzed individually for the Tucuruí, Ilha Solteira, Salto Santiago and Luiz Gonzaga powerplants. Table 23 provides the copula information for Tucuruí.

Table 23. Vine Copula for Tucuruí

Tree	Edge	Copula		Dependence measures		
		Family	Parameters	Kendall´s tau	Upper tail	Lower tail
1	(4,3)	Frank	-5.39	-0.48		
	(1,2)	Gaussian	0.58	0.40		
	(4,5)	BB8	2.66/0.87	0.36		
	(6,1)	Frank	4.00	0.39		
	(6,4)	TawnII90*	-3.52/0.79	-0.59		
2	(6,1|2)	Gumbel	1.24	0.20	0.25	
	(3,2|6)	Clayton90	-0.47	-0.19		
	(6,4|3)	Gumbel90	-1.10	-0.09		
	(5,3|6)	Independent	-	0.00		
3	(3,1|6,2)	Independent	-	0.00		
	(4,2|3,6)	Independent	-	0.00		
	(5,4|6,3)	Independent	-	0.00		
4	(4,1|3,6,2)	Independent	-	0.00		
	(5,2|4,3,6)	Clayton270*	-0.36	-0.15		
5	(5,1|4,3,6,2)	Independent	-	0.00		

Note: * means the copula is rotated to the degrees presented in the family's name.

Source: own elaboration.

Several notable differences are observed in the case of Tucuruí in contrast to the run-of-river powerplants. First, the correlation between energy generation and water volume, while still significant, is not as strong (0.40) as it was for affluent flow. Furthermore, it is nearly identical to the correlation between energy generation and humidity (0.39). Second, the strong dependence observed in the lower tail between variables in run-of-river powerplants is no longer present for Tucuruí. In this case, there is no strong dependence in the lower tail between any two variables. Finally, the presence of conditional independence relationships given the unconditional dependence, such as wind speed and precipitation being independent given humidity. However, there is no longer a structured dependence between wind and precipitation unconditionally.

These findings suggest a more diffuse set of dependencies, making it challenging to infer causal relationships when constructing the network structure. The dependencies between variables in Tucuruí exhibit a different pattern than those in run-of-river powerplants.

Figure 52. Network representing Tucuruí's Vine Copula

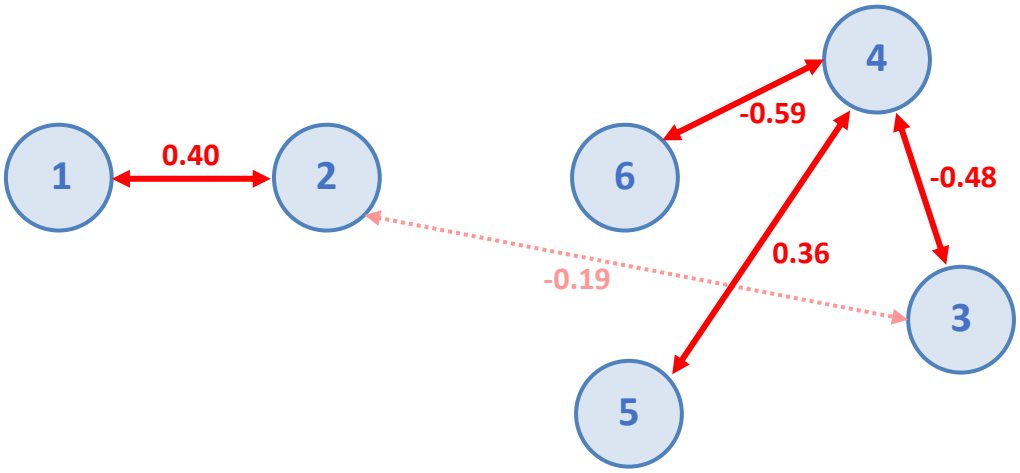

Source: own elaboration

The same diffuse patterns are observed in the case of other water storage powerplants. In these instances, either there is a weak dependency between energy generation (1) and water

volume (2) with no observable dependency between energy generation and other variables (as seen in the case of Ilha Solteira), or a causal relationship cannot be firmly established within this dependency structure, as observed in the cases of Salto Santiago and Luiz Gonzaga.

The bidirectionality in the pair (1,2) can be due to the operational characteristics of water storage powerplants, especially the higher human intervention. As the water flow that leaves the reservoirs can be controlled to meet the energy demand (Enel Green Power, n.d.), at certain times the volume remaining in the reservoirs can be caused by the expected energy generation levels, while, at the other end, the amount of generated energy depends on the available water volume.

This diffuse nature of these relationships suggests that this study is limited to parameterizing insurance contracts exclusively for run-of-river powerplants. This is because there is no clear and well-defined relationship between energy generation and other variables for water storage powerplants that would allow obtaining the calculation of necessary quantiles to price the insurance.

Furthermore, if we were to set only the water volume as index, in an attempt of standardization with the copulas model for run-of-river powerplants, we would incur in the same problem pointed out when analyzing Figure 30, where we saw that the claims frequency would end up being much higher than actually necessary. This may happen because these powerplants' structure allows for greater control of the water use, in response to the energy demand and available water volume. Also, this human managing characteristic could, in some cases, induce moral hazards, as the water volume could be intentionally put to a lower level to activate the insurance, while the energy generation would not immediately be jeopardized. Therefore, with this methodology, we will limit the insurance design to run-of-river powerplants.

4.6.3. The relation between Energy Generation and Affluent Flow at the run-of-river powerplants

Considering the findings presented in sections 4.6.1 and 4.6.2, we analyzed the dependence structure between affluent flow and energy generation specifically for the run-of-river powerplants. To do so, we must identify the copula family and its corresponding parameter value(s) that were derived for each power plant, as summarized in Table 24.

Table 24. Bivariate Estimated Copulas for Energy Generation and Affluent Flow

Powerplant	Copula	Parameter(s)
Itaipu	TawnII180*	3.07/0.64
Belo Monte	SurvGumbel	4.31
Xingó	t-Student	0.98/2.00
Porto Primavera	TawnII180*	6.31/0.84

Note: * means the copula is rotated to the degrees presented in the family's name.

Source: own elaboration.

Figure 53 shows the dependency structures' copula density for each plant.

Figure 53. Bivariate Copulas Densities

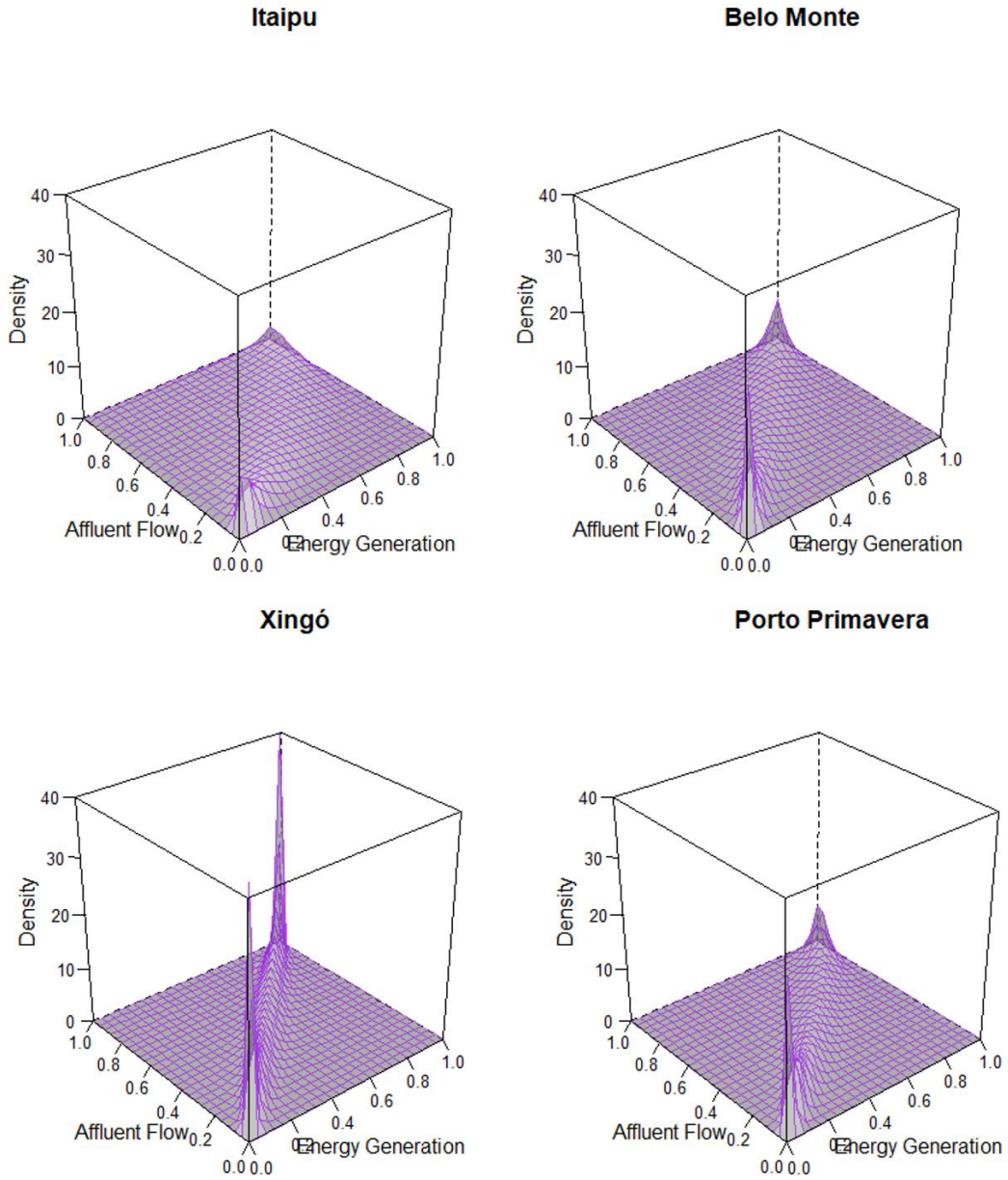

Source: own elaboration.

In all cases the densities are highly concentrated on the main diagonals of the cubes, which represents some form of linear association (as it was already shown on Table 9, these two variables have an 0.89 Pearson's correlation). Interestingly, the highest densities are always in the tails, our main interest, particularly the lower tails. The estimated distributions, as presented on Table 24, are best fitted to model heavy-tailed distributions, and the 180º rotation, especially, is best to capture dependence in the lower tails.

Comparing the density functions of these four powerplants, Xingó presents the heaviest tails and Itaipu the lightest. This may be due to the influence of other variables onto energy generation or affluent flow in the case of Itaipu. As it is shown in Figure 48, there is a direct and unconditional relationship between these two variables, with a 0.47 correlation,

however, they are also impacted by the other variables to some extent. The other powerplants, conversely, present stronger correlations between energy generation and affluent flow, from 0.72 in Porto Primavera to 0.88 in Xingó, so their distributions present higher densities, as the relation between the variables is stronger and less influenced by the other variables in the network.

With the use of these copulas, we are able to develop a PI scheme, similar to what was done in sections 4.4 and 4.5. This time, we utilize solely the affluent flow as trigger, given the results of the first-level estimated vine copulas, presented in section 4.6.1. To measure the energy levels associated with the affluent flow levels (which was previously done by the coefficients of the spatial models), we utilize the copulas' estimated distributions, extracting the expected value of generation within the interval of affluent flow thresholds (limited between 0.5% and 5% quantiles of the energy generation, as an attempt to standardize the indemnifications levels with the frequency observed in the previous model). As for the frequency probabilities, they can be directly assessed with the copula density $c(F_E, F_A)$ of energy generation and affluent flow.

These concepts are illustrated in Figure 54. The premium calculation can be expressed as in Equations 27-30.

Figure 54. Pricing through copulas - illustration

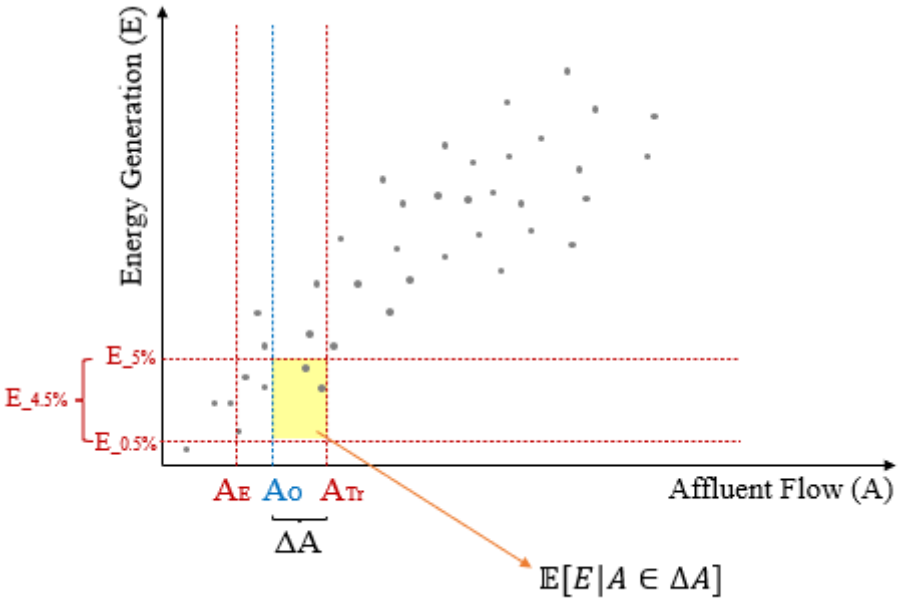

Source: own elaboration.

$$P = G_w \times \sum_{A \in \Delta A} \mathbb{E}[E|A \in \Delta A] \times \mathbb{P}[A \in \Delta A] \tag{27}$$

$$P = G_w \times \sum_{A \in \Delta A} \sum_{E} e \times \mathbb{P}[E = e|A \in \Delta A] \times \mathbb{P}[A \in \Delta A] \tag{28}$$

$$P = G_w \times \sum_{A \in \Delta A} \sum_{E} e \times \frac{\mathbb{P}[E = e, A \in \Delta A]}{\mathbb{P}[A \in \Delta A]} \times \mathbb{P}[A \in \Delta A] \tag{29}$$

$$P = G_w \times \sum_{A \in \Delta A} \sum_{E} e \times c(F_E, F_A) \tag{30}$$

where E is the energy generation, A is the Affluent Flow, ΔA is the difference between the trigger and the observed affluent flow ($A_{Tr} - A_O$), or between the trigger and the exit threshold ($A_{Tr} - A_E$), when $A_o < A_E$, is the on-grid power price and $c(F_E, F_A)$ is the copula density. The monthly premium is simply $P_m = \frac{P}{m}$. The Payout is the term $G_w \times \sum_{A \in \Delta A} \sum_E E$ of Equation 30.

To ensure comparability between the econometric and the copulas designs, we will utilize the same affluent flow triggers and exit thresholds defined in Table 19, which were chosen through the k-means clusters. The results of this insurance design are presented on Table 25.

Table 25. Insurance results through copulas

Powerplant	Expected Frequency ($c(F_E, F_A)$)	Claims Frequency	Total Payout	Annual Risk Premium	Loss ratio	Payouts during droughts of 2014-2016 or 2021-2022?
Itaipu	0.4%	8.3%	R$ 3,750,851,384,377.34	R$ 73,407,913.25	300564.76 %	Yes
Belo Monte	3.3%	4.4%	R$ 3,002,022,470,305.01	R$ 526,596,850.45	33534.11%	Yes
Xingó	0.8%	12.3%	R$ 2,256,691,459,358.79	R$ 51,430,492.34	258108.66 %	No

Source: own elaboration.

We were not able to obtain valid results for Porto Primavera due to the lack of observations of lower occurrences of energy generation and water flow, jeopardizing a correct assessment of the probabilities.

It is noteworthy that, compared to the spatial econometrics results, this design presents lower expected frequencies and consequently lower premiums. The payout values, however, are much higher. This is most likely due to the construction of the energy generation prediction in both models: with the spatial econometrics, the predicted value was a result of the difference between the observed affluent flow and the trigger pondered by the model coefficients; in the copulas model, the observed energy level is used directly, subtracted from a predicted energy (through the estimation of a theoretical copula with the same parameters found in table 24) associated with the affluent flow trigger (at the 5% energy quantile).

When utilizing one trigger instead of two, the insurance design becomes less restrictive, causing the claims ratio to be higher. The fact that the copulas were not able to correctly estimate the frequencies (except for Belo Monte, where the estimation is more approximate to the observed values) could be due to this estimation being made statically over time. The densities reflect very low probabilities of occurrence for values in the lower tails, however, the empirical data shows these values have occurred with a higher frequency than predicted. Our hypothesis is that the data distribution has been changing over time, as climate change increases the frequency of extreme events, the static copula no longer reflects the current probabilities. Since the copula for Belo Monte only comprehends data spanning from 2020-2022, it adjusts better to the real occurrences.

This combination of low premiums and high payouts leads to extremally high loss ratios, which make it unviable to offer this insurance product. In this sense, the spatial

econometrics design is more robust, and the copulas analyses serve as support for the construction of the spatial regression, ensuring the non-endogeneity of the model.

To improve the insurance designs, a dynamic structure should be incorporated (in both the SARAR and the copulas), accounting for the changes in the data distribution over time and the increasing climate change effects. Moreover, the payout values could be defined in different ways or even be a fixed value. Different triggers can also be tested, and the discount rate could be reintroduced into the premium for long term contracts, as the claims are sparse over time.

5. CONCLUDING REMARKS

This study aimed to design a parametric insurance product for Brazilian hydroelectric companies, addressing an insurance protection gap. Such product could improve the companies' operations sustainability and mitigate effects of drought crises, as the Brazilian electricity system is highly dependent on water and subject to systemic hydrological risk, especially with the increasing climate changes and drought periods.

We were pioneers into designing a parametric insurance for energy generators utilizing spatial econometrics, and also in applying the models to Brazilian hydroelectric generators, as most studies in the literature observe other energy sources, such as wind, most common in other countries. This study also stands out for utilizing copulas as an endogeneity robustness check.

There are two main types of hydroelectric powerplants, each with its unique operational characteristics and contributions to the nation's energy mix. The run-of-river powerplants utilize the natural flow of watercourses to generate energy and are valued for their minimal environmental impact. The water storage powerplants utilize reservoirs and the energy generation occurs through the water release, which can be controlled to meet the energy demand.

These powerplants ensure flexibility in managing the electricity supply and play a significant role in providing a reliable and sustainable source of electricity in line with Brazil's commitment to environmental sustainability and energy security. However, as hydroelectricity represents 65% of Brazil's energy matrix, in times of rain scarcity there can be severe energy crises.

Besides initiatives toward diversifying its energy matrix, Brazil counts with an accounting balancing mechanism, the MRE, which promotes the sharing of hydrological risk among the participating powerplants, minimizing the financial repercussions of fluctuating energy generation. While MRE enhances the generators financial stability and the energy security, it does not mitigate systemic risk. Given this scenario, we propose the parametric insurance design.

We evaluated two different methodologies to price this product: (i) spatial econometrics, and (ii) vine copulas models. Spatial econometrics expands the traditional actuarial pricing GLM models by incorporating relations among the observed powerplant and its neighbors, a key feature when dealing with climate subjected models, as weather and location are intrinsically related, most of all in a country as extensive and diverse as Brazil. Vine copulas models allow us to elucidate the intricate conditional non-linear dependency structures that exist among the model's variables in each powerplant, therefore providing a better understanding of which variables can be considered causal to the energy generation. In both cases, we used a k-means clustering technique to define the triggers and exit thresholds that limit the insurance claims.

Given the diverse characteristics of each powerplant, we found better results when designing the insurance differently for run-of-river and water storage powerplants. Also, the threshold levels needed to be defined individually, to account for the different levels of energy generation typical of each plant and for the climate characteristics of each location, with different levels of precipitation, for instance.

This product would initially be indexed on Brazil's National Institute of Meteorology (INMET) rainfall index, but our results show that an insurance indexed solely on this parameter would not be feasible, as this variable presents low correlation with the amount of generated energy. Instead, the spatial econometrics model points to the joint use of

precipitation and water flow or volume, depending on the powerplant type, whilst the copulas models allow a sole trigger of affluent flow for run-of-river powerplants, but do not point a clear path for water storage powerplants, as the networks show diffuse relations and no specific variable can be highlighted as main cause for the energy generation.

Our main finding is that energy generation levels for hydroelectric powerplants can be robustly modeled by spatial econometrics, with significant gains towards the traditional models. This is especially interesting for climate-related applications, given the intrinsic relation of weather and location, and integrated systems such as Brazil's electricity system.

The most suitable model to explain and predict the powerplant's energy generation was a fixed-effects SARAR. This model possesses both an autoregressive and an error term associated with the neighborhood matrix. This translates to the powerplant's energy generation being explainable not only by its own measurements of water flow/volume and the regional meteorological conditions, but also by the energy generated by its neighboring powerplants. Hence, the conditions of a powerplant are closely related to those of its nearest neighbors, often sharing the same basin and, as a result, experiencing similar watercourses and meteorological conditions. Furthermore, random shocks effects on neighboring powerplants negatively affect the energy generation of the observed powerplant. One such effect could be the MRE mechanism. Given the highly interconnected nature of the Brazilian electrical system, with minimum energy generation targets established for each powerplant and periodically revised by ONS, a powerplant's energy generation is also contingent on the energy demand and the generated levels by all other suppliers in the electrical system.

The copulas models for the individual powerplants endorse the non-endogeneity of the SARAR, especially for run-of-river powerplants, as they show that generation is indeed dependent on the other variables, with a directional causality from meteorological conditions to the affluent flow and then to the generated energy, and not the way around. It, therefore, serves as a robustness check for physical implication. However, it is worth pointing out that other possible endogeneity sources, such as omitted variables or measurement errors, are not captured by this methodology.

The insurance design results show that Parametric Insurance can be a practical option for alleviating hydrological risk in energy generation, particularly during drought crises. The design of this insurance product must be tailored to each powerplant's unique characteristics. It is especially well-suited for run-of-river powerplants, while water storage powerplants present more diffuse results, likely due to the operation differences among these plants. Run-of-river powerplants are more subjected to climate conditions and water availability, while water storage plants can control, to a certain point, the water levels in the reservoir and its release to meet energy demands, taking a longer time to suffer the effects of drought crises.

Furthermore, the substantial loss ratio, premiums and payouts associated with this product make it more suitable for offerings backed by reinsurance companies. The premium proportion in relation to the powerplants' revenues points this product as viable and attractive for customers. The high loss ratios, however, suggest that improvements in the design must be made before insurers would offer such contract. Measures that aim to reduce the payout values should be taken to ensure the feasibility of this product for the insurers.

Future studies can delve into improvements of these estimations, such as, but not limited to: (i) incorporating time dynamics into both the spatial and copulas models, accounting for the changes in the data distribution through time and the increasing climate change effects; (ii) assessing different estimations of the payouts, to reduce the expressive loss ratios; (iii) estimating regional models or a GWR, to account for the diversity of Brazil's climate, hence utilizing coefficients more adherent to each powerplant and not simply the

global means; (iv) verifying other techniques to define the trigger and exit threshold values; (v) price the insurance as a long term contract, including a discount rate, as the loss occurrence is concentrated in a few crises windows sparse over time; (vi) include variables predictive of climate change as instruments in the model, such as indicators of El Niño or La Niña occurrence and GHG levels.

Furthermore, this study can be extended for other renewable energy sources and/or other countries. Different methods, such as machine learning algorithms, can also be tested against the already presented models.

6. REFERENCES

Actuaries Institute Australia. (2020). *Climate Change – Information Note for Appointed Actuaries* (Issue November, pp. 1–28). https://www.actuaries.asn.au/Library/Standards/MultiPractice/2020/INCCFinal121120.pdf

Agnese, P., & Giacomini, E. (2023). Bank's funding costs: Do ESG factors really matter? *Finance Research Letters*, *51*, 103437. https://doi.org/10.1016/J.FRL.2022.103437

Aguiar, J. T. de, & Lobo, M. (2020). Reliability and discrepancies of rainfall and temperatures from remote sensing and Brazilian ground weather stations. *Remote Sensing Applications: Society and Environment*, *18*(January), 100301. https://doi.org/10.1016/j.rsase.2020.100301

Andersen, D. A., & Bonat, W. H. (2017). Double generalized linear compound poisson models to insurance claims data. *Electronic Journal of Applied Statistical Analysis*, *10*(2). https://doi.org/10.1285/i20705948v10n2p384

Anselin, L. (1988). Spatial Econometrics: Metodhs and Models. In *Kluwer Academic Publishers, Deodrecht*.

Antonio, Y., Indratno, S. W., & Saputro, S. W. (2021). Pricing of cyber insurance premiums using a Markov-based dynamic model with clustering structure. *PLoS ONE*, *16*(10 October). https://doi.org/10.1371/journal.pone.0258867

Arumugam, S., & Bhargavi, R. (2019). A survey on driving behavior analysis in usage based insurance using big data. *Journal of Big Data*, *6*(1). https://doi.org/10.1186/s40537-019-0249-5

Assed, G., & Assed, C. (2020). A regulação de energia elétrica no Brasil e a teoria dos leilões. *Revista Políticas Públicas & Cidades*. https://doi.org/10.23900/2359-1552v9-n4-2-2020-2-4-4

Ayuso, M., Guillén, M., & Pérez-Marín, A. M. (2014). Time and distance to first accident and driving patterns of young drivers with pay-as-you-drive insurance. *Accident Analysis and Prevention*, *73*, 125–131. https://doi.org/10.1016/j.aap.2014.08.017

Barroso, L., Porrua, F., Thome, L., & Pereira, M. (2007). Planning for Big Things in Brazil. *IEEE Power and Energy Magazine*, *5*(5), 54–63. https://doi.org/10.1109/MPE.2007.904763

Bellapu, R. P., Mylsamy, S., Rama Krishna, S., & Kundu, P. (2021). Developing and evaluation of machine learning models in the insurance sector. *Materials Today: Proceedings*. https://doi.org/10.1016/j.matpr.2020.12.866

Bentemuller, R. P. P. (2018). Poder Judiciário e deferência administrativa: o caso Fator GSF. *Revista de Direito Setorial e Regulatório*, *4*(1), 21–38. https://search.ebscohost.com.sbproxy.fgv.br/login.aspx?direct=true&db=edsdoj&AN=edsdoj.9b9217016724107a28a7e8ccef6d57d&lang=pt-br&site=eds-live

Bergel, A. I., Cardoso, R. M. R., Egídio, A. D., & Rodríguez-martínez, E. V. (2013). The Cramér-Lundberg and the dual risk models : Ruin , dividend problems and duality features. *30th International Congress of Actuaries*, 1–16.

Biener, C., Eling, M., & Wirfs, J. H. (2015). Insurability of cyber risk: An empirical analysis. *Geneva Papers on Risk and Insurance: Issues and Practice*, *40*(1). https://doi.org/10.1057/gpp.2014.19

Bokusheva, R. (2018). Using copulas for rating weather index insurance contracts. *Https://Doi.Org/10.1080/02664763.2017.1420146*, *45*(13), 2328–2356. https://doi.org/10.1080/02664763.2017.1420146

Boldeanu, F. T., Clemente-Almendros, J. A., Tache, I., & Seguí-Amortegui, L. A. (2022). Is ESG Relevant to Electricity Companies during Pandemics? A Case Study on European Firms during COVID-19. *Sustainability (Switzerland)*, *14*(2). https://doi.org/10.3390/su14020852

Bolton, P., Despres, M., Pereira Da Silva, L. A., Samama, F., & Svartzman, R. (2020). *The green swan: Central banking in the age of climate change*. Bank for International Settlements. https://www.bis.org/publ/othp31.pdf

Borba, P. C. S., Sousa, W. C., Shadman, M., & Pfenninger, S. (2023). Enhancing drought resilience and energy security through complementing hydro by offshore wind power—The case of Brazil. *Energy Conversion and Management*, *277*, 116616. https://doi.org/10.1016/J.ENCONMAN.2022.116616

Bowers, N. L., Gerber, H. U., Hickman, J. C., Jones, D. A., & Nesbitt, C. J. (1987). Actuarial mathematics. . Actuarial Mathematics by Bowers, Hickman, Gerber, Jones and Nesbitt [Published in 1986 by The Society of Actuaries]. *Transactions of the Faculty of Actuaries*, *41*. https://doi.org/10.1017/s0071368600009812

Boyle, C. F. H., Haas, J., & Kern, J. D. (2021). Development of an irradiance-based weather derivative to hedge cloud risk for solar energy systems. *Renewable Energy*, *164*, 1230–1243. https://doi.org/10.1016/j.renene.2020.10.091

Braun, A., & Schreiber, F. (2017). The Current InsurTech Landscape: Business Models and Disruptive Potential. *Institute of Insurance Economics I.VW-HSG, University of St. Gallen,*.

Broberg, M. (2020). Parametric loss and damage insurance schemes as a means to enhance climate change resilience in developing countries. *Climate Policy*, *20*(6), 693–703. https://doi.org/10.1080/14693062.2019.1641461

Caceres, A. L., Jaramillo, P., Matthews, H. S., Samaras, C., & Nijssen, B. (2021). Hydropower under climate uncertainty: Characterizing the usable capacity of Brazilian, Colombian and Peruvian power plants under climate scenarios. *Energy for Sustainable Development*, *61*, 217–229. https://doi.org/10.1016/J.ESD.2021.02.006

Campiglio, E., Dafermos, Y., Monnin, P., Ryan-Collins, J., Schotten, G., & Tanaka, M. (2018). Climate change challenges for central banks and financial regulators. *Nature Climate Change*, *8*(6), 462–468. https://doi.org/10.1038/s41558-018-0175-0

Campos, A. F., Silva, N. F. da, Pereira, M. G., & Siman, R. R. (2020). Deregulation, flexibilization and privatization: historical and critical perspective of the brazilian electric sector. *Electricity Journal*, *33*(7). https://doi.org/10.1016/j.tej.2020.106796

Can, A., & Musulin, R. (2023). Climate Change Risk (and Opportunity) for the P&C Actuary. *Actuarial Review*. https://ar.casact.org/climate-change-risk-and-opportunity-for-the-pc-actuary/

Cankaya, S., & Naeem, N. (2022). Does ESG performance affect the financial performance of environmentally sensitive industries A comparison between emerging and developed markets. *Pressacademia*, *14*(1). https://doi.org/10.17261/pressacademia.2021.1509

Carneiro, R. (2000). *Estado, mercado eo desenvolvimento do setor elétrico brasileiro*. Universidade Federal de Minas Gerais.

Carvalho, J. V. F., & Bonetti, R. S. F. (2023). Longitudinal Effects of Sectoral Concentration on the Brazilian Insurance Market Performance. *Revista de Administração Contemporânea*, *27*(1). https://doi.org/10.1590/1982-7849rac2022210311.en

Carvalho, J. V. F., & Guimarães, A. S. (2023). Systemic Risk Assessment using Complex Networks Approach: evidence from the Brazilian (Re)Insurance Market. *Research in International Business and Finance*, 102065. https://doi.org/10.1016/j.ribaf.2023.102065

Castilho, D. (2019). Hidrelétricas na Amazônia Brasileira: Da Expansão à Espoliação. In *La electricidad y la transformación de la vida urbana y socia* (pp. 68–87). Geocrítica.

Cataia, M. (2019). Macrossistema elétrico brasileiro: integração nacional e centralização do poder. *V Simposio Internacional de La Historia de La Electrificación: La Electricidad y La Transformación de La Vida Urbana y Social.*, 581–602.

CCEE. (2023). *Mecanismo de Realocação de Energia (MRE)* (pp. 1–56). CCEE - Câmara de Comercialização de Energia Elétrica. https://www.ccee.org.br/mercado/regras-de-comercializacao

Cesarini, L., Figueiredo, R., Monteleone, B., & Martina, M. L. V. (2021). The potential of machine learning for weather index insurance. *Natural Hazards and Earth System Sciences*, *21*(8), 2379–2405. https://doi.org/10.5194/nhess-21-2379-2021

Chang, B., & Joe, H. (2019). Prediction based on conditional distributions of vine copulas. *Computational Statistics and Data Analysis*, *139*. https://doi.org/10.1016/j.csda.2019.04.015

Chang, L., & Fairley, W. B. (1979). Pricing Automobile Insurance under Multivariate Classification of Risks: Additive versus Multiplicative. *The Journal of Risk and Insurance*, *46*(1), 75. https://doi.org/10.2307/251634

Chen, H.-M., Kuo, T.-C., & Chen, J.-L. (2022). Impacts on the ESG and financial performances of companies in the manufacturing industry based on the climate change related risks. *Journal of Cleaner Production*, 134951. https://doi.org/10.1016/J.JCLEPRO.2022.134951

Chenet, H., Ryan-Collins, J., & van Lerven, F. (2021). Finance, climate-change and radical uncertainty: Towards a precautionary approach to financial policy. *Ecological Economics*, *183*, 106957. https://doi.org/10.1016/J.ECOLECON.2021.106957

Citterio, A., & King, T. (2023). The role of Environmental, Social, and Governance (ESG) in predicting bank financial distress. *Finance Research Letters*, *51*, 103411. https://doi.org/10.1016/J.FRL.2022.103411

Clarke, D. J. (2016). A theory of rational demand for index insurance. *American Economic Journal: Microeconomics*, *8*(1). https://doi.org/10.1257/mic.20140103

Clauberg, A. P. C., Henkes, J. A., & Becegato, V. A. (2021). Fontes hídricas: setor energético brasileiro e o incremento das pequenas centrais hidrelétricas. *Revista Brasileira De Meio Ambiente &Amp; Sustentabilidade*, *1*(4), 134–174. https://rbmaes.emnuvens.com.br/revista/article/view/95

Cole, S., Stein, D., & Tobacman, J. (2014). Dynamics of demand for index insurance: Evidence from a long-run field experiment. *American Economic Review*, *104*(5). https://doi.org/10.1257/aer.104.5.284

Corradin, A., Denuit, M., Detyniecki, M., Grari, V., Sammarco, M., & Trufin, J. (2022). JOINT MODELING OF CLAIM FREQUENCIES AND BEHAVIORAL SIGNALS IN

MOTOR INSURANCE. *ASTIN Bulletin*, *52*(1). https://doi.org/10.1017/asb.2021.24

Costa, V. B. F., Bonatto, B. D., & Silva, P. F. (2022). Optimizing Brazil's regulated electricity market in the context of time-of-use rates and prosumers with energy storage systems. *Utilities Policy*, *79*, 101441. https://doi.org/10.1016/J.JUP.2022.101441

Costa, V. B. F., Capaz, R. S., Silva, P. F., Doyle, G., Aquila, G., Coelho, É. O., de Lorenci, E., Pereira, L. C., Maciel, L. B., Balestrassi, P. P., Bonatto, B. D., & da Silva, L. C. (2022). Socioeconomic and environmental consequences of a new law for regulating distributed generation in Brazil: A holistic assessment. *Energy Policy*, *169*, 113176. https://doi.org/10.1016/J.ENPOL.2022.113176

Cummins, J. D. (1991). Statistical and Financial Models of Insurance Pricing and the Insurance Firm. *The Journal of Risk and Insurance*, *58*(2), 261. https://doi.org/10.2307/253237

Czado, C. (2019). Analyzing dependent data with vine copulas: A practical guide with R. In *Lecture Notes in Statistics* (Vol. 222). https://doi.org/10.1007/978-3-030-13785-4_1

David, M. (2015). Auto Insurance Premium Calculation Using Generalized Linear Models. *Procedia Economics and Finance*, *20*. https://doi.org/10.1016/s2212-5671(15)00059-3

de Jong, P., Kiperstok, A., Sánchez, A. S., Dargaville, R., & Torres, E. A. (2016). Integrating large scale wind power into the electricity grid in the Northeast of Brazil. *Energy*, *100*, 401–415. https://doi.org/10.1016/J.ENERGY.2015.12.026

De Jong, P., Sánchez, A. S., Esquerre, K., Kalid, R. A., & Torres, E. A. (2013). Solar and wind energy production in relation to the electricity load curve and hydroelectricity in the northeast region of Brazil. *Renewable and Sustainable Energy Reviews*, *23*, 526–535. https://doi.org/10.1016/J.RSER.2013.01.050

Deng, M., Leippold, M., Wagner, A. F., & Wang, Q. (2022). *Stock Prices and the Russia-Ukraine War: Sanctions, Energy and ESG*. https://papers.ssrn.com/abstract=4121382

Denuit, M., Charpentier, A., & Trufin, J. (2021). Autocalibration and Tweedie-dominance for insurance pricing with machine learning. *Insurance: Mathematics and Economics*, *101*. https://doi.org/10.1016/j.insmatheco.2021.09.001

Denuit, M., Guillen, M., & Trufin, J. (2019). Multivariate credibility modelling for usage-based motor insurance pricing with behavioural data. *Annals of Actuarial Science*, *13*(2). https://doi.org/10.1017/S1748499518000349

Diffenbaugh, N. S., Singh, D., & Mankin, J. S. (2018). Unprecedented climate events: Historical changes, aspirational targets, and national commitments. *Science Advances*, *4*(2). https://doi.org/10.1126/sciadv.aao3354

Dijksterhuis, C., Lewis-Evans, B., Jelijs, B., De Waard, D., Brookhuis, K., & Tucha, O. (2015). The impact of immediate or delayed feedback on driving behaviour in a simulated Pay-As-You-Drive system. *Accident Analysis and Prevention*, *75*. https://doi.org/10.1016/j.aap.2014.11.017

Domínguez-Tuda, M., & Gutiérrez-Jurado, H. A. (2021). Global analysis of the hydrologic sensitivity to climate variability. *Journal of Hydrology*, *603*, 126720. https://doi.org/10.1016/J.JHYDROL.2021.126720

Drewing, B., & Lanavère, F. (2021). *When the wind blows ; the role of parametric insurance in renewable energy*. AXA XL. https://axaxl.com/fast-fast-forward/articles/when-the-wind-blows-the-role-of-parametric-insurance-in-renewable-energy

Eabrasu, M. (2021). Bet against yourself: Integrating insurance and entrepreneurship. *Journal of Institutional Economics*, *May*. https://doi.org/10.1017/S1744137421000394

Eling, M., & Zhu, J. (2018). Which Insurers Write Cyber Insurance? Evidence from the U.S. Property and Casualty Insurance Industry. In *Journal of Insurance Issues* (Vol. 41, Issue 1).

Embrechts, P., & Wüthrich, M. V. (2022). Recent Challenges in Actuarial Science. *Annual Review of Statistics and Its Application*, *9*, 119–140. https://doi.org/10.1146/annurev-statistics-040120-030244

Enel Green Power. (n.d.). *Energia hidráulica*. Retrieved October 11, 2023, from https://www.enelgreenpower.com/pt/learning-hub/energias-renoveveis/energia-hidraulica

Enríquez, S., Hyman, E., Ramírez-Leiva, L., Reyes, E., Cardona, L. M., & González-Rivera, C. (2020). *Parametric Insurance for Renewable Electric Power Producers in Central America*. https://www.climatelinks.org/sites/default/files/asset/document/2020_USAID_CEADIR_Parametric-Insurance-for-Renewable-Electric-Power-Producers-in-Central-America.pdf

Escobar-Anel, M. (2022). Multivariate risk aversion utility, application to ESG investments. *The North American Journal of Economics and Finance*, *63*, 101790. https://doi.org/10.1016/J.NAJEF.2022.101790

Esposito, A. S. (2018). Energia elétrica. In *O BNDES e as agendas setoriais : contribuições para a transição de governo* (pp. 57–67). http://web.bndes.gov.br/bib/jspui/handle/1408/18041

Fafaliou, I., Giaka, M., Konstantios, D., & Polemis, M. (2022). Firms' ESG reputational risk and market longevity: A firm-level analysis for the United States. *Journal of Business Research*, *149*, 161–177. https://doi.org/10.1016/J.JBUSRES.2022.05.010

Fahrenwaldt, M. A., Weber, S., & Weske, K. (2018). Pricing of cyber insurance contracts in a network model. *ASTIN Bulletin*, *48*(3). https://doi.org/10.1017/asb.2018.23

Fairley, W. B., Tomberlin, T. J., & Weisberg, H. I. (1981). Pricing Automobile Insurance under a Cross-Classification of Risks: Evidence from New Jersey. *The Journal of Risk and Insurance*, *48*(3), 505. https://doi.org/10.2307/252727

Falcão, Â. W. D. S., Nunes, R. V., De Assis, C. W. C., Adriano, N. D. A., & Siebra, A. A. (2019). Os reflexos da crise hídrica brasileira na estrutura de custos das empresas do setor de energia elétrica. *ABCustos*, *14*(2), 1–36. https://doi.org/10.47179/abcustos.v14i2.475

Fernandes, G., Lima Gomes, L., & Teixeira Brandão, L. E. (2019). Mitigating Hydrological Risk with Energy Derivatives. *Energy Economics*, *81*, 528–535. https://doi.org/10.1016/J.ENECO.2019.05.001

Ferreira, P. G. C., Oliveira, F. L. C., & Souza, R. C. (2015). The stochastic effects on the Brazilian Electrical Sector. *Energy Economics*, *49*, 328–335. https://doi.org/10.1016/j.eneco.2015.03.004

Figueiredo, R., Martina, M. L. V., Stephenson, D. B., & Youngman, B. D. (2018). A Probabilistic Paradigm for the Parametric Insurance of Natural Hazards. *Risk Analysis*, *38*(11), 2400–2414. https://doi.org/10.1111/risa.13122

Florax, R. J. G. M., Folmer, H., & Rey, S. J. (2003). Specification searches in spatial

econometrics: The relevance of Hendry's methodology. *Regional Science and Urban Economics*, *33*(5), 557–579. https://doi.org/10.1016/S0166-0462(03)00002-4

Ford, J. M., Gehricke, S. A., & Zhang, J. E. (2022). Option traders are concerned about climate risks: ESG ratings and short-term sentiment. *Journal of Behavioral and Experimental Finance*, *35*, 100687. https://doi.org/10.1016/J.JBEF.2022.100687

Frees, E. W. (2015). Analytics of Insurance Markets. *Annual Review of Financial Economics*, *7*. https://doi.org/10.1146/annurev-financial-111914-041815

Fridgen, G., Halbrügge, S., Olenberger, C., & Weibelzahl, M. (2020). The insurance effect of renewable distributed energy resources against uncertain electricity price developments. *Energy Economics*, *91*. https://doi.org/10.1016/j.eneco.2020.104887

Galletta, S., Mazzù, S., & Naciti, V. (2022). A bibliometric analysis of ESG performance in the banking industry: From the current status to future directions. *Research in International Business and Finance*, *62*, 101684. https://doi.org/10.1016/J.RIBAF.2022.101684

Ganim, A. (2009). *Setor Elétrico Brasileiro: Aspectos Regulamentares, Tributários e Contábeis* (2nd ed.). Synergia.

Getirana, A., Libonati, R., & Cataldi, M. (2021). Brazil is in water crisis — it needs a drought plan. *Nature*, *600*, 218–220. https://doi.org/https://doi.org/10.1038/d41586-021-03625-w

Golfetto, V. de C. (2023). *A judicialização do setor elétrico: os impactos das escolhas regulatórias do setor na esfera judicial - Editora Dialética*. Dialética.

Gonçalves, R. C., & Mueller, B. (2019). *Repactuação do Risco Hidrológico no Mercado de Energia Elátrica: Uma Análise a partir das Teorias Positivas e Normativas da Regulação*. Escola Superior do Tribunal de Contas da União.

Guelman, L., Guillén, M., & Pérez-Marín, A. M. (2014). A survey of personalized treatment models for pricing strategies in insurance. *Insurance: Mathematics and Economics*, *58*(1), 68–76. https://doi.org/10.1016/J.INSMATHECO.2014.06.009

Gürtürk, M., Ucar, F., & Erdem, M. (2022). A novel approach to investigate the effects of global warming and exchange rate on the solar power plants. *Energy*, *239*, 122344. https://doi.org/10.1016/J.ENERGY.2021.122344

Hair Jr, J. F., Black, W. C., Barry, B. J., & Anderson, R. E. (2014). Multivariate Data Analysis. In *British Library Cataloguing*.

Han, X., Zhang, G., Xie, Y., Yin, J., Zhou, H., Yang, Y., Li, J., & Bai, W. (2019). Weather index insurance for wind energy. *Global Energy Interconnection*, *2*(6), 541–548. https://doi.org/10.1016/j.gloei.2020.01.008

Havlová, K. (2015). What Integrated Reporting Changed: The Case Study of Early Adopters. *Procedia Economics and Finance*, *34*, 231–237. https://doi.org/10.1016/S2212-5671(15)01624-X

Henckaerts, R., Côté, M. P., Antonio, K., & Verbelen, R. (2020). Boosting Insights in Insurance Tariff Plans with Tree-Based Machine Learning Methods. *North American Actuarial Journal*, 1–31. https://doi.org/10.1080/10920277.2020.1745656/SUPPL_FILE/UAAJ_A_1745656_SM9618.HTML

Hermes de Araújo, J. L. R. (2006). The Case of Brazil: Reform by Trial and Error? In *Electricity Market Reform* (pp. 565–594). Elsevier. https://doi.org/10.1016/B978-

008045030-8/50018-7

Hochberg, M., & Poudineh, R. (2021). The Brazilian electricity market architecture: An analysis of instruments and misalignments. *Utilities Policy*, *72*(August), 101267. https://doi.org/10.1016/j.jup.2021.101267

Horton, J. (2018). Parametric Insurance as an Alternative to Liability for Compensating Climate Harms. *Carbon & Climate Law Review*, *12*(4), 285–296. https://doi.org/10.21552/cclr/2018/4/4

Horton, J., Lefale, P., & Keith, D. (2021). Parametric Insurance for Solar Geoengineering: Insights from the Pacific Catastrophe Risk Assessment and Financing Initiative. *Global Policy*, *12*(S1). https://doi.org/10.1111/1758-5899.12864

Huang, Q., Li, Y., Lin, M., & McBrayer, G. A. (2022). Natural disasters, risk salience, and corporate ESG disclosure. *Journal of Corporate Finance*, *72*, 102152. https://doi.org/10.1016/J.JCORPFIN.2021.102152

Huang, Y., & Meng, S. (2020). A Bayesian nonparametric model and its application in insurance loss prediction. *Insurance: Mathematics and Economics*, *93*, 84–94. https://doi.org/10.1016/j.insmatheco.2020.04.010

Hunt, J. D., Stilpen, D., & Freitas, M. A. V. De. (2018). A review of the causes , impacts and solutions for electricity supply crises in Brazil. *Renewable and Sustainable Energy Reviews*, *88*(February), 208–222. https://doi.org/10.1016/j.rser.2018.02.030

Itaipu Binacional. (2022). *RELATÓRIO ANUAL ITAIPU BINACIONAL*. https://www.itaipu.gov.br/sites/default/files/af_df/RelAnual_2022_.pdf

Jha, S. (2012). Punishing the Lemon: The Ethics of Actuarial Fairness. *Journal of the American College of Radiology*, *9*(12), 887–893. https://doi.org/10.1016/J.JACR.2012.09.012

Jibril, M., Raffar, N., Zulkafli, Z., Nurulhuda, K., Mohamed, B., Melissa, F., Ain, N., & Tangang, F. (2022). International Journal of Disaster Risk Reduction Index-based insurance and hydroclimatic risk management in agriculture : A systematic review of index selection and yield-index modelling methods. *International Journal of Disaster Risk Reduction*, *67*(October 2021), 102653. https://doi.org/10.1016/j.ijdrr.2021.102653

Joe, H. (1996). *Families of m-variate distributions with given margins and m(m-1)/2 bivariate dependence parameters*. https://doi.org/10.1214/lnms/1215452614

Jong, P., & Heller, G. Z. (2008). Generalized Linear Models for Insurance Data. In *Generalized Linear Models for Insurance Data*. Cambridge University Press. https://doi.org/10.1017/CBO9780511755408

Kaas, R., Goovaerts, M., Dhaene, J., & Denuit, M. (2008). Modern Actuarial Risk Theory. In *Modern Actuarial Risk Theory*. Springer Berlin, Heidelberg. https://doi.org/10.1007/978-3-540-70998-5

Kapphan, I., Calanca, P., & Holzkaemper, A. (2012). Climate change, weather insurance design and hedging effectiveness. *Geneva Papers on Risk and Insurance: Issues and Practice*, *37*(2), 286–317. https://doi.org/10.1057/gpp.2012.8

Karim, M., & Mutaqin, A. K. (2020). Modeling Claim Frequency in Indonesia Auto Insurance Using Generalized Poisson-Lindley Linear Model. *Jurnal Matematika, Statistika Dan Komputasi*, *16*(3). https://doi.org/10.20956/jmsk.v16i3.9315

Kelejian, H., & Piras, G. (2017). *Spatial Econometrics*. Academic Press.

Khakifirooz, M., Fathi, M., Wu, J.-Z., & Yu, K. (2021). The Key Factors to Promote the Pay-As-You-Drive Insurance in Taiwan. *Journal of Insurance Issues*, *44*(2), 1–30. https://www.researchgate.net/profile/Mahdi-Fathi/publication/349961266_The_Key_Factors_to_Promote_the_Pay-As-You-Drive_Insurance_in_Taiwan/links/6049392292851c1bd4def8bb/The-Key-Factors-to-Promote-the-Pay-As-You-Drive-Insurance-in-Taiwan.pdf%0Ahttps://www

Kubara, M., & Kopczewska, K. (2023). Akaike information criterion in choosing the optimal k-nearest neighbours of the spatial weight matrix. *Spatial Economic Analysis*, 1–19. https://doi.org/10.1080/17421772.2023.2176539

Kumar, S. (2023). Funding Issues and Challenges of Conventional Energy Market in the ESG Conscious World. *Academy of Marketing Studies Journal*, *27*(1), 1–10.

Kusuma, A., Jackson, B., & Noy, I. (2018). A viable and cost-effective weather index insurance for rice in Indonesia. *GENEVA Risk and Insurance Review*, *43*(2). https://doi.org/10.1057/s10713-018-0033-z

Laas, D., Schmeiser, H., & Wagner, J. (2016). Empirical findings on motor insurance pricing in Germany, Austria and Switzerland. *Geneva Papers on Risk and Insurance: Issues and Practice*, *41*(3), 398–431. https://doi.org/10.1057/gpp.2015.30

Lai, X., & Zhang, F. (2022). Can ESG certification help company get out of over-indebtedness? Evidence from China. *Pacific-Basin Finance Journal*, *76*, 101878. https://doi.org/10.1016/J.PACFIN.2022.101878

Laudagé, C., Desmettre, S., & Wenzel, J. (2019). Severity modeling of extreme insurance claims for tariffication. *Insurance: Mathematics and Economics*, *88*. https://doi.org/10.1016/j.insmatheco.2019.06.002

Lee, C. C., Li, X., Yu, C. H., & Zhao, J. (2022). The contribution of climate finance toward environmental sustainability: New global evidence. *Energy Economics*, *111*, 106072. https://doi.org/10.1016/J.ENECO.2022.106072

Lee, M. T., Raschke, R. L., & Krishen, A. S. (2022). Signaling green! firm ESG signals in an interconnected environment that promote brand valuation. *Journal of Business Research*, *138*, 1–11. https://doi.org/10.1016/J.JBUSRES.2021.08.061

Leonel, L. D., Balan, M. H., Camargo, L. A. S., Rego, E. E., Ramos, D. S., & Lima, R. M. F. (2019). Game theory application in hydropower's firm energy monthly allocation process. *IEEE Latin America Transactions*, *17*(1), 85–92. https://doi.org/10.1109/TLA.2019.8826699

LeSage, J., & Pace, R. K. (2009). Introduction to spatial econometrics. In *Introduction to Spatial Econometrics*. https://doi.org/10.1111/j.1467-985x.2010.00681_13.x

Lesk, C., Coffel, E., Winter, J., Ray, D., Zscheischler, J., Seneviratne, S. I., & Horton, R. (2021). Stronger temperature–moisture couplings exacerbate the impact of climate warming on global crop yields. *Nature Food*, *2*(9). https://doi.org/10.1038/s43016-021-00341-6

Li, Q., Sheng, B., Huang, J., Li, C., Song, Z., Chao, L., Sun, W., Yang, Y., Jiao, B., Guo, Z., Liao, L., Li, X., Sun, C., Li, W., Huang, B., Dong, W., & Jones, P. (2022). Different climate response persistence causes warming trend unevenness at continental scales. *Nature Climate Change 2022*, 1–7. https://doi.org/10.1038/s41558-022-01313-9

Lima, F. V. M. S., Gonçalves, R. M., Montecino, H. D., Carvalho, R. A. V. N., & Mutti, P. R. (2022). Multi-sensor geodetic observations for drought characterization in the Northeast

Atlantic Eastern Hydrographic Region, Brazil. *Science of The Total Environment*, *846*, 157426. https://doi.org/10.1016/J.SCITOTENV.2022.157426

Lin, X., & Kwon, W. J. (2020). Application of parametric insurance in principle-compliant and innovative ways. *Risk Management and Insurance Review*, *23*(2), 121–150. https://doi.org/10.1111/rmir.12146

Linnerooth-Bayer, J., Warner, K., Bals, C., Höppe, P., Burton, I., Loster, T., & Haas, A. (2009). Insurance, developing countries and climate change. *Geneva Papers on Risk and Insurance: Issues and Practice*, *34*(3), 381–400. https://doi.org/10.1057/gpp.2009.15

Liu, P., Zhu, B., Yang, M., & Chu, X. (2022). ESG and financial performance: A qualitative comparative analysis in China's new energy companies. *Journal of Cleaner Production*, *379*, 134721. https://doi.org/10.1016/J.JCLEPRO.2022.134721

Lööf, H., Sahamkhadam, M., & Stephan, A. (2022). Is Corporate Social Responsibility investing a free lunch? The relationship between ESG, tail risk, and upside potential of stocks before and during the COVID-19 crisis. *Finance Research Letters*, *46*, 102499. https://doi.org/10.1016/J.FRL.2021.102499

Lovick, A. C., & Lee, P. K. W. (2012). Redefining the deviance objective for generalised linear models. *British Actuarial Journal*, *17*(3). https://doi.org/10.1017/s1357321712000190

Maceira, M. E. P., Marzano, L. G. B., Penna, D. D. J., Diniz, A. L., & Justino, T. C. (2015). Application of CVaR risk aversion approach in the expansion and operation planning and for setting the spot price in the Brazilian hydrothermal interconnected system. *International Journal of Electrical Power & Energy Systems*, *72*, 126–135. https://doi.org/10.1016/J.IJEPES.2015.02.025

Machado, B. G. F., & Bhagwat, P. C. (2020). The impact of the generation mix on the current regulatory framework for hydropower remuneration in Brazil. *Energy Policy*, *137*(February 2019), 111129. https://doi.org/10.1016/j.enpol.2019.111129

Maestri, C. O. N. M., & Andrade, M. E. M. C. (2022). Priorities for tariff compensation of distributed electricity generation in Brazil. *Utilities Policy*, *76*(March). https://doi.org/10.1016/j.jup.2022.101374

Malavasi, M., Peters, G., Shevchenko, P. V., Trueck, S., Jang, J., & Sofronov, G. (2021). Cyber Risk Frequency, Severity and Insurance Viability. *SSRN Electronic Journal*. https://doi.org/10.2139/ssrn.3940329

Mansoor, S., Farooq, I., Kachroo, M. M., Mahmoud, A. E. D., Fawzy, M., Popescu, S. M., Alyemeni, M. N., Sonne, C., Rinklebe, J., & Ahmad, P. (2022). Elevation in wildfire frequencies with respect to the climate change. *Journal of Environmental Management*, *301*, 113769. https://doi.org/10.1016/J.JENVMAN.2021.113769

Martins, H. C. (2022). Competition and ESG practices in emerging markets: Evidence from a difference-in-differences model. *Finance Research Letters*, *46*, 102371. https://doi.org/10.1016/J.FRL.2021.102371

Mayon, P., & Parodi, M. (2018). *Setor Elétrico Brasileiro 2012-2018: Resiliência ou Transição?* Synergia.

McNeil, A. J., Frey, R., & Embrechts, P. (2005). Quantitative risk management: Concepts, techniques, and tools. In *Quantitative Risk Management: Concepts, Techniques, and Tools*. https://doi.org/10.1198/jasa.2006.s156

Melo, A. C. G., Rodrigues, A. F., Batista, F. . R. S., Marzano, L. G. B., & Maceira, M. E. P. (2019). Estratégias dominantes de contratação de usinas hidroelétricas no Brasil considerando incertezas hidrológicas. *Cadernos Do IME - Série Estatística*, *45*, 34. https://doi.org/10.12957/cadest.2018.44400

Mendes-Da-Silva, W., Lucas, E. C., & Carvalho, J. V. F. (2021). Flood insurance: The propensity and attitudes of informed people with disabilities towards risk. *Journal of Environmental Management*, *294*, 113032. https://doi.org/10.1016/j.jenvman.2021.113032

Mendes, A. L. S., De Castro, N., Brandao, R., Camara, L., & Moszkowicz, M. (2016). The role of imbalance settlement mechanisms in electricity markets: A comparative analysis between UK and Brazil. *International Conference on the European Energy Market, EEM*, *2016-July*. https://doi.org/10.1109/EEM.2016.7521348

Michel-Kerjan, E., & Morlaye, F. (2008). Extreme events, global warming, and insurance-linked securities: How to trigger the "tipping point." *Geneva Papers on Risk and Insurance: Issues and Practice*, *33*(1), 153–176. https://doi.org/10.1057/palgrave.gpp.2510159

Minkova, L. D. (2012). *Distributions in Insurance Risk Models*. Sofia University, Bulgaria.

Montoya, M. A., Allegretti, G., Sleimann Bertussi, L. A., & Talamini, E. (2021). Renewable and Non-renewable in the energy-emissions-climate nexus: Brazilian contributions to climate change via international trade. *Journal of Cleaner Production*, *312*(May). https://doi.org/10.1016/j.jclepro.2021.127700

Moran, P. A. P. (1948). The Interpretation of Statistical Maps. *Journal of the Royal Statistical Society: Series B (Methodological)*, *10*(2). https://doi.org/10.1111/j.2517-6161.1948.tb00012.x

Moro, E. D. (2020). Towards an economic cyber loss index for parametric cover based on IT security indicator: A preliminary analysis. *Risks*, *8*(2). https://doi.org/10.3390/risks8020045

Mourdoukoutas, F., Boonen, T. J., Koo, B., & Pantelous, A. A. (2021). Pricing in a competitive stochastic insurance market. *Insurance: Mathematics and Economics*, *97*, 44–56. https://doi.org/10.1016/J.INSMATHECO.2021.01.003

Mu, W., Liu, K., Tao, Y., & Ye, Y. (2023). Digital finance and corporate ESG. *Finance Research Letters*, *51*, 103426. https://doi.org/10.1016/J.FRL.2022.103426

Mukhopadhyay, A., Chatterjee, S., Saha, D., Mahanti, A., & Sadhukhan, S. K. (2013). Cyber-risk decision models: To insure IT or not? *Decision Support Systems*, *56*(1). https://doi.org/10.1016/j.dss.2013.04.004

Nascimento, M. M. S., Shadman, M., Silva, C., Assad, L. P. de F., Estefen, S. F., & Landau, L. (2022). Offshore wind and solar complementarity in Brazil: A theoretical and technical potential assessment. *Energy Conversion and Management*, *270*, 116194. https://doi.org/10.1016/J.ENCONMAN.2022.116194

Nelsen, R. B. (2006). *An Introduction to Copulas* (Second). Springer Series in Statistics.

Nielsen, S. F. (2010). Generalized linear models for insurance data. *Journal of Applied Statistics*, *37*(4). https://doi.org/10.1080/02664760902811571

Ohlsson, E., & Johansson, B. (2010). Non-Life Insurance Pricing with Generalized Linear Models. In *EAA Lecture Notes*.

Omerašević, A., & Selimović, J. (2020). Risk factors selection with data mining methods for insurance premium ratemaking. *Zbornik Radova Ekonomskog Fakultet Au Rijeci*, *38*(2). https://doi.org/10.18045/zbefri.2020.2.667

ONS, & SIN. (n.d.). *Mapas*. Retrieved October 12, 2023, from https://www.ons.org.br/paginas/sobre-o-sin/mapas

Paelinck, J. H. P., & Klaasen, L. H. (1979). Spatial econometrics. In *Spatial econometrics.* Saxon House. https://books.google.com/books/about/Spatial_Econometrics.html?hl=pt-BR&id=mVTaAAAAMAAJ

Pai, J., Li, Y., Yang, A., & Li, C. (2022). Earthquake parametric insurance with Bayesian spatial quantile regression. *Insurance: Mathematics and Economics*, *106*, 1–12. https://doi.org/10.1016/j.insmatheco.2022.04.007

Paim, M. A., Dalmarco, A. R., Yang, C. H., Salas, P., Lindner, S., Mercure, J. F., de Andrade Guerra, J. B. S. O., Derani, C., Bruce da Silva, T., & Viñuales, J. E. (2019). Evaluating regulatory strategies for mitigating hydrological risk in Brazil through diversification of its electricity mix. *Energy Policy*, *128*(May 2018), 393–401. https://doi.org/10.1016/j.enpol.2018.12.064

Paltán, H. A., Pant, R., Plummer Braeckman, J., & Dadson, S. J. (2021). Increased water risks to global hydropower in 1.5 °C and 2.0 °C Warmer Worlds. *Journal of Hydrology*, *599*, 126503. https://doi.org/10.1016/J.JHYDROL.2021.126503

Pereira, R. B., Rocha, S. P. da, Machado-Coelho, T. M., Oliveira, B. A. G. de, Ekel, P. I., & Soares, G. L. (2018). AGREGAÇÃO DE MÉTRICAS DE RISCO COM O OPERADOR OWA APLICADA A COMERCIALIZAÇÃO DE ENERGIA. *Proceedings XXII Congresso Brasileiro de Automática*. https://doi.org/10.20906/CPS/CBA2018-1219

Pineau, E., Le, P., & Estran, R. (2022). Importance of ESG factors in sovereign credit ratings. *Finance Research Letters*, *49*, 102966. https://doi.org/10.1016/J.FRL.2022.102966

Pinheiro Neto, D., Domingues, E. G., Coimbra, A. P., de Almeida, A. T., Alves, A. J., & Calixto, W. P. (2017). Portfolio optimization of renewable energy assets: Hydro, wind, and photovoltaic energy in the regulated market in Brazil. *Energy Economics*, *64*, 238–250. https://doi.org/10.1016/J.ENECO.2017.03.020

Prol, J. L., & Kim, K. (2022). Risk-return performance of optimized ESG equity portfolios in the NYSE. *Finance Research Letters*, *50*, 103312. https://doi.org/10.1016/J.FRL.2022.103312

PWC. (2023). *Demonstrações financeiras consolidadas e individuais em 31 de dezembro de 2022 e relatório dos auditores independentes - Auren Energia S.A.* https://api.mziq.com/mzfilemanager/v2/d/691c9da5-45e0-458f-a3da-41982b1730fc/79ed366b-e250-904d-9948-fd438d491ec2?origin=1

Qi, W., Feng, L., Yang, H., & Liu, J. (2022). Warming winter, drying spring and shifting hydrological regimes in Northeast China under climate change. *Journal of Hydrology*, *606*, 127390. https://doi.org/10.1016/J.JHYDROL.2021.127390

Qian, W., Yang, Y., & Zou, H. (2016). Tweedie's Compound Poisson Model With Grouped Elastic Net. *Journal of Computational and Graphical Statistics*, *25*(2). https://doi.org/10.1080/10618600.2015.1005213

Reimers, I., & Shiller, B. R. (2019). The impacts of telematics on competition and consumer behavior in insurance. *Journal of Law and Economics*, *62*(4). https://doi.org/10.1086/705119

Rodrigues, R. de S. (2022). *A Financeirização do Dado Meteorológico como mitigação das consequências da crise hídrica*. https://portal.inmet.gov.br/noticias/a-financeirização-do-dado-meteorológico-como-mitigação-das-consequências-da-crise-hídrica

Sant, D. T. (1980). Estimating Expected Losses in Auto Insurance. *The Journal of Risk and Insurance*, *47*(1), 133. https://doi.org/10.2307/252686

Schanz, K.-U. (2018). *Understanding and Addressing Global Insurance Protection Gaps* (Issue April). www.genevaassociation.org

Shanaev, S., & Ghimire, B. (2022). When ESG meets AAA: The effect of ESG rating changes on stock returns. *Finance Research Letters*, *46*, 102302. https://doi.org/10.1016/J.FRL.2021.102302

Shi, P., Feng, X., & Boucher, J. P. (2016). Multilevel modeling of insurance claims using copulas. *Annals of Applied Statistics*, *10*(2). https://doi.org/10.1214/16-AOAS914

Shin, J., Moon, J. J., & Kang, J. (2022). Where does ESG pay? The role of national culture in moderating the relationship between ESG performance and financial performance. *International Business Review*, 102071. https://doi.org/10.1016/J.IBUSREV.2022.102071

Silva, V. O., de Mello, C. R., & Chou, S. C. (2022). Projections of severe droughts in future climate in Southeast Brazil: a case study in Southern Minas Gerais State, Brazil. *Theoretical and Applied Climatology 2022*, 1–14. https://doi.org/10.1007/S00704-022-03993-X

Singer, A. W. (2019). The evolution of parametric insurance. *Risk Management*, *66*(3), 32–36. http://www.rmmagazine.com/articles/article/2019/04/01/-The-Evolution-of-Parametric-Insurance-

Song, M. L., & Carvalho, J. V. de F. (2022). "Divide et impera"? A financial assessment of the (de)concentration in the Brazilian reinsurance market. In *22º USP International Conference in Accounting*. University of São Paulo. https://congressousp.fipecafi.org/anais/22UspInternational/ArtigosDownload/3621.pdf

Stoeckli, E., Dremel, C., & Uebernickel, F. (2018). Exploring characteristics and transformational capabilities of InsurTech innovations to understand insurance value creation in a digital world. *Electronic Markets*, *28*(3). https://doi.org/10.1007/s12525-018-0304-7

Strupczewski, G. (2021). Defining cyber risk. *Safety Science*, *135*. https://doi.org/10.1016/j.ssci.2020.105143

Tan, Y., & Zhu, Z. (2022). The effect of ESG rating events on corporate green innovation in China: The mediating role of financial constraints and managers' environmental awareness. *Technology in Society*, *68*, 101906. https://doi.org/10.1016/J.TECHSOC.2022.101906

Tettamanzi, P., Venturini, G., & Murgolo, M. (2022). Sustainability and Financial Accounting: a Critical Review on the ESG Dynamics. *Environmental Science and Pollution Research 2022 29:11*, *29*(11), 16758–16761. https://doi.org/10.1007/S11356-022-18596-2

Tollefson, J. (2021). Top climate scientists are sceptical that nations will rein in global warming. In *Nature* (Vol. 599, Issue 7883). https://doi.org/10.1038/d41586-021-02990-w

Tolmasquim, M. T., de Barros Correia, T., Addas Porto, N., & Kruger, W. (2021). Electricity market design and renewable energy auctions: The case of Brazil. *Energy Policy*, *158*, 112558. https://doi.org/10.1016/J.ENPOL.2021.112558

Tselentis, D. I., Theofilatos, A., Yannis, G., & Konstantinopoulos, M. (2018). Public opinion on usage-based motor insurance schemes: A stated preference approach. *Travel Behaviour and Society*, *11*. https://doi.org/10.1016/j.tbs.2018.02.003

Umar, M., Mirza, N., Rizvi, S. K. A., & Naqvi, B. (2022). ESG scores and target price accuracy: Evidence from sell-side recommendations in BRICS. *International Review of Financial Analysis*, *84*, 102389. https://doi.org/10.1016/J.IRFA.2022.102389

van Houtan, K. S., Tanaka, K. R., Gagné, T. O., & Becker, S. L. (2021). The geographic disparity of historical greenhouse emissions and projected climate change. *Science Advances*, *7*(29). https://doi.org/10.1126/sciadv.abe4342

Vaughan, E., & Vaughan, T. (2008). Fundamentals of Risk and Insurance 10e. In *John Wiley & Sons, Inc*.

Verma, A. K. (2021). Influence of Climate Change on Balanced Ecosystem, Biodiversity and Sustainable Development: an Overview. *International Journal of Biological Innovations*, *03*(02), 331–337. https://doi.org/10.46505/ijbi.2021.3213

Verschuren, R. M. (2021). Predictive Claim Scores for Dynamic Multi-Product Risk Classification in Insurance. *ASTIN Bulletin*, *51*(1). https://doi.org/10.1017/asb.2020.34

Verschuren, R. M. (2022). Customer price sensitivities in competitive insurance markets. *Expert Systems with Applications*, *202*, 117133. https://doi.org/10.1016/J.ESWA.2022.117133

Volosovych, S., Zelenitsa, I., Kondratenko, D., Szymla, W., & Mamchur, R. (2021). Transformation of insurance technologies in the context of a pandemic. *Insurance Markets and Companies*, *12*(1). https://doi.org/10.21511/INS.12(1).2021.01

Wen, H., Gao, J., Yu, L., & Ho, K. C. (2022). The fundamental effects of ESG disclosure quality in boosting the growth of ESG investing. *Journal of International Financial Markets, Institutions and Money*, *81*, 101655. https://doi.org/10.1016/J.INTFIN.2022.101655

Wolny-Dominiak, A., & Żædlo, T. (2022). Copula-based risk measures in non-life insurance portfolio. *Procedia Computer Science*, *207*, 2610–2617. https://doi.org/10.1016/J.PROCS.2022.09.319

Wu, C., J.-F. Yeh, P., Chen, Y. Y., Lv, W., Hu, B. X., & Huang, G. (2021). Copula-based risk evaluation of global meteorological drought in the 21st century based on CMIP5 multi-model ensemble projections. *Journal of Hydrology*, *598*, 126265. https://doi.org/10.1016/J.JHYDROL.2021.126265

Wuthrich, M. V., & Buser, C. (2018). Data Analytics for Non-Life Insurance Pricing. *SSRN Electronic Journal*. https://doi.org/10.2139/ssrn.2870308

Xu, M., & Hua, L. (2019). Cybersecurity Insurance: Modeling and Pricing. *North American Actuarial Journal*, *23*(2). https://doi.org/10.1080/10920277.2019.1566076

Yeo, A. C., Smith, K. A., Willis, R. J., & Brooks, M. (2002). A mathematical programming approach to optimise insurance premium pricing within a data mining framework. *Journal of the Operational Research Society*, *53*(11). https://doi.org/10.1057/palgrave.jors.2601413

Yu, W., Guan, G., Li, J., Wang, Q., Xie, X., Zhang, Y., Huang, Y., Yu, X., & Cui, C. (2021). Claim Amount Forecasting and Pricing of Automobile Insurance Based on the BP Neural Network. *Complexity*, *2021*. https://doi.org/10.1155/2021/6616121

Zhang, C., Yang, Y., Yang, D., & Wu, X. (2021). Multidimensional assessment of global dryland changes under future warming in climate projections. *Journal of Hydrology*, *592*, 125618. https://doi.org/10.1016/J.JHYDROL.2020.125618

Zhang, D., Mohsin, M., & Taghizadeh-Hesary, F. (2022). Does green finance counteract the climate change mitigation: Asymmetric effect of renewable energy investment and R&D. *Energy Economics*, *113*, 106183. https://doi.org/10.1016/j.eneco.2022.106183

Zhang, W., Furtado, K., Wu, P., Zhou, T., Chadwick, R., Marzin, C., Rostron, J., & Sexton, D. (2021). Increasing precipitation variability on daily-to-multiyear time scales in a warmer world. *Science Advances*, *7*(31). https://doi.org/10.1126/sciadv.abf8021

Annex 1

In the following table, we present the results for the chosen OLS regression using both the balanced and unbalanced data.

	Balanced	**Unbalanced**
Formula	V*R_3M+A*R_3M+WS*H	V*R_3M+A*R_3M+WS*H
V	1602.6***	1842***
	(73.568)	(75.597)
A	87.791***	81.668***
	(1.0809)	(1.2234)
R_3M	16.065***	23.667***
	(1.9687)	(2.2137)
WS	54884***	60266***
	(9840.5)	(10412)
H	1533.9***	1434.8***
	(387.82)	(415.89)
V*R_3M	-0.0806*	-0.1449***
	(0.0372)	(0.0378)
A*R_3M	-0.0103***	-0.0099***
	(0.0004)	(0.0004)
WS*H	-706.18***	-685.23***
	(149.11)	(158.59)
Adjusted R-Square	0.33371	0.25821
AIC	832,619.9	698610.2
BIC	833,953.5	699916.3
n	151	151
t	204	8-204

Source: own elaboration.